Exploring novel molecular approaches to promote repair of the damaged nervous system: A role for Neuronal Pentraxin 2

by

Ushananthini Shanmugalingam

A thesis submitted to the Faculty of Graduate and Postdoctoral Affairs in partial fulfillment of the requirements for the degree of

Doctor of Philosophy

in

Neuroscience

Carleton University

Ottawa, Ontario

Abstract

The mammalian central nervous system (CNS) does not spontaneously regenerate, thereby limiting functional recovery following numerous CNS injuries. Neural repair is restricted due to both the inhibitory extracellular environment post-injury and the limited intrinsic capabilities of adult neurons. The visual system, including retinal ganglion cells (RGCs), and their axons, the optic nerve, is widely used as a model to study molecular mechanisms associated with neuroprotection and regeneration following CNS injury. Many potential therapeutic strategies have been discovered using this model with variable success in terms of promoting axon regeneration. Recent work has suggested that modulating neural activity can protect neurons and promote axon regeneration after injury; however, this area of research remains in its infancy. Activity-dependent signalling molecules, such as neuronal pentraxin 2 (NP2), have been suggested as critical modulators of neuroplasticity but have not been previously implicated in CNS neuroprotection or axon regeneration. This thesis examined the role of NP2 in protecting RGCs and promoting axon regeneration, using *in vitro, ex vivo* and *in vivo* (optic nerve injury) techniques. Given that previous work has supported the notion that RGCs lose intrinsic capacity for regeneration with age, the developmental expression pattern of NP2 was characterized. Additionally, the impact of NP2 treatment on RGC survival, using an *in vitro* RGC culture model, was evaluated. Furthermore, the ability of NP2 to enhance RGC neurite outgrowth using both *in vitro* and *ex vivo* model systems was examined. To assess the *in vivo* impact of exogenous NP2 administration on RGC survival and axon

regeneration, a well-established optic nerve crush (ONC) model was utilized. The effect of NP2 administration on functional recovery following ONC was also evaluated using electroretinography and visual evoked potentials. Taken together, the results indicated a decline in NP2 protein expression with an increase in age and revealed that treatment with NP2 promotes survival and neurite outgrowth in both embryonic and postnatal RGCs. Furthermore, the data demonstrated that exogenous administration of NP2 promotes RGC survival but does not measurably improve functional outcomes post ONC. Collectively, these results illustrate that NP2 holds potential as a survival-inducing factor.

Acknowledgements

Firstly, I thank God for giving me the strength to persevere and successfully complete this chapter of my life.

I would like to express my sincerest gratitude to many people for their support and encouragement throughout my studies. I would like to start by thanking and expressing my immeasurable amount of gratitude to my supervisor, Dr. Patrice D. Smith. Anytime I was uncertain how to proceed, her door was always open; she always answered every question with a smile. Her guidance and support helped me build confidence in myself and made me a better researcher. It was a privilege to work under Dr. Smith's guidance and the completion of this thesis is a testament to her endless patience and constant encouragement. I would like to thank my thesis committee members, Dr. Hayley and Dr. Hildebrand, for their time, insight into my thesis and for their continued support. I would like to express my sincere appreciation to Dr. Tsilfidis and her lab members, especially Dr. Pamela Lagali. Also, I am forever grateful to all my teachers and mentors.

A special thank you to all my friends and my lab colleagues for their encouragement and laughter throughout this journey. Dennis Chan, Georgina Chapman Lau, Meagan Milton and Hyung-Suk Yoo – thank you for making my graduate research experience memorable. A special shout-out to Hyung-Suk Yoo – running experiments on the weekends just would not have been the same without you! Working in the Smith lab is an experience that I will truly cherish for the rest of my life.

Finally, my most important thanks go to my family. Thank you to my Appa, Shanmugalingam, Amma, Nagarajeswary and spouse, Krishanthan, for their unconditional support, kindness, and selflessness. I would also like to thank my siblings for their unwavering support, encouragement, and avid belief in me that kept me going. To my nieces and nephews: thank you for always putting a smile on my face. None of my accomplishments would have been possible without everything my family has done for me.

The knowledge and skills I have gained during my doctoral studies has had a profound impact on my life. My sincerest thanks go to everyone who has helped me along this educational journey!

Table of Contents

Abstract ..... **ii**
Acknowledgements ..... **iv**
Table of Contents ..... **vi**
List of Tables ..... **viii**
List of Figures ..... **ix**
List of Abbreviations ..... **x**

Chapter 1: General Introduction **1**
1.1 The Need for Axon Regeneration 1
1.2 Modeling Central Nervous System Injuries using the Visual System 3
1.2.1 Structural organization of the Visual System 3
1.2.2 Using the Retina and Optic nerve to study Axon Regeneration 7
1.2.3 *In vitro, Ex vivo* and *In vivo* Models 9
1.2.4 Visual electrophysiology 13
1.3 Regeneration in the Mammalian Central Nervous System 18
1.3.1 Overview 18
1.3.2 Extrinsic: The hostile environment 19
1.3.3 Intrinsic: Developmental changes in neuron's regenerative ability 24
1.4 Pentraxins 27
1.4.1 Pentraxin Family 27
1.4.2 Biochemistry and Structure of NP2 29
1.4.3 Expression pattern and Function of NP2 31
1.4.4 The role of NP2 in Regeneration 35

Chapter 2: Research Objectives **38**

Chapter 3: Neuronal Pentraxin 2 promotes cell survival and enhances neurite outgrowth of retinal ganglion cells *in vitro* and *ex vivo* **41**
3.1 Abstract 41
3.2 Introduction 42
3.3 Methods 43
3.3.1 Animals 43
3.3.2 Western blot 43
3.3.3 Enzymatic deglycosylation through digestion with peptide N-glycosidase F (PNGase F) 44
3.3.4 Dissociated retinal cell cultures 44
3.3.5 Immunostaining and assessment of neurite length in retinal cultures 45
3.3.6 Retinal explants 46
3.3.7 Statistical analysis 47
3.4 Results/Discussion 47
3.4.1 NP2 protein is expressed in the developing and adult mouse retina 47
3.4.2 Decline in N-glycosylated NP2 protein expression with retinal development 51
3.4.3 NP2 promotes survival and neurite outgrowth of P7 retinal cultures 53

3.4.4 NP2 promotes axon growth of P14 retinal cultures 56
3.4.5 NP2 promote neurite outgrowth of E18 and P7 retinal explants. 57
3.5 Conclusion 61
3.6 Supplemental Figure 61

Chapter 4: Neuronal Pentraxin 2 promotes cell survival following optic nerve crush 62
4.1 Abstract 62
4.2 Introduction 63
4.3 Methods 65
4.3.1 Animals 65
4.3.2 Optic nerve crush surgery and intravitreal injection 65
4.3.3 Anesthesia for electrophysiology 66
4.3.4 Visual electrophysiology 66
4.3.5 Visual electrophysiology analysis 68
4.3.6 Western blot for quantifying NP2 expression post ONC 68
4.3.7 *In Vivo* retinal ganglion cell survival analysis, using retinal wholemounts 69
4.3.8 Axonal cryosection 70
4.3.9 Statistical analysis 70
4.4 Results/Discussion 71
4.4.1 NP2 expression is altered following optic nerve crush 71
4.4.2 NP2 promotes RGC survival *in vivo* after optic nerve crush 73
4.4.3 NP2 does not enhance functional recovery after optic nerve crush 76
4.5 Conclusion 89

Chapter 5: General Discussion 90

Chapter 6: Conclusion 100

References 101

List of Tables

Table 1: Homolog of NP2 29

List of Figures

Figure 1-1: Schematic illustration of the mammalian (A) visual system and (B) retinal cell layers. 4
Figure 1-2: Schematic illustration of *in vitro* primary retinal ganglion cell culture method..... 10
Figure 1-3: Schematic illustration of *ex vivo* retinal explant culture method. 12
Figure 1-4: Schematic illustration of in vivo optic nerve crush method. 13
Figure 1-5: Full-field scotopic flash electroretinography waveform of a C57BL/6J mouse. 14
Figure 1-6: Pattern electroretinography waveform of a C57BL/6J mouse. 16
Figure 1-7: Flash Visual Evoked Potential waveform of a C57BL/6J mouse. 17

Figure 3-1: Developmental decline in NP2 protein expression in retina. 49
Figure 3-2: Decline in N-glycosylated NP2 protein expression with retinal development. 52
Figure 3-3: NP2 promotes survival and neurite outgrowth in P7 retinal cultures. 55
Figure 3-4: NP2 promotes axon growth in P14 retinal cultures. 56
Figure 3-5: NP2 promote neurite outgrowth in E18 and P7 retinal explants. 58
Figure 3-6: NP2 promote neurite outgrowth in E18 and P7 retinal explants. 59

Figure 4-1: NP2 expression is altered following optic nerve crush. 72
Figure 4-2: NP2 administration promotes adult RGC survival post ONC injury. 75
Figure 4-3: *In vivo* functional analysis experimental design. 76
Figure 4-4: The function of photoreceptors and bipolar cells remains intact following ONC. 78
Figure 4-5: NP2 does not protect against RGC dysfunction following ONC. 80
Figure 4-6: NP2 does not protect against optic nerve dysfunction following ONC. 87

List of Abbreviations

AA	Amino acid
AMPA	α-amino-3-hydroxy-5-methylisoxazole-4-propionic acid
ANOVA	Analysis of variance
BBB	Blood-brain barrier
BDNF	Brain-derived neurotrophic factor
BRB	Blood-retinal barrier
Ca^{2+}	Calcium ions
CCAC	Canadian Council on Animal Care
CNS	Central nervous system
CNTF	Ciliary neurotrophic factor
CRP	C-reactive protein
CSPG	Chondroitin sulphate proteoglycans
CTB	Cholera toxin β subunit
DAPI	4′,6-diamidino-2-phenylindole
dLGN	Dorsal lateral geniculate nucleus
DNase I	Deoxyribonuclease I
DPBS	Dulbecco's phosphate buffered saline
E18	Embryonic day 18
ECM	Extracellular matrix
ERG	Electroretinography or electroretinogram
GAD	Glutamate decarboxylase or glutamic acid decarboxylase
GAPDH	Glyceraldehyde 3-phosphate dehydrogenase
GCL	Ganglion cell layer
GFAP	Glial fibrillary acidic protein
Hz	Hertz
IEG	Immediate early gene
kDa	Kilodalton
LGN	Lateral geniculate nucleus
MAG	Myelin-associated glycoproteins
MAIs	Myelin-associated inhibitors
MAP2	Microtubule-associated protein 2
MECS	Maximal electroconvulsive seizures
mRNA	Messenger ribonucleic acid
mTOR	Mechanistic/mammalian target of rapamycin
Narp	Neuronal activity regulated pentraxin

Nogo	Neurite outgrowth inhibitor
NP1	Neuronal pentraxin 1
NP2	Neuronal pentraxin 2
NPR	Neuronal pentraxin receptor
NPTX1	Neuronal pentraxin 1
NPTX2	Neuronal pentraxin 2
NPTXR	Neuronal pentraxin receptor
OGD	Oxygen-glucose deprivation
OMgP	Oligodendrocyte myelin glycoprotein
ONC	Optic nerve crush
P1	Postnatal day 1
PBS	Phosphate buffered saline
PDL	Poly-D-lysine
Pen/Strep	Penicillin-streptomycin
PERG	Pattern electroretinography or electroretinogram
PFA	Paraformaldehyde
PNGase F	Peptide:N-Glycosidase F
PNS	Peripheral nervous system
PTEN	Phosphatase/tensin homolog
PTX1	Pentraxin 1
PTX2	Pentraxin 2
PTX3	Pentraxin 3
PTX4	Pentraxin 4
PVDF	Polyvinylidene fluoride
RBPMS	RNA-binding protein with multiple splicing
RGC(s)	Retinal ganglion cell(s)
RIPA	Radioimmunoprecipitation assay
SAP	Serum amyloid P component
SCI	Spinal cord injury
SOCS3	Suppressor of cytokine signaling 3
TACE	Tumor Necrosis Factor-alpha Converting Enzyme
TBI	Traumatic brain injury
Trk	Tyrosine kinase
TSG-14	TNF-inducible gene 14 protein
TTX	Tetrodotoxin
VEPs	Visual evoked potentials
WD	Wallerian Degeneration

Chapter 1: **General Introduction**

1.1 The Need for Axon Regeneration

The mammalian nervous system is one of the most intricate and enigmatic systems in the body. It is anatomically divided into two main components: the central nervous system (CNS) and the peripheral nervous system (PNS). The CNS is comprised of the brain and the spinal cord, whereas the PNS consists of motor and sensory nerve fibres as well as all the neurons outside the CNS. The CNS communicates with the rest of the body via nerves of the PNS, which carry sensory information into the CNS and motor instructions from the CNS to the rest of the body. Many researchers suggest that the visual system is a natural extension of the brain and while controversy remains regarding whether the visual system forms part of the CNS, it is clear from numerous studies that RGCs retain many of the intrinsic characteristics seen in neurons derived from the brain, including the developmentally regulated loss of axon growth ability (London et al., 2013). Traumatic CNS injuries result from physical insults that cause damage, such as in traumatic brain injury (TBI), spinal cord injury (SCI) or optic nerve injury. Traumatic injuries can result in permanent disability depending on the mode, severity and anatomical location of the injury (Shoichet et al., 2008).

Traumatic injuries contribute to morbidity and mortality in both developed as well as developing countries. The incidence and prevalence of SCI in Canada is estimated to be approximately 109 per million and 1200 per million, respectively (Noonan et al., 2012). Globally, most non-fatal cases of both TBI and SCI are due to falls and road injuries,

which means these injuries are somewhat preventable (James et al., 2019), but are highly prevalent. Traumatic CNS injuries not only cause great personal hardship for the individual, but it can have profound consequences for their families and society in general (Wyndaele and Wyndaele, 2006). Dysfunction resulting from CNS injuries is persistent and requires prolonged medical treatment and rehabilitation. Over the individual's lifetime, they will have to spend over $1 million in healthcare-associated costs (McKinley et al., 1999). Therefore, it is vital that viable therapeutic interventions that promote axon regeneration and functional recovery are developed to help alleviate the pressure on the health care system and help individuals suffering from CNS injuries.

Currently, there are no effective therapeutic strategies to promote functional recovery after CNS injury. Moreover, neurons of the adult mammalian CNS do not spontaneously regenerate their axons post-injury, unlike their PNS counterparts. Following traumatic CNS insult, the axons and dendrites of the neurons at the site of injury, that have lost their connection to their original neural pathways, degenerate, leading to neuron loss (Crair and Mason, 2016; Laha et al., 2017). The underlying pathophysiological processes are very complex and despite extensive research efforts, they are still not completely understood. Potential therapeutic interventions would need to address neuronal loss, repair of the injured pathway, target innervation and restoration of function (Benowitz and Yin, 2008).

To better understand these processes and to discover potential new therapeutic strategies, a simple and relatively accessible research model is useful. Anatomically and developmentally, the mammalian visual system is an extension of the brain. Studies

examining regeneration using the visual system have been informative and broadly applicable to other CNS regions (Fawcett, 2018). Most of the molecular pathways that have been discovered using the optic nerve crush (ONC) technique as a model of CNS injury have consistently shown promising results for regeneration in the corticospinal tract (Nathan et al., 2020). Therefore, RGCs and their axons are often used as a model in which to study the possible mechanisms associated with neuroprotection and axon regeneration in the damaged CNS.

1.2 Modeling Central Nervous System Injuries using the Visual System

1.2.1 Structural organization of the Visual System

The coordination of visual cues from the eye to the brain allows for the processing of visual information. The mammalian visual system is comprised of the eye, the optic nerve which projects through to the optic tract, and various parts of the brain such as the lateral geniculate nucleus (LGN), superior colliculus, and the visual cortex (Figure 1-1A). The eye encompasses three major tissues: the cornea, the lens and the retina (Baker et al., 2014). Briefly, visual information is transmitted as light through the cornea. The cornea is a clear, transparent outer covering of the eye and it lies directly in front of the iris and pupil. The light then passes through the lens followed by the vitreous body and finally reaches the retina (Leinonen and Tanila, 2018). The lens is a crystalline capsule-like structure involved in focusing light. The vitreous body is a large gelatinous structure that allows for the passage of light. The retina is located posteriorly and is the light-

processing structure of the eye, wherein light energy is converted to electrical impulses (Baker et al., 2014).

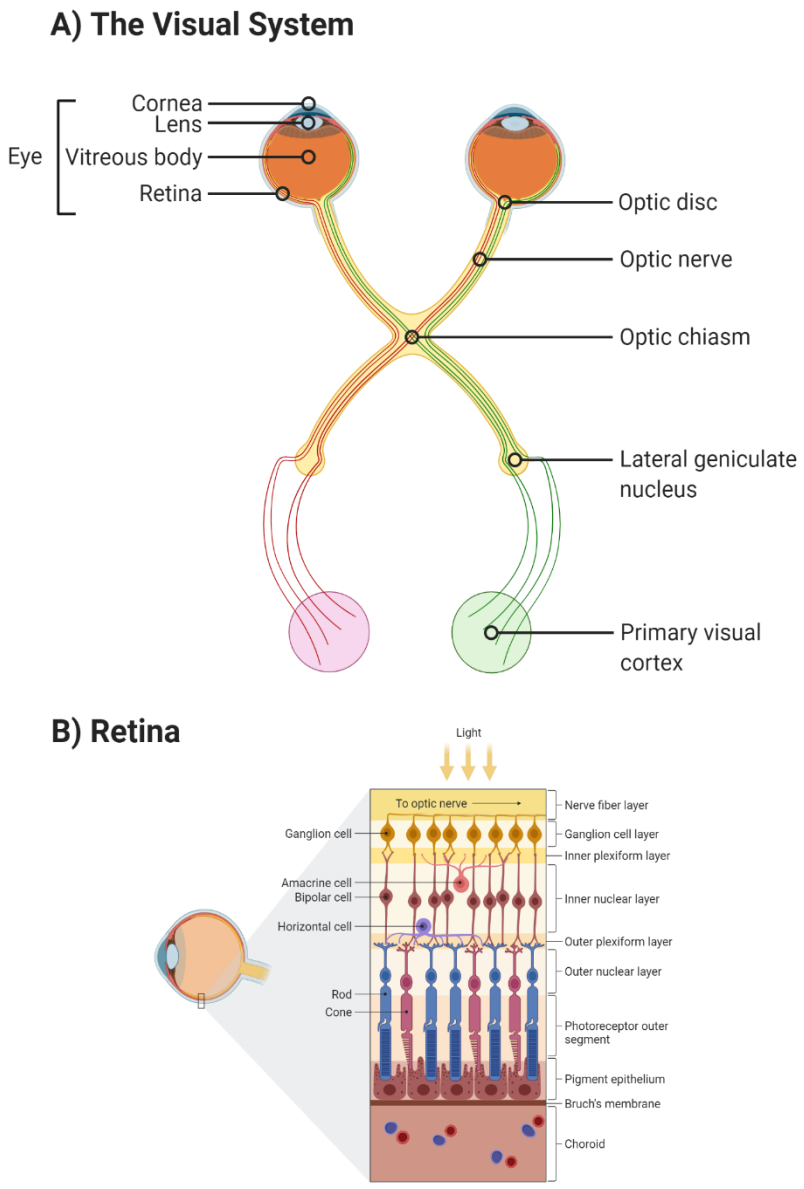

Figure 1-1: Schematic illustration of the mammalian (A) visual system and (B) retinal cell layers. (A) The visual system is comprised of the eye, the optic nerve, and various parts of the brain such as the lateral geniculate nucleus and the visual cortex. The eye is comprised of several different structure including but not limited to the cornea, lens, vitreous body, and retina. Axons of the retinal ganglion cell converge to form the optic nerve. (B) Magnification of the retina illustrating the different layers and cell composition. Bipolar cells (dark red) synapse with and transfer information between photoreceptors (blue and red) and retinal ganglion cells (yellow). Horizontal (purple) and amacrine (light red) modulate the activity of the retinal neurons. Created with BioRender.com

The mammalian retina is composed of layers of interconnecting neuron and glial cells (Figure 1-1B). The neurosensory retina is organized into three main cell layers: outer nuclear layer, inner nuclear layer, and ganglion cell layer (GCL). These layers are separated by two synaptic layers: outer and inner plexiform layers (Baker et al., 2014). There are five major types of retinal neurons: photoreceptors, bipolar cells, horizontal cells, amacrine cells and RGCs (Baker et al., 2014). There are three main types of glial cells found within the mammalian retina: Müller cells, microglial and astrocytes (Vecino et al., 2016). Rods and cones, collectively called photoreceptors, are located in the farthest layer of the retina with respect to the vitreous body while the RGCs are localized to the innermost cell layer on the vitreous side (GCL). The other cells are found between these two cell layers.

The outermost layer is known as the retinal pigment epithelium layer which is a monolayer of highly pigmented cells (Strauss, 2005). The retinal pigment epithelium is not part of the neurosensory retina, rather if forms a part of the blood-retinal barrier (BRB) functioning as a selective barrier and provides nourishment to the retinal cells (Strauss, 2005). The photoreceptor's outer segments are located within the photoreceptor layer while their soma is located within the outer nuclear layer. Photoreceptors form synaptic connections with both bipolar cells and horizontal cells in the outer plexiform layer. The cell bodies of the horizontal, bipolar and amacrine cells are located in the inner nuclear layer. The axonal processes of bipolar cells and amacrine cells make synaptic contacts onto the dendritic processes of the RGCs in the inner plexiform layer. The RGCs and displaced amacrine cell bodies are found within the GCL, while RGC axons form the nerve fibre layer (Baker et al., 2014).

The glial cells play a vital role in maintaining retinal homeostasis. The Müller cells span the retina radially and help support and maintain neuronal functions (Bringmann et al., 2006). The cell body of Müller cells are found in the INL (Baker et al., 2014). The astrocytes are located in the nerve fiber layer and are associated with the blood vessels in the inner nuclear layer. In addition to their significant role in ion homeostasis, they provide neurotrophic support and the maintenance of the BRB (Vecino et al., 2016). The microglial cells are found throughout the retina. In addition to their involvement in phagocytic functions, they also respond to specific stimuli by secreting cytokines and neurotrophic factors (Vecino et al., 2016).

As light reaches the retina, it traverses through all retinal layers before being absorbed by the photopigments in photoreceptors. Photoreceptors transduce light energy into electrical signal. The most direct pathway by which visual signal is transmitted through the retina is from the photoreceptor to the bipolar cells and then to the RGCs (London et al., 2013). Along this direct pathway, horizontal and amacrine cells, which are interneurons, modulate the electrical activity of the other neurons in the retina via lateral interactions (Leinonen and Tanila, 2018). The RGCs integrate electrical signal from the other neurons in the retina and convey visual information from the retina to the brain via the optic nerve. The axons of the RGCs run along the innermost surface of the retina towards a region termed the optic disc where they converge and exit the eye to form the optic nerve. The optic disc is also known the “blind spot” since there are no retinal cells in this region.

The optic nerve is comprised of approximately 1.2 million axons (Saadati et al, 1998). The optic nerve from both eyes cross at the optic chiasm. Around 97% of the optic nerve

axons radiate to the contralateral side of the brain in the mouse, while only 60% do so in humans (Dräger, 1974; Viczian and Zuber, 2014). Post optic chiasm, the axons are collectively called the optic tract. The optic tract projects to various areas in the brain including the LGN, which is the visual part of the thalamus, the superior colliculus, which is located at the roof of the mid-brain and helps coordinate head and eye movement, the superchiasmatic nucleus, which is in the hypothalamus and plays a role in the circadian rhythm, and the mid-brain nuclei, which plays a role in regulating the pupil size (Leinonen and Tanila, 2018). Astrocytes and oligodendrocytes closely interact with the optic nerve. As with other axons of the CNS, oligodendrocytes myelinate the optic nerve fibers. Astrocytes provide biochemical support within the optic nerve (Cooper et al., 2018) and aid in organizing the axons into bundles (Lye-Barthel et al., 2013).

Since RGCs are the only pathway by which external signals are transmitted from the retina to the brain, RGC injury or optic nerve injury directly leads to visual disturbances. Therefore, the rodent visual system has been widely used as a model system to study neuronal survival, growth, and regeneration. The structure and function of the retina is somewhat similar between rodents and primates, which facilitates translational research (Leinonen and Tanila, 2018).

1.2.2 Using the Retina and Optic nerve to study Axon Regeneration

The retina is an ideal model system to study regeneration since it shares several characteristics with the CNS, its relatively accessible for experimental manipulation and has a well-known anatomy and physiology (London et al., 2013). Developmentally, the retina, the cell layer found within the eye, extend from the diencephalon, which gives rise

to anterior forebrain structures (Baker et al., 2014; London et al., 2013). Moreover, the different components of the visual system exhibit many attributes similar to the CNS. For instance, the eye is surrounded by the BRB which resembles the CNS' blood-brain barrier (BBB) and the anterior chamber of the eye, contains anti-inflammatory and immunoregulatory factors, which resembles the cerebrospinal fluid in the brain and spinal cord (London et al., 2013). The optic nerve is myelinated by oligodendrocytes similarly to axons residing in the CNS. Finally, in response to insult, the RGCs and its axons, present the same features as the rest of the CNS – lack of spontaneous regeneration. Optic nerve injury results in the loss of RGC in addition to retrograde and anterograde degeneration, glial scar formation, myelin degradation, and the formation of a neurotoxic environment which all lead to regenerative failure (London et al., 2013). In addition to their similarities with the CNS, it is the accessibility and the structural architecture of the retina and the optic nerve that makes them a valuable model.

The eye, retina and the optic nerve can be easily experimentally manipulated. The retina is composed of relatively few and distinguishable cell types that are arranged in layers (Varadarajan and Huberman, 2018). This highly organized structural architecture allows for the examination of specific cell types and their interactions with connecting cells. Due to the anatomical location of RGCs within the retina and being outside the skull, RGCs are much more easily accessible for targeted neuronal cell body manipulation compared to other CNS structures. Exogenous factors, such as therapeutic agents, can be delivered to the retina through intravitreal injections without disturbing the BRB, making the eye readily amenable to scientific investigation (London et al., 2013).

In a SCI model, both descending motor axons and ascending sensory axons need to reconnect to their targets for full restorative function. In contrast to the complex network of connections of the spinal cord, the optic nerve arises from a single neuronal cell population, the RGCs. Spinal cord lesions affect multiple neuronal populations whereas optic nerve injury is directly connected only to the RGC population. Moreover, the optic nerve is a continuous structure that is not disrupted by interneurons (London et al., 2013). These advantageous features allow for focus on a specific population of neurons and axons upon injury. Taken together, the retina and the optic nerve are highly attractive structures of the visual system that can be manipulated and studied in *in vitro*, *ex vivo* and *in vivo* settings to better understand the molecular mechanisms underlying the pathology of CNS injury.

1.2.3 *In vitro, Ex vivo* and *In vivo* Models

A multitude of models have been used to characterize and study CNS injuries including dorsal root ganglion cultures, PNS nerve grafts and spinal cord transection animal models (Fawcett, 2018). The visual system is one of the finest model systems to study CNS injuries due to its unique position and highly organized structure (Crair and Mason, 2016). The rodent visual system serves as a valuable model for testing several cellular functions such as cell survival and axon growth via the following unique and informative scientifically manipulative tools: *in vitro* primary RGC culture, *ex vivo* retinal explants and *in vivo* optic nerve crush.

Primary RGC culture assays (Figure 1-2) are a useful tool to study the molecular and cellular mechanisms underlying axon regeneration and cell survival (Maekawa et al.,

2016). One of the major benefits of the dissociated RGC culture assay is that the neuroprotective and regeneration-inducing potential of factors or pharmacological agents and their most potent concentration can be screened in a short period of time using less animals (Romano and Hicks, 2007). Using immunostaining techniques, the number of RGCs in the wells can be counted as an indicator for cell survival (Legacy et al., 2013). The effect on neurite or axon length can be elucidated by measuring the length of β3-Tubulin or Tau-1-positive processes protruding away from the RGC soma, respectively (Legacy et al., 2013).

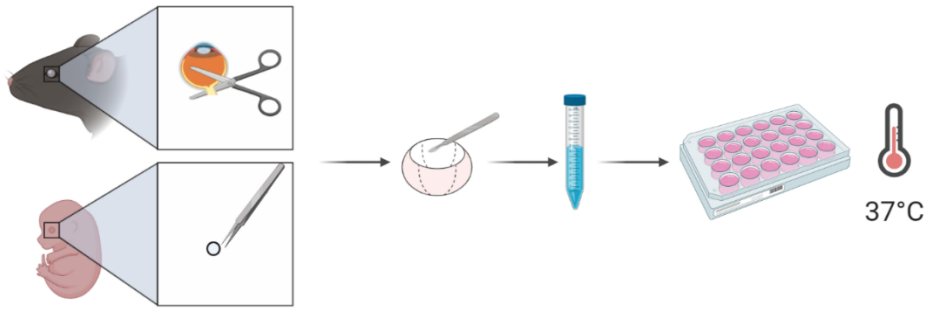

Figure 1-2: Schematic illustration of *in vitro* primary retinal ganglion cell culture method. Embryonic, postnatal, or adult mouse eyes are enucleated and dissected to obtain the optic cup. The cells are then dissociated before being plated in 24-well plates coated with poly-D-lysine and laminin. The cell culture medium contained Neurobasal A supplemented with 2% B-27, 0.3% L-glutamine and 0.5% penicillin-streptomycin. The cells are incubated at 37°C and 5% CO_2 for 3 days. Created with BioRender.com

The RGC culture assay can be used to determine RGC's intrinsic response to an exogenous factor by isolating the RGCs from their normal environment (Romano and Hicks, 2007). Since the dissociated RGCs are cultured in serum-free medium, it provides the investigator with some control over the cellular environment to address questions related to the effect of a particular chemical on the intrinsic regenerative capacity of RGCs (Maekawa et al., 2016). Furthermore, it is a useful model to elucidate the specific molecular mechanisms behind the RGC's response. However, the drawback is that RGCs usually die within several days of culture due to the lack of required neurotrophic factors.

Another drawback is that while RGCs from embryonic and early postnatal animals can be successfully cultured, it is very difficult to culture adult RGCs for an extended period of time (Romano and Hicks, 2007). Furthermore, since the retinal tissue is dissociated during the isolation procedure, it does not as closely mirror the *in vivo* environment.

The *ex vivo* retinal explants cultures (Figure 1-3) involve the isolation of intact retinae tissue (Hanea et al., 2016). Similar to *in vitro* RGC cultures, retinal explants can be used for screening studies when looking for potential therapeutic agents (Bull et al., 2011; Hanea et al., 2016; Schaeffer et al., 2020). The retinal explant system serves as an intermediate between *in vitro* dissociated RGC cultures and an *in vivo* animal model. It closely mimics the *in vivo* environment as complex neuronal connections are preserved and other functionally important non-neuronal cells of the retina are retained (Hanea et al., 2016; Murali et al., 2019; Schaeffer et al., 2020). Therefore, the cellular responses can be studied *in situ* rather than in isolation.

When the retina is removed from the eyeball during dissection, even though the cellular composition is intact, the RGC axons are damaged creating an injury model in a dish. Therefore, the neurites from RGCs can be examined to assess their outgrowth, in response to injury (Hanea et al., 2016). However, like the primary RGC cultures it is not possible to culture these explants for a long period of time (Hanea et al., 2016; Kretz et al., 2007). In addition to the increased number of animals needed to perform this technique, one of the major drawbacks of retinal explant cultures is that it is a technically advanced tool that must be mastered to allow effective reproducibility and assessment.

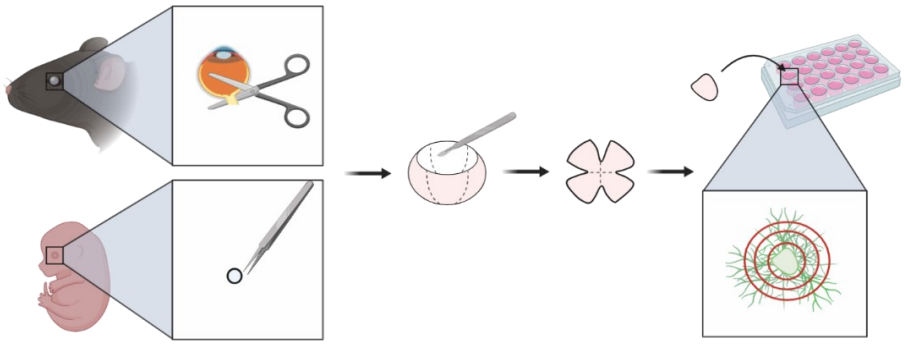

Figure 1-3: Schematic illustration of *ex vivo* retinal explant culture method.
Embryonic, postnatal, or adult mouse eyes are enucleated and dissected to obtain the optic cup. The optic cup is cut into 4-quarants and one of the quadrants is incubated per well in 24-well plates coated with poly-D-lysine and laminin. The culture medium contained Neurobasal A supplemented with 2% B-27, 0.3% L-glutamine and 0.5% penicillin-streptomycin. The explants are incubated at 37°C and 5% CO_2 for 3 days. In retinal explants the cellular architecture of the retina and the interactions between the cells are maintained. Created with BioRender.com

The *in vivo* adult mouse ONC model (Figure 1-4) is a predominantly used model to address the molecular and cellular mechanisms behind CNS axon regeneration and RGC survival post injury (Gobrecht et al., 2016; Park et al., 2008; Smith et al., 2009). In this model, a constant pressure is applied, using fine forceps, to the optic nerve at a certain distance from the optic disc. Due to the accessibility and anatomy of the eye, potential growth-stimulating factors can be administered intravitreally into the eye. These factors can readily diffuse to reach RGCs without compromising the BRB (Templeton and Geisert, 2012). The extent of regeneration can then be quantified using an anterograde or retrograde tracer. *In vivo* studies have shown that the adult RGCs can be stimulated to overcome axonal injury to extend their axons past the lesion site and to reinnervate their original targets (Lima et al., 2012).

A wide variety of growth and survival promoting factors have been identified using *in vitro*, *ex vivo* and *in vivo* models (Hanea et al., 2016; Legacy et al., 2013; Park et al., 2008; Smith et al., 2009). Current literature continues to focus on identifying new and

more effective therapeutic factors. While these results are promising, functional recovery is a necessary parameter that should also be examined to determine treatment efficacy.

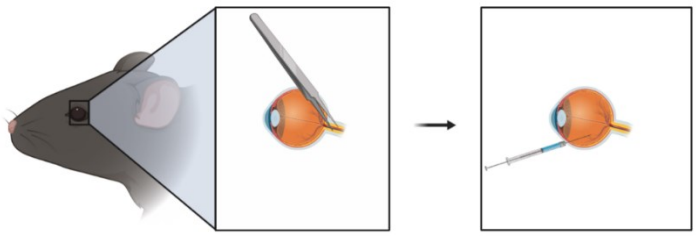

Figure 1-4: Schematic illustration of in vivo optic nerve crush method.
Adult mice are anaesthetized, and the optic nerve is exposed by making an incision on the conjunctiva and crushed at a point ~ 1 mm behind the optic disc for 10 seconds with jeweler's forceps. Immediately after the optic nerve crush, a Hamilton syringe is used to withdraw 1 µL of vitreous solution, followed immediately by an injection of 1 µL of factor of interest. Created with BioRender.com

1.2.4 Visual electrophysiology

Electroretinography or electroretinogram (ERG) and visual evoked potentials (VEPs) are two types of visual electrophysiology assessments used to assess the *in vivo* functional integrity of the visual pathway. These tests are valuable tools to non-invasively measure the electrical activity of the visual pathways in response to visual stimulation (Leinonen and Tanila, 2018). While the ERG reflects retinal activity, VEPs reflect neural activity in the visual cortex. These tests were primarily designed for patient testing but have been adapted for use in rodents and other animal models (Leinonen and Tanila, 2018).

ERG is measured via the placement of electrodes on the corneal surface of the mouse eye (Leinonen and Tanila, 2018). The corneal electrode is grounded by the insertion of needle electrodes in the tail and head of the animal. The ERG response is based on the change in electrical activity of retinal cells generated in response to a light stimulus. Two types of ERG tests are used to assess retinal function: the full-field scotopic flash ERG and the

pattern ERG (PERG). The full-field scotopic flash ERG waveform is based on the summation of electrical responses from a variety of retinal neurons and glial cells to a flash of light. Retinal cells that are radially oriented with respect to the cornea such as the photoreceptors and bipolar cells, contribute mainly to the formation of this waveform. The resulting waveform is composed of two key components that can be traced back to these distinct retinal cell types (Figure 1-5). The first negative deflection is termed the "a-wave" and is primarily driven by photoreceptor activation, whereas the positive peaks are termed "b-waves" and correspond mainly to the activation of bipolar cells (Heckenlively et al., 2006). The amplitudes and latencies of the a- and b-waves are analyzed to assess change in function.

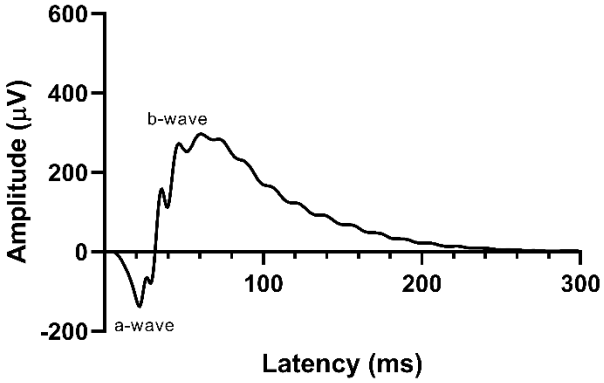

Figure 1-5: Full-field scotopic flash electroretinography waveform from a C57BL/6J mouse.
An example of a full-field scotopic flash electroretinography trace. The y-axis displays the change in amplitude in microvolts whereas the x-axis indicates the latency in milliseconds. A flash stimulus was presented to the eye at a frequency of 1 Hz and an intensity of 0.05 cd.s/m^2. For the flash stimulus, 100 traces were averaged to achieve one readout (pictured above). The negative-going-a-wave is labelled as "a" and the positive-going-b-wave is labelled as "B".

While the full-field scotopic flash ERG provides information on the functionality of most of the retinal cells, RGC's functionality, which are the cells of primary interest in ONC model, can not be assessed using this test (Liu et al., 2014). To assess RGC function, the

PERG test is used. In contrast to the flash light stimulus used in the full-field scotopic flash ERG, during PERG recording the mean luminance is kept unaltered but the eye is stimulated by alternating black and white bars or checkerboards pattern (Leinonen and Tanila, 2018). The contrast-reversing pattern stimulus causes the linear signals that produce the a- and b-waves to cancel, leaving only the non-linear signals which generate the PERG waveform (Porciatti, 2015). Non-linear signals that compose the PERG are known to depend upon the functional integrity of RGCs (Leinonen and Tanila, 2018).

The PERG waveform is composed of three key components (Figure 1-6). There is an small negative trough (termed N1), followed by a positive peak (termed P1) and a board second negative trough (termed N2) (Porciatti, 2015). The exact source of N1, P1 and N2 components in the rodent retina is debated but it is accepted that they provide information about RGC function (Porciatti, 2015). There are over 30-types of RGCs and they can be functionally divided into two major subgroups: ON- and OFF-center ganglion cells (van Wyk et al., 2009). The P1 and N2 components of the mouse PERG are believed to originate in part from the ON- and OFF-centre ganglion cells, respectively (Miura et al., 2009). The source of the N1 component has not be determined.

The PERG is the most sensitive method to test RGC function (Leinonen and Tanila, 2018). PERG responses are eliminated, while a- and b-waves of the flash ERG are still present following ONC or optic nerve injury which causes degeneration of RGC axons and subsequently, their cell bodies to degenerate (Berardi et al., 1990; Harrison et al., 1987; Porciatti, 2015; Porciatti et al., 1996). While ERGs provide information regarding

retinal cell function, the effects of ONC extend beyond the retina and affects the rest of the visual pathway.

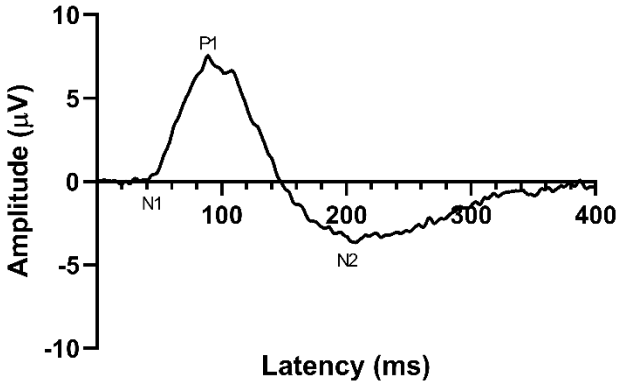

Figure 1-6: Pattern electroretinography waveform from a C57BL/6J mouse.
An example of a pattern electroretinography trace. The y-axis displays the change in amplitude in microvolts whereas the x-axis indicates the latency in milliseconds. A pattern stimulus consisting of alternating horizontal black and white bars was presented to the eye at a frequency of 0.155 cycles/degree with 2.1 reversals/second and at 100% contrast. For the pattern stimulus, 300 traces were averaged to achieve one readout (pictured above). There is an initial small negative trough (termed N1), followed by a positive peak (termed P1) and a board second negative trough (termed N2).

VEPs are used to assess whether RGC axons are capable of carrying retinal signals from the retina to the visual cortex (Chou et al., 2013). Thus, VEPs also provide information about RGC functionality. Light stimuli are introduced to the eye via corneal electrodes, but unlike in ERG, the responses are measured from the skull surface overlying the visual cortex via a subdermal electrode. Therefore, the VEP is a gross electrical potential measure from the visual cortex in response to a visual stimulus (Ridder and Nusinowitz, 2006). The VEPs test result in a waveform with three components: a small positive peak (termed P1), followed by a negative trough (termed N1) and a second positive peak (termed P2) (You et al., 2011). The exact source of the P1, N1 and P2 components of the VEP are not clearly defined (Marenna et al., 2019). The amplitude of these components and the structure of the waveforms are believed to be correlated with the extent of axonal

damage of the RGCs. The latency is believed to be reflective of the speed of signal conduction along the visual pathway and is considered an accurate measurement of optic nerve myelination (Marenna et al., 2019). A normal VEP waveform requires an intact visual pathway from the retina to the primary visual cortex, therefore, changes in VEP waveform structure is indicative of abnormalities in the visual pathway induced by ONC (Ridder and Nusinowitz, 2006).

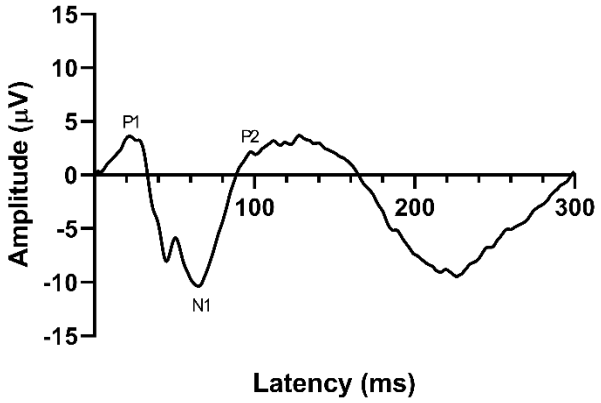

Figure 1-7: Flash Visual Evoked Potential waveform from a C57BL/6J mouse.
An example of a flash visual evoked potential trace. The y-axis displays the change in amplitude in microvolts whereas the x-axis indicates the latency in milliseconds. A flash stimulus was presented to the eye at a frequency of 1 Hz and an intensity of 0.05 cd.s/m^2. For the flash stimulus, 100 traces were averaged to achieve one readout (pictured above). There is a small positive peak (termed P1), followed by a negative trough (termed N1) and a second positive peak (termed P2).

Overall, these three assessments provide important information regarding the general health of the different components of the visual pathway. These tests provide a comprehensive view of the functional integrity of the visual pathway from the retina to the brain (Ridder and Nusinowitz, 2006). These assessments are valuable tools to assess functional recovery following therapeutic intervention post injury. When combined with histology findings, these tests will provide a thorough picture of the therapeutic potential of neuroprotective and/or regeneration-inducing factors.

1.3 Regeneration in the Mammalian Central Nervous System

1.3.1 Overview

Dramatic loss of neurons and axonal projections are hallmarks of several neurological conditions such as TBI and SCI. Indeed, unlike the neurons from the PNS and the developing mammalian CNS that have the capability to regenerate axons, those in the adult mammalian CNS do not regenerate axons spontaneously after injury (Fawcett and Verhaagen, 2018). The prevailing dogma for many years has been that the adult mammalian CNS is unable to regenerate injured or diseased axons. Santiago Ramon y Cajal, who is recognized as the father of modern neuroscience, stated: “In adult centres, the nerve paths are something fixed, ended, and immutable. Everything may die, nothing may be regenerated. It is key for the science of the future to change, if possible, this decree.” (Ramon y Cajal and May, 1928). This statement still resonates with the current challenges we face with understanding axon regeneration in the CNS - what precisely prevents axons from regenerating in the injured CNS environment?

Following several advances in the field of axon regeneration, the long-held assumption that axons in the mammalian CNS are incapable of regeneration has been recognized as no longer acceptable: CNS neurons are capable of regenerating their axons if provided with the appropriate conditions (David and Aguayo, 1981; Park et al., 2008). Accumulating evidence indicate that the lack of axon-growth ability seen within the CNS is due to the generation of a growth-inhibiting environment at the lesion site and the loss of intrinsic factors important in promoting growth in mature neurons. Multitude of key extrinsic and intrinsic factors which prevent damaged axons from re-growing and reforming functional connections post injury have been discovered, propelling us an inch

forward in solving the regeneration puzzle. Current findings suggest that regeneration can be promoted by manipulating these extrinsic and intrinsic factors.

1.3.2 Extrinsic: The hostile environment

The CNS is composed of intricate networks of neurons that relay information to one another in an environment supported by glial cells and an extracellular matrix. CNS injury disrupts these connections and causes alterations at the lesion site that impedes regeneration (Benowitz et al., 2017). The nonpermissive nature of the mature mammalian CNS in terms of regeneration is partially accredited to the inhibitory environment created by the glial scar, breakdown products of the myelin sheath of oligodendrocytes, presence of growth inhibiting molecules, insufficient support via growth factors and lack of permissive growth substate (Lee et al., 2010; Vargas and Barres, 2007).

The earliest data that indicated that CNS axons might be capable of regeneration if provided with a permissive environment was conducted by Tello and Cajal (Fawcett, 2018). They grafted a section of peripheral nerve into the brain and observed axons growing from the brain into the nerve graft. Since the source of the axons were not delineated, these findings were met with much controversy (Fawcett, 2018). A seminal study by David & Aguayo (1981) using axon tracing methods showed that CNS axons (from spinal cord) were capable of regenerating into nerve grafts (David and Aguayo, 1981). Furthermore, when the optic nerve was grafted into a peripheral nerve injury, the optic nerve tissue was nonpermissive to regeneration of PNS axons (David and Aguayo, 1981; Fawcett, 2018). These findings demonstrated that the reason for failed growth within the CNS is due to the inhibitory environment of the damaged CNS. One aspect of

regeneration research has focused on manipulating the injured CNS environment to resemble more closely that of the PNS, a region with some regenerative capacities.

Following both PNS and CNS nerve injury, the axon is divided into two segments: the proximal axon segment that remains attached to the cell body and the detached distal segment. In both segments, the rupturing of the cell membrane leads to membrane depolarization and subsequent influx of calcium ions (Ca^{2+}) activating intracellular Ca^{2+}-dependent pathways that trigger a period of acute axonal degeneration and axon retraction (Huebner and Strittmatter, 2009). Following this initial dieback, in the PNS, the proximal axon segment initiates a multi-step process of regeneration that includes the repair of the broken cytoplasmic membrane, Ca^{2+} activated proteins that mediate the disintegration and remodeling of the cytoskeletal components to support the formation of a new growth cone to promote axon extension and increase in the expression of pro-regenerative genes and inhibition of expression of pro-degenerative genes (Vargas and Barres, 2007). In the damaged adult mammalian CNS, growth cones are not formed, rather end bulbs are formed that do not permit regrowth form at the tips of the proximal segment (Ertürk et al., 2007).

On the other hand, the distal axon segment which is cut off from the cell body undergoes a process called Wallerian Degeneration (WD). During WD, the influx of Ca^{2+} leads to axon disintegration and degeneration by activating downstream pathways that for example initiate the degradation of cytoskeletal structures (Vargas and Barres, 2007). Subsequent to the fragmentation of axons, myelin that once surrounded the axon also becomes disintegrated and is released into the microenvironment before being removed.

While the WD process takes approximately 7-14 days in the PNS (George and Griffin, 1994), it takes months to years in the CNS (Vargas and Barres, 2007). The dramatic difference in the rate of WD between the PNS and CNS is attributed to the lack of mechanism for clearing CNS myelin debris (George and Griffin, 1994; Vargas and Barres, 2007).

The axons in the PNS are myelinated by Schwann cells whereas in the CNS, myelin sheaths are formed by oligodendrocytes. While Schwann cells play a crucial role in providing a permissive environment for regrowth, oligodendrocytes on the other hand have an inhibitory effect on axon regeneration (Wong et al., 2017). Following axonal degeneration in the PNS, initially Schwann cells clear up the myelin debris by breaking down myelin into smaller myelin ovoids and performing phagocytoses before recruiting macrophages (Vargas and Barres, 2007). The influx of macrophages increases the rate of myelin debris clearance. The PNS axon degeneration also increases the permeability of the blood-tissue barrier allowing blood-circulating opsonin to enter and attach to the degenerating PNS nerve, where these compounds facilitate the phagocytic myelin clearance by macrophages (Vargas and Barres, 2007). Therefore, there is rapid clearance of myelin debris in the PNS.

During CNS WD, like Schwann cells, oligodendrocytes also shed their myelin sheaths although at a slower rate (Ludwin, 1990). Furthermore, upon injury, oligodendrocytes either undergo apoptosis or enter a quiescent state (Ludwin, 1990). In comparison to Schwann cells, oligodendrocytes cannot digest myelin debris and do not recruit macrophages for myelin debris removal (Vargas and Barres, 2007). Instead of

macrophages, microglia in the CNS play a vital role in clearing myelin debris. However, they are recruited at a slower rate and they are not as efficient as macrophages. Also, the BBB permeability does not increase to the same extent as the blood-tissue barrier in the PNS, thereby limiting the influx of serum opsonins and recruitment of peripheral macrophages to the degenerating CNS axon (Vargas and Barres, 2007). Altogether, these factors contribute to the delay in the myelin debris clearance process in the CNS.

The injured myelin in both the CNS and PNS releases factors such as neurite outgrowth inhibitor (Nogo), myelin-associated glycoproteins (MAG) and oligodendrocyte myelin glycoprotein (OMgP) that are collectively known as myelin-associated inhibitors (MAIs) (BrosiusLutz and Barres, 2014). The rapid WD in the PNS results in the elimination of MAIs, whereas the slow WD in the CNS results in the prolonged presence of these inhibitory factors suggesting that slow WD creates an inhibitory environment that may be partly responsible for the regenerative failure observed in the CNS (Vargas and Barres, 2007). This suggests that triggering rapid CNS myelin clearance or removal of MAIs may enhance CNS regenerative ability. In support of this notion, multiple studies have found that removal of these molecules induced axonal regrowth in neurons. For example, in a study by Lee and colleagues (2010), axon sprouting was seen in Nogo, MAG and OMgp deficient mice (Lee et al., 2010). Alternatively, other studies have found little or no regeneration following the removal of these proteins (Zheng et al., 2003). Taken together, these findings suggest that while MAIs have a role in creating an inhibitory CNS environment following injury, they are not the only determinants of regeneration failure.

The formation of glial scar tissue by reactive astrocytes, oligodendrocytes, oligodendrocyte precursors, and microglia at the lesion site is a morphological hallmark of CNS injury (Fischer and Leibinger, 2012). This scar often develops perpendicular to the lesion site and was initially believed to act as a physical and chemical barrier to regeneration due to its dense fibrous meshwork structure and the presence of inhibitory molecules such as chondroitin sulphate proteoglycans (CSPG) (Laha et al., 2017; Yiu and He, 2006). Notably, in a 3-dimensional glial cultures, astrocytes cultures formed a barrier that prevented axonal growth from mature but not embryonic neurons while Schwann cultures were supportive to axonal growth from both the two populations (Fawcett et al., 1989). Furthermore, the digestion of CSPGs by chondroitinase, enhanced sprouting and regeneration after SCI (Fawcett, 2015). On the contrarily, other work show that the glial scar actually aids regeneration in the rodent spinal cord (Anderson et al., 2016). A study by Anderson and colleagues (2016) demonstrated that preventing astrocyte scar formation following SCI failed to promote axon regeneration. Instead they found that astrocytes and non-astrocytes at the lesion site express multiple axon-growth-supporting molecules (Anderson et al., 2016). Interestingly, prior to these findings Faulkner and colleagues (2004) found that depletion of reactive astrocytes following SCI resulted in larger inflammatory regions around the lesion site resulting in larger lesion volume and increased motor deficits (Faulkner et al., 2004). These findings were indicative of the notion that the glial scar is beneficial for the prevention of inflammatory processes from propagating to the surrounding healthy tissue. Altogether, these studies highlight the importance of the formation of the glial scar at the lesion site and indicate that it may be beneficial under certain circumstances.

Multiple studies have focused on characterizing the environmental inhibitory molecules in the adult CNS and blocking these inhibitory signals to promote axon regeneration; however, the efficacy of this approach remains controversial. Removing just the environmental influence does not appear to be enough to enhance growth ability to promote recovery suggesting the possibility of other contributing factors such as those responsible for the developmental loss of axon growth ability (Goldberg et al., 2002a). Therefore, another piece to this puzzle lies within the neuron – its intrinsic regenerative ability. Stimulating intrinsic growth potential by inhibiting negative regulators of axonal growth has been shown to induce strikingly long-distance axon regeneration after CNS injury (Park et al., 2008; Smith et al., 2009). This indicated that robust neuron-intrinsic growth mechanisms can potentially overcome the inhibitory extrinsic environment of the injured CNS (Fawcett and Verhaagen, 2018; He and Jin, 2016). Therefore, although the extrinsic environment plays a role in determining regenerative ability, the intrinsic properties of the neuron also play a critical role.

1.3.3 Intrinsic: Developmental changes in neuron's regenerative ability

Another avenue of regeneration research has focused on modifying the intrinsic environment to resemble more closely that of the developing neuron, a region with regenerative capacities. During CNS development, the presence and activation of intrinsic growth promoting signals and pathways in neurons, allow for enhanced axon growth (Benowitz, 2010; Goldberg et al., 2002a). However, this ability diminishes with age, indicating that a neuron's growth ability varies developmentally (Goldberg et al., 2002a). As development nears completion, many of the growth-promoting signals are down regulated and many in fact change their function to instead inhibit growth (Smith et

al., 2009). This shift in signal is key as it indicates the end of development and is necessary to prevent overgrowth and to prevent improper connections from being made (Li et al., 2017). However, the loss of the intrinsic growth ability creates a barrier in terms of regeneration of damaged axons.

The loss of neurons' intrinsic axon growth ability was elegantly demonstrated by Goldberg *et al.* (2002) using purified embryonic and postnatal RGC cultures (Goldberg et al., 2002b). They cultured purified embryonic day 20 (E20) and postnatal day 8 (P8) rat RGCs over three days and examined axon growth in terms of length and speed. Although initially both groups of cells extended axons to the same degree, after three days in culture, E20 RGCs extended longer axons at a faster rate (approximately 7x longer and 10x faster) in comparison to postnatal RGCs (Goldberg et al., 2002b). Even in a growth permissive environment, culture media containing trophic factors *in vitro* or transplantation of cells into a developing brain *in vivo*, the extent of regeneration among the two age groups differed, indicating that the loss of axon growth ability is intrinsic to the neuron rather than being dependent on the external environment. They further delineated that retinal maturation prompts neonatal RGCs to irreversibly switch from an axonal to dendritic growth mode (Goldberg et al., 2002b). While embryonic RGCs extend more axons than dendrites, the reverse was seen in postnatal RGCs. Therefore, cellular changes during development make the maturing mammalian CNS unable to undergo prominent axon regeneration.

Maturational changes also drastically decrease a neuron's capacity to reinnervate target tissue (Chen et al., 1995). Using explant cocultures of hamster retinae and tectum tissue,

it was demonstrated that while retinae harvested from animals aged E14 through P0 showed extensive fiber growth and re-innervation of tectal tissue, animals aged P2 and older showed little growth and re-innervation. This was also the case when the tectum was of the same age or younger, indicating that the age of target tissue does not account for the regenerative failure of the older retinal axons (Chen et al., 1995). The reason neurons lose their regenerative ability when they mature are believed to be due to intrinsic factors and genetic changes. As RGCs mature, they down regulate the expression of several growth-relating pathways such as the mammalian target of rapamycin (mTOR) pathway (Park et al., 2008). Moreover, in the CNS, pro-axon regenerative pathways are switched off after injury (Belin et al., 2015). Analysis of the change in gene expression following lesion of the adult PNS indicates that successful adult PNS regeneration is a consequence of both reactivated developmental mechanisms and newly activated injury-dependent reactions (Bosse et al., 2006).

Several studies have focused on examining the molecular mechanisms behind the discrepancy between adult and young neuron's ability to regenerate. Using various CNS injury models, such as ONC injury and SCI models, a deeper understanding of the genes, proteins, their receptor targets and the signal transduction pathways that are involved have been uncovered. Many studies have shown enhancement of axon regrowth by reactivating developmental growth pathways and/or suppressing growth-inhibiting pathways in neurons (Benowitz et al., 2017; Crair and Mason, 2016). These manipulations include but are not limited to increasing positive regulators of growth such as mTOR (Lee et al., 2014) and ciliary neurotrophic factor (CNTF) (Müller et al., 2009) and inhibiting negative regulators of growth such as phosphatase/tensin homolog (PTEN)

(Park et al., 2008) and suppressor of cytokine signaling (SOCS3) (Smith et al., 2009). In some of these studies, axons regenerated past the lesion site all the way to the optic chiasm.

When considering the clinical application of some of these candidate factors that show robust axon regeneration there are many caveats that need to be addressed. First, the induction of mTOR has to be in place before axon injury in order for regeneration to occur (Lim et al., 2016). Second, these regenerative molecules are also known to be oncogenic factors (Park et al., 2008). This means any therapeutic approach modulating PTEN and mTOR levels would need to be carefully safeguarded. Third, manipulation of these factors only induces axon regeneration to the optic chiasm and not the full distance back to the brain (Lim et al., 2016; Park et al., 2008). While the discovery of these factors has revealed possible targets for therapeutic intervention after injury, more research is still needed to uncover other therapeutic factors.

1.4 Pentraxins

1.4.1 Pentraxin Family

Pentraxins are a superfamily of phylogenetically conserved proteins characterized by their sequence homology and cyclic multimeric architecture (Agrawal et al., 2009). The members of the family are identified by an ~200 amino acid (AA) long pentraxin domain sequence that is located at the C terminal. Within the pentraxin domain, there is a conserved 8 AA-long sequence called the pentraxin family signature which is His-x-Cys-x-Ser/Thr-Trp-x-Ser, where x is any AA (Breviarios et al., 1992). Based on the length of the protein sequence, the pentraxin family is broadly grouped into two subgroups: the

short pentraxins and long pentraxins. The short pentraxins include the C-reactive protein (CRP) also known as pentraxin 1 (PTX1; Whitehead et al. 1990) and the serum amyloid P component (SAP) also known as pentraxin 2 (PTX2; Dowton and McGrew 1990). The long pentraxins include the neuronal pentraxins, pentraxin 3 also known as TNF-inducible gene 14 protein (PTX3, TSG-14; G. W. Lee, Lee, & Vilcek, 1993) and pentraxin 4 (PTX4; Martinez de la Torre et al., 2010). The neuronal pentraxins include neuronal pentraxin 1 (NP1; Schlimgen et al. 1995), neuronal pentraxin 2 (NP2; Hsu & Perin, 1995), and neuronal pentraxin receptor (NPR; Dodds et al. 1997).

Pentraxins are defined by their structural organization of five identical subunits arranged covalently in pentameric radial symmetry that may further dimerize to form decameric structures (Tsui et al., 1996). Pentraxins are able to bind to saccharides, and this lectin property is thought to be essential for their biological function (Tsui et al., 1996). Also, the pentraxin family bind to ligands in a calcium-dependent manner (Hsu and Perin, 1995; Schwalbe et al., 1992). The pentraxin family are multifunctional proteins that regulate many processes in the brain as well as in the periphery. The short pentraxins are acute-phase proteins that regulate the innate immune response and are primarily produced in the liver and transported through the blood stream to other tissues (Agrawal et al., 2009). PTX3 plays a regulatory role in inflammation in addition to its role in innate immune response (Balhara et al., 2013). PTX4's function is not well-defined (Martinez de la Torre et al., 2010).

Neuronal pentraxins have been implicated in α-amino-3-hydroxy-5-methylisoxazole-4-propionic acid (AMPA) receptor-mediated excitatory synapse assembly (Lee et al.,

2017). NP1 and NP2 are secreted glycoproteins. NP1 is mainly expressed in neurons (Omeis et al., 1996; Schlimgen et al., 1995), whereas NP2 is expressed in various tissues such as the brain, testes, liver and kidneys (Hsu and Perin, 1995; Tsui et al., 1996). NPR is a type-II transmembrane protein mostly expressed in the brain and is the only pentraxin family member anchored to the cell membrane (Dodds et al., 1997).

1.4.2 Biochemistry and Structure of NP2

Like the other pentraxin molecules, NP2 is evolutionary-conserved and has been identified in several species (Table 1). There are varying degrees of homology amongst the different protein variants. NP2 is known as apexin/p50 in guinea pig (Reid and Blobel, 1994), neuronal activity-regulated pentraxin (Narp) in rat (Tsui et al., 1996), and NPTX2 in humans (Hsu and Perin, 1995). Apexin is localized to the acrosome of mature sperm (Tsui et al., 1996). The human homologue of NP2 was identified by Hsu and Perin in 1995. They identified the protein as NPTX2 and the gene as *NPTX2*. The human NPTX2 gene is located on chromosome 7q21-q22 (Hsu and Perin, 1995). The rat homologue of NP2 was identified by Tsui and colleagues in 1996. They termed the protein as Narp and the gene as *Narp* (Tsui et al., 1996). NP2 is about 50% identical to NP1 and NPR (Tsui et al., 1996).

Table 1 Homolog of NP2

	Human	**Guinea Pig**	**Rat**
Protein	NPTX2/NPII	Apexin/p50	Narp
Homology with NPTX2		88%	94%

While the precise structure of NP2 is not yet known, key molecular groups have been identified based on the protein sequence such as 3 potential N-glycosylation sites,

putative ligand- and calcium-binding sites, and several cysteines (Tsui et al., 1996). The location of the calcium-binding sites and cysteines are homologous to other pentraxin family members (Tsui et al., 1996). The calcium-binding sites is thought to be important for the pentraxin family's ability to bind to saccharides in a calcium-dependent manner attributing to their lectin property (Tsui et al., 1996). The binding specificity of each pentraxin member is distinct from one another. For example, Narp has been shown to bind to agar but not to agarose (Tsui et al., 1996). The significance of this binding difference remains to be determined.

NP2 does not have a transmembrane domain. However, it does have a N-terminal secretory signal peptide sequence, indicative of NP2 being a secreted protein (Kirkpatrick et al., 2000; Tsui et al., 1996). The C-terminal pentraxin domain of NP2 has been shown to interact with the N-terminus of glutamatergic AMPA receptor subunits (Sia et al., 2007; Xu et al., 2003). In addition to the C-terminal domain, NP2 has a longer N-terminal that is predicted to form coiled-coils (Dodds et al., 1997; Goodman et al., 1996; O'Brien et al., 1999; Tsui et al., 1996; Xu et al., 2003). Narp encodes seven cysteines, with three in the N-terminal and four in the C-terminal (Xu et al., 2003). It has been shown that the cysteines in the coiled-coil N-terminal are important for forming intermolecular disulfide bonds during multimerization (Xu et al., 2003).

Pentraxins can multimerize forming homo- or hetero-multimers (Kirkpatrick et al., 2000; Xu et al., 2003). NP2 can be self-arranged into highly organized complexes via covalent disulfide bonds or it can form hetero-multimers with NP1 by both protein-protein and disulfide mediated interactions (Xu et al., 2003). Th exact function of this

multimerization is unclear, but the relative ratio of NP1 and NP2 in the complex is dynamically dependent upon the neuron's activity (Xu et al., 2003). It has been suggested that NP1 is constitutively expressed in neurons and upon neuron activity NP2 expression is increased, leading to the integration of NP2 protein into NP1-NP2 hetero-multimers (Xu et al., 2003). It is important to note that NP1 expression is not dynamically responsive to neuronal activity. Furthermore, although NP1 and NP2 are secreted proteins they can be tethered to the cell membrane when expressed as hetero-multimers with NPR (Kirkpatrick et al., 2000).

NPTX2 and Narp are about 430-432 amino acid in length (Hsu and Perin, 1995; Tsui et al., 1996; Xu et al., 2003). The predicted molecular weight of NP2 is ~46.2 kDa. Narp appears as a single broad protein band around ~46-60 kDa on western blots of rat brain tissues (Dodds et al., 1997; O'Brien et al., 1999; Reti and Baraban, 2000; Tsui et al., 1996; Xu et al., 2003). Treatment with endoglycosidase H results in a downward shift of the band to ~45 kDa due to the removal of N-glycans (Tsui et al., 1996; Xu et al., 2003). Under non-reducing conditions, Narp migrates as a multimer with a size > 220 kDa (Reti and Baraban, 2000; Xu et al., 2003). These observations are consistent with the fact that Narp is a glycosylated protein and that it can form cysteine-linked multimers (O'Brien et al., 1999; Xu et al., 2003).

1.4.3 Expression pattern and Function of NP2

Unlike the other neuronal pentraxins that are expressed mainly in the CNS and more specifically in neurons, NPTX2 mRNA is expressed in multiple tissues with the highest expression being in testis. More specifically, NPTX2 mRNA is expressed in the brain,

testis, pancreas, liver, skeletal muscle, and heart (Hsu and Perin, 1995). In contrast to NPTX2 mRNA, Narp mRNA expression shows a more restricted distribution; it is expressed almost exclusively in the CNS with low levels found in the testis and ovaries (Tsui et al., 1996). Similarly, Narp protein has been reported to be present in rat testes but not in other peripheral tissues (O'Brien et al., 1999). However, recently, it has been shown that Narp protein is expressed in peripheral tissue such as the liver (Kozaczek et al., 2019).

Endogenous Narp mRNA expression is developmentally regulated. In the forebrain, Narp mRNA is first detected around embryonic day 14 and its expression increases monotonically to peak levels between postnatal day 16-21, with levels remaining high throughout adulthood (Tsui et al., 1996). Using hippocampi tissue it was shown that there is low Narp protein expression at the time of birth but the levels peak at around 7 weeks of age (Xu et al., 2003). However, NP2 is not ubiquitously expressed throughout the brain. It has been noted that NP2 displays highly heterogenous pattern of expression (Reti et al., 2002a). In terms of the visual system, i*n situ hybridization* has revealed that NP2 mRNA is expressed in the GCL and the inner nuclear layer of the retina (Bjartmar et al., 2006). NP1 and NPR mRNA are also expressed in the retina, although at lower levels compared to NP2 (Bjartmar et al., 2006). NP2 protein expression in postnatal mice was evident in the GCL, inner nuclear and inner plexiform layers. NP2 protein was also found in the optic nerve. Furthermore, NP2 labels RGC axons in culture (Bjartmar et al., 2006).

NP2 is expressed primarily in excitatory neurons and does not colocalize with glutamic acid decarboxylase (GAD), which is marker for inhibitory axons (O'Brien et al., 1999;

Reti et al., 2002b), nor the glial maker, glial fibrillary acidic protein (GFAP) (Chang et al., 2018). NPTX2 protein has been localized specifically to excitatory synapses in primary neuronal cultures and in adult brain. It has been found to be present in both pre- and postsynaptic compartments (O'Brien et al., 1999; Xu et al., 2003). Narp's prominent expression in the presynaptic cell is associated with synaptic vesicles (O'Brien et al., 1999). It has been shown that Narp could accumulate at synapses either by secretion from the presynaptic terminal or by lateral diffusion on the postsynaptic dendrite (O'Brien et al., 1999).

In terms of cellular localization, Narp has been localized to the somatodendritic areas of neurons (Mariga et al., 2015; O'Brien et al., 1999) and has also been identified in axonal projections and terminals areas (Bjartmar et al., 2006; Mariga et al., 2015; O'Brien et al., 1999; Reti et al., 2002b). Mariga and colleagues (2015) found that in addition to Narp expression being enhanced in the somatodendritic compartments, Narp colocalizes with both MAP2 (dendrites) and Tau (axon) staining in cultured hippocampal neurons (Mariga et al., 2015). Whereas, Reti and colleagues (2002) found that Narp displayed minimal dendritic localization and was found prominently in axonal pathways in hippocampal slices (Reti et al., 2002b). To further support the notion that Narp is preferentially targeted to axonal projections, Bjartmar and colleagues (2006) found that NP2 colocalizes with anterograde tracing of RGC axons in the dLGN (Bjartmar et al., 2006). It has been suggested that Narp is induced by neural activity and is then rapidly transported to axon terminals where it co-assembles with NP1 (Xu et al., 2003).

NP2 was originally isolated as an immediate early gene (IEG) induced by seizures in the rat hippocampus (Tsui et al., 1996). Upon neuronal activity, NP2 expression increases in excitatory neurons (Tsui et al., 1996). Brain derived neurotrophic factor (BDNF) is also able to induce NP2 expression in the absence of neuronal activity (Mariga et al., 2015). Previous studies have shown that NP2 overexpression can increase excitatory synapse formation, while downregulation of NP2 decreases excitatory synapse formation indicating a role in synaptogenesis (O'Brien et al., 2002, 1999). Following secretion, NP2 forms heteromultimers with NP1 and binds to and clusters AMPA receptors (Xu et al., 2003). The NP1-NP2 complex can also associate with NPR, which is anchored to the membrane through its transmembrane domain (Cho et al., 2008; Dodds et al., 1997). When NPR is cleaved by Tumor Necrosis Factor-alpha Converting Enzyme (TACE), there is internalization of the neuronal pentraxin complex and the associated AMPA receptors via endocytosis (Cho et al., 2008). Collectively, these studies indicate a role of the neuronal pentraxins in AMPA receptor aggregation and internalization. NP2 has also been implicated in pathological states. For example, the expression of NP2 is reduced in human Alzheimer's disease and is correlated with cognitive decline (Hanson, 2017; Xiao et al., 2017). Recently, NP2 has been shown to have neuroprotective function against *in vitro* ischemia oxygen-glucose deprivation (OGD) induced cytotoxicity (Cai et al., 2019). The overexpression of NP2 mRNA in primary neuronal cultures showed approximately 50% protection against OGD-induced cell death (Cai et al., 2019). Although NP2 has been implicated in the above-mentioned processes, the underlying mechanism of how and to what extent NP2 impacts these processes has not be fully elucidated (Chapman et al., 2020).

1.4.4 The role of NP2 in Regeneration

NP2 has been mainly implicated in AMPA receptor clustering, however, it is important to emphasize that it may have other functions in the CNS (Chapman et al., 2020). Despite compelling evidence, the role of NP2 as a potential regeneration inducing factor is an area of research that has not be fully explored. For example, Narp has been shown to stimulate dendritic outgrowth in cortical neurons (Tsui et al., 1996). Thus, additional studies on NP2's functional role are needed to fully elucidate its role in the CNS.

Increasing neuronal activity has a neuroprotective effect and promotes axon growth. *In vivo* and *in vitro* experiments have demonstrated that electrical stimulation can enhance neuronal survival and axonal regeneration in the CNS after injury (Corredor and Goldberg, 2009; Lee and Chiao, 2016; Miyake et al., 2007). For example, it has been shown that stimulating the retina with a trans-corneal electrode increases RGC survival and protect axons from degeneration in a model of ONC *in vivo* when compared to unstimulated controls (Miyake et al., 2007; Morimoto et al., 2005). Furthermore, in another *in vivo* study, it was found that if the activity of RGCs was increased by visual stimulation in combination with the activation of mTOR, the RGC axons regenerate long distances (Lim et al., 2016). These effects have been related to the intrinsic signaling pathways which regulate axonal growth, such as neurotrophic signaling (Corredor and Goldberg, 2009). Taken together, these studies strongly support the idea that increased neural activity is an effective therapeutic strategy that is likely to promote cell survival and bring about axon RGC regeneration. However, the use of direct electrical stimulation has limited therapeutic value.

NP2 mRNA expression is rapidly induced in neurons by electrical stimulation (Tsui et al., 1996). As an IEG, NP2 is upregulated in response to synaptic activity (Tsui et al., 1996; Xu et al., 2003). Narp mRNA is dynamically regulated by physiological synaptic activity in the adult visual cortex. When tetrodotoxin (TTX), a sodium channel antagonist, was injected intravitreally to cause the blockage of the consensual pupillary light reflex, resulting in the interruption of afferent visual input, there was a rapid reduction in Narp mRNA expression in the primary visual cortex (Tsui et al., 1996). This means basal expression of Narp mRNA in dependent on natural synaptic activity. Therefore, it can be hypothesized that post ONC injury, when there is a loss of visual input, there would be a decrease in NP2 expression, indicating a need for exogenous NP2.

Mature RGCs normally fail to regenerate their axons following injury. However, they can be stimulated to promote regeneration by activating macrophages in the eye by inducing lens injury (Fischer, 2004). In an experiment comparing differences in gene profile between axotomy alone and axotomy combined with lens injury it was found that the gene expression of *Narp* declined after axotomy alone but increased above baseline after axotomy combined with lens injury. In terms of changes in RGC's Narp protein expression, Narp was undetectable 4 days post axotomy but was strongly elevated in the axotomy combined with lens injury group (Fischer, 2004). How and whether Narp contributes to the regenerative state following combined axotomy and lens injury has not been explored.

Using *ex vivo* postnatal day 1 rat cortical explants, Narp was found to promote neurite outgrowth and migration of neurons from cortical explants (Tsui et al., 1996). It is important to note that these neurites labelled positive for MAP2, which is a marker for neuronal dendrites, however Tau (neuronal axon marker) labelling was not detected. Indicating that NP2 may play a role in promoting neuronal dendritic outgrowth. In addition, it was found that ~40 ng/mL was the most effective concentration in promoting outgrowth (Tsui et al., 1996).

Taken together, these findings indicate that NP2 may play a role in axon regeneration making it an ideal candidate for inducing optic nerve regeneration. Despite these findings, current literature has yet to explore the role of NP2 in the visual system by studying the impact on neurite outgrowth *in vitro* and following optic nerve crush *in vivo*. This thesis sought to explore this avenue of research and evaluate the role of NP2 in the repair of damaged CNS neurons.

Chapter 2: **Research Objectives**

Within the broader goal of understanding the fundamental process of axon regeneration post injury by manipulating intrinsic mechanisms, the specific objective of this dissertation was to elucidate the role of NP2 in promoting RGC survival and enhancing the regenerative ability of RGCs post injury. It was hypothesized that treatment of RGCs with exogenous NP2 will promote neurite outgrowth *in vitro* and *ex vivo* and induce axon regeneration following optic nerve crush injury *in vivo*. Therefore, the studies proposed in this dissertation are intended to fill a critical void in the understanding of NP2's effect on RGCs and its' role in promoting RGC survival and axon regeneration in the optic nerve. This knowledge is critical for the development of therapies aimed at repairing the damaged central visual pathway and hold promise regarding repair following injury to the brain and spinal cord. This thesis is comprised of five major aims that were collectively pursued to address the role of NP2 in RGC survival and optic nerve regeneration. The **five major aims** of this dissertation are:

1. To determine the developmental time course of NP2 expression in mouse retina and compare the developmental changes in NP2 expression to previously established developmental decline in intrinsic growth ability of retinal ganglion cells.

   Hypothesis: I hypothesized that similar to the trend in loss of intrinsic growth ability of retinal ganglion cells, the expression of NP2 in mouse retina would decrease throughout retina development.

2. To determine the time-course and pattern of NP2 expression in the retina following optic nerve crush.

   Hypothesis: I hypothesized that the expression pattern of NP2 will remain largely unaltered, with a potential increase 1-day post optic nerve crush injury, based predominantly on the notion that NP2 is considered an early immediate gene.

3. To determine the optimal NP2 dosing paradigm for promoting cell survival and neurite growth *in vitro* and *ex vivo.*

   Hypothesis: I hypothesized that cell survival and neurite growth will be optimal with 1 nM treatment of NP2, based upon prior evidence suggesting this dose was effective in promoting dendritic growth in cortical neurons *in vitro*.

4. To determine the impact of NP2 administration on neuroprotection and axon regeneration following optic nerve crush injury *in vivo*.

   Hypothesis: I hypothesized that NP2 will promote neuroprotection and axon regeneration following optic nerve crush injury.

5. To determine the impact of NP2 administration on functional recovery post optic nerve crush injury using electroretinography.

   Hypothesis: I hypothesized that NP2 will promote functional recovery following optic nerve crush injury.

NP2 is a relatively understudied protein whose roles in axon regeneration has not been fully explored. My work will provide a framework to dissect how NP2 modulates axon regeneration of RGCs post injury. The studies pursued in this thesis took the critical step toward defining the role of NP2 in neuroprotection and axon growth, using *in vitro* RGC derived cell culture system, *ex vivo* retinal explants and *in vivo* optic nerve crush mouse

models, with critical functional assessments. Results from these experiments could lead to a new understanding of how mammalian optic nerve and its' function can be protected in response to injury. Knowledge gained from the studies in this dissertation will have direct impact on the understanding of axon regeneration and has relevance to restoration of function following injuries such as glaucoma and SCI. In the following chapters, I present two manuscripts detailing the rationale, methodology, results, and discussion exploring the five major aims of this thesis. The first manuscript focuses on screening for the optimal NP2 dosage to promote RGC survival and neurite outgrowth while the second manuscript critically explores *in vivo* effects on RGC survival and regeneration with assessment of functional outcomes.

Chapter 3: **Neuronal Pentraxin 2 promotes cell survival and enhances neurite outgrowth of retinal ganglion cells *in vitro* and ex *vivo***

3.1 Abstract

Activity-dependent signaling molecules, such as neuronal pentraxin 2 (NP2), play a significant role in neuroplasticity. However, the developmental expression pattern of NP2 in the retina and the potential regenerative effect of NP2 on mammalian retinal ganglion cells (RGCs) remain unknown. We designed experiments to investigate the developmental time course of NP2 expression in mouse retina and to determine whether NP2 had any beneficial effects on neurite outgrowth, using both an *in vitro* and *ex vivo* retinal model. Western blot analysis revealed a distinct pattern of NP2 protein expression; E18 and early postnatal retina samples showed a unique band that was not present in adult retina samples. We hypothesized that this higher molecular weight band could be due to post-translational modification of NP2. Treatment with Peptide: N-glycosidase F resulted in a lower molecular weight band that likely represents deglycosylated NP2. Given the established developmental decline in RGC neurite growth, we conducted experiments to examine the effect of NP2 treatment on neurite growth. NP2 enhanced neurite growth in both E18 and P7 retinal explants and axon growth in cultured P14 RGCs when compared to controls. Taken together, our data suggest that NP2 is a developmentally regulated neurite growth-inducing factor that could be targeted toward promoting regeneration and repair of the damaged CNS.

Keywords: Retina, RGC survival, pentraxin, neurite growth, NP2, glycosylation

3.2 Introduction

Adult mammalian central nervous system (CNS) axons generally do not regenerate, creating an obstacle for effective repair and recovery post injury. Retinal ganglion cells (RGCs) are CNS neurons whose axons carry visual signal from the eye to various parts of the brain. Many therapeutic strategies have been discovered with variable success in promoting axon regeneration. For instance, it has been shown that electrical stimulation is able to enhance RGC survival and neurite outgrowth (Corredor and Goldberg, 2009; Goldberg et al., 2002a; Lee and Chiao, 2016). Furthermore, in an *in vivo* study, it was found that if the activity of RGCs was increased by visual stimulation in combination with the activation of mTOR, the RGC axons regenerate long distances (Lim et al., 2016). Although the use of direct electrical stimulation has limited therapeutic value, these findings do suggest that increasing neural activity may hold potential in promoting regeneration.

Neuronal pentraxin 2 (NP2), in humans, referred to as NPTX2 (Hsu and Perin, 1995) and in rodents referred to as neuronal-activity-regulated pentraxin (Narp) (Tsui et al., 1996), is a secreted glycoprotein and is part of the highly conserved pentraxin family (Tsui et al., 1996). The NP2 protein has been localized to the ganglion cell layer (GCL) of early postnatal retinal tissue (Bjartmar et al., 2006) and is expressed in the brain (Tsui et al., 1996). NP2 mRNA expression is developmentally regulated and its expression is rapidly induced in neurons by electrical stimulation (Tsui et al., 1996). Furthermore, it has been reported that NP2 promotes dendritic outgrowth in postnatal day one cortical explant

(Tsui et al., 1996). Taken together, these findings indicate that NP2 might hold regeneration-inducing potential. However, this idea has not been fully explored.

The aim of this study was two-fold, first, we conducted experiments to characterize NP2 protein expression across the lifespan in mouse retina to determine whether there was a relationship between developmental changes in NP2 expression and established decline in axon regeneration ability of RGCs (Goldberg et al., 2002a). Secondly, we designed experiments to evaluate the impact of NP2 treatment on RGC neurite growth, using both an *in vitro* retinal culture system and an *ex vivo* retinal explant model. Our results showed a decline in NP2 protein expression with an increase in age. Furthermore, our data revealed that treatment with NP2 promotes neurite outgrowth in both embryonic and postnatal RGCs.

3.3 Methods

3.3.1 Animals

All experiments were conducted according to the guidelines of the Canadian Council on Animal Care (CCAC) and approved by the Carleton University Animal Care Committee. All experiments were performed on C57BL/6N wild-type female and/or male mice purchased from Charles River Laboratories (Montreal, Quebec, Canada). All animals were housed with consistent 12-hour light-dark cycle, with access to food and water *ad libitum*.

3.3.2 Western blot

Eyes from embryonic day 18 (E18), postnatal day 1 (P1), P4, P7, P14, P21 and adult mice were enucleated and used to extract protein in RIPA buffer containing phosphatase

and proteinase inhibitors (Cell Signalling). Proteins were separated by SDS-PAGE and transferred to polyvinylidene fluoride (PVDF) membranes. Primary antibodies for NPTX2 (1:250; ThermoFisher Scientific) and glyceraldehyde 3-phosphate dehydrogenase (GAPDH; 1:10 000; Cell Signalling) were used overnight. Primary antibodies were visualized with infrared dye 680/800 CW goat anti-rabbit IgG (1:10 000, LiCor Biosciences). Membrane was imaged with the Odyssey Imaging System (LI-COR; 680/800 channel). Bands were quantified by densitometry using Image Studio Lite (LI-COR) and normalized to glyceraldehyde 3-phosphate dehydrogenase (GAPDH) signal.

3.3.3 Enzymatic deglycosylation through digestion with peptide N-glycosidase F (PNGase F)

Protein extracts (40 μg) from E18 and 6-8 weeks old adult eye samples were de-glycosylated using Peptide:N-Glycosidase F (PNGase F, New England BioLabs) following manufacturer's protocol. Control samples were treated with phosphate buffered saline (PBS) and subject to same treatment as PNGase samples. Deglycosylated and control protein samples were assessed using Western Blot.

3.3.4 Dissociated retinal cell cultures

RGCs were isolated from pooled retinas from a single litter of mouse pups. Postnatal day 7 (P7) or P14 pups were anesthetized by hypothermia and euthanized by decapitation with surgical scissors. Mouse eyes were enucleated and placed in cold Dulbecco's phosphate buffered saline (DPBS) without Ca^{2+} and Mg^{2+} (Life Technologies). The retinae were removed by dissection on ice and dissociated using a papain system according to the manufacturer's protocol (Worthington Biochem, NJ. USA). Briefly, the

retinae were incubated in papain dissociation solution at 37 ℃ for 30 minutes with agitation. The cells were then triturated in papain inhibitor and deoxyribonuclease I (DNase I), followed by centrifugation. The dissociated RGCs were immediately resuspended in cell culture medium containing Neurobasal A containing 2% B-27 supplement, 0.3% L-glutamine and 0.5% penicillin-streptomycin (Pen/Strep), as previously described by our lab (Legacy et al., 2013). Dissociated retinal cells (7.5×10^3), containing retinal ganglion cells (RGCs), were plated in 24-well cell culture plates (Sarstedt) coated with 20 μg/mL poly-D-lysine (PDL) and 10 μg/mL laminin.

Retinal cultures were grown in the presence of vehicle control and 0.1, 1 or 10 nM of Recombinant Human NP2 protein (NPTX2; R&D Systems). The vehicle control was PBS. The cells were incubated for three days at 37℃ in a humidified 5% CO_2 atmosphere.

3.3.5 Immunostaining and assessment of neurite length in retinal cultures

After incubation for three days, cells were fixed in 4% paraformaldehyde (PFA) in PBS for 30 minutes before immunostaining. Briefly, cells were washed three times in PBS, permeabilized in 0.1% Triton X-100 in PBS for 5 minutes and were blocked for nonspecific protein binding with 10% normal goat serum in PBS for 1 hour at room temperature. Primary antibodies diluted in PBS were added to wells and incubated overnight at 4°C. Cells were stained with rabbit anti-RNA-binding protein with multiple splicing (RBPMS; 1:500; Millipore) and mouse anti-β3-Tubulin (1:500, New England BioLabs) or mouse anti-Tau-1 (1:500; Millipore). Staining was visualized with Alexa Fluor 555-conjugated anti-rabbit (Cell Signalling) and Alexa Fluor 488-conjugated anti-

mouse (Cell Signalling) at a dilution of 1:250 in PBS for 1 hour at room temperature followed by three PBS washes. Cells were counterstained with 4′,6-diamidino-2-phenylindole (DAPI) (1:10000, Thermo Scientific).

For RGC survival quantification, 5 fields of each cell culture well were visualized using a Zeiss Axiovert Inverted Microscope (Zeiss) equipped with a camera and collected using Infinity Analyze software (Lumenera Corporation); 3 biological replicates. The number of RGCs in each field was manually counted using ImageJ software (NIH). To determine the number of RGCs bearing neurites, the number of $RBPMS^+$ RGCs extending neurite(s) over a length greater than the diameter of the somata were counted using ImageJ software (NIH); 4 biological replicates.

For neurite or axon length quantification, the longest β3-Tubulin or Tau-1-labelled process protruding away from the cell body in each frame were measurement using ImageJ software (NIH); 4-5 biological replicates.

3.3.6 Retinal explants

An *ex vivo* retinal explant system as previously described by Hanea *et al.* was utilized to study neurite outgrowth (Hanea et al., 2016). Fresh enucleated E18 and P7 mouse eyes were obtained. Retinal explants were prepared and exposed to either vehicle control or 1 nM of Recombinant Human NP2 protein (NPTX2; R&D Systems) in cell culture media for three days. The vehicle control was PBS. The explant tissues were then fixed with 4% PFA and immunostained with anti-β3-Tubulin (1:500, New England BioLabs). Three fluorescent images were taken per explant; four E18 explants and five P7 explants per treatment were analyzed. Using ImageJ software (NIH), the number of fibers that grew

from the edge of the explant was quantified at different lengths. Manual counts were verified using Neurite-J, an Image-J plug-in (Torres-Espín et al., 2014).

3.3.7 Statistical analysis

Statistical analysis was performed using GraphPad Prism (version 6.0). One-way analysis of variance (ANOVA) or student's t-test was used to compare the difference between experimental groups. Significant findings were followed up using Bonferroni's posthoc test. For explant data repeated measures ANOVA was performed. In all analyses, a *p*-value of < 0.05 was considered significant. All data are presented as mean ± standard error of the mean (SEM).

3.4 Results/Discussion

3.4.1 NP2 protein is expressed in the developing and adult mouse retina

NP2 is widely expressed in different regions of the developing and adult brain (Dodds et al., 1997; Hsu and Perin, 1995; Schlimgen et al., 1995; Tsui et al., 1996). Previously, *in situ* hybridization and immunohistochemistry was used to show the presence of NP2 in early postnatal mouse retina (Bjartmar et al., 2006). We were interested in utilizing a quantitative approach towards evaluating NP2 protein expression in embryonic, postnatal, and adult retinae. For this, we conducted Western Blot assay on homogenized tissue from E18, P1, P4, P7, P14, P21 and adult mouse retina. The predicted molecular weight of monomeric NP2 is 46.2 kDa (Tsui et al., 1996), but there is ample evidence supporting post-translational modification of the protein (Tsui et al., 1996; Xu et al., 2003).

Immunoblot of whole retina extract under reducing conditions revealed bands at ~52 (double band), ~62 and ~72 kDa with varying levels of expression depending on age (Figure 3-1A). The ~52 kDa bands were present at all ages at comparable levels (Figure 3-1B; $F(3,17) = 0.8195$, $p > 0.05$). Additionally, we observed a band at ~62 kDa that progressively diminished with development. Beyond P7, the level of expression of the ~62 kDa band was significantly decreased compared to embryonic samples (Figure 3-1C; $F(3,17) = 7.042$, $p < 0.01$). Similarly, protein extract from E18 up to P7 showed a unique band at ~72 kDa that was barely detectable in adult retina samples (Figure 3-1A). Determination of the relative abundance by densitometry revealed that the level of expression of the ~72 kDa NP2 were greater in the embryonic samples but progressively diminished with increase in age (Figure 3-1D; $F(3,17) = 16.64$, $p < 0.0001$). E18 samples showed the highest level of expression compared to P7, P14 and adult samples. Beyond P7, the NP2 expression was scarce. When all bands were quantified together, the maximal NP2 expression peaked at P7 before declining (*data not shown*). Under reducing conditions, the recombinant Human Neuronal Pentraxin 2 Protein (NPTX2; R&D Systems) appeared as a doublet at ~52 kDa (Figure S3-1). Overall, the expression of NP2 appears to be developmentally regulated, with adult retina expressing the lowest levels of NP2 relative to the other age groups.

In the dorsal lateral geniculate nucleus (dLGN), NP2 protein expression (immunohistochemistry) peaks over the first week of postnatal development and remains elevated at least until P14 (Bjartmar et al., 2006). These findings are partly similar to our western blot analysis results, where we found that overall NP2 expression peaked at P7. Conversely, in hippocampi tissue, it has been shown that there is low expression of NP2

protein at the time of birth but that the levels increase and peak at around 5 weeks of age (Xu et al., 2003) before stabilizing. Variation in tissue type and assessment time may account partially for the difference in the findings. Late postnatal assessment points by Xu *et al.* included P11, P23, P33 and P66, whereas we assessed expression at P14, P21 and then adult (~P56) (Xu et al., 2003). It is possible that we missed the P33 peak, however, it is less likely since at P21 and adult there were similar expression level of NP2.

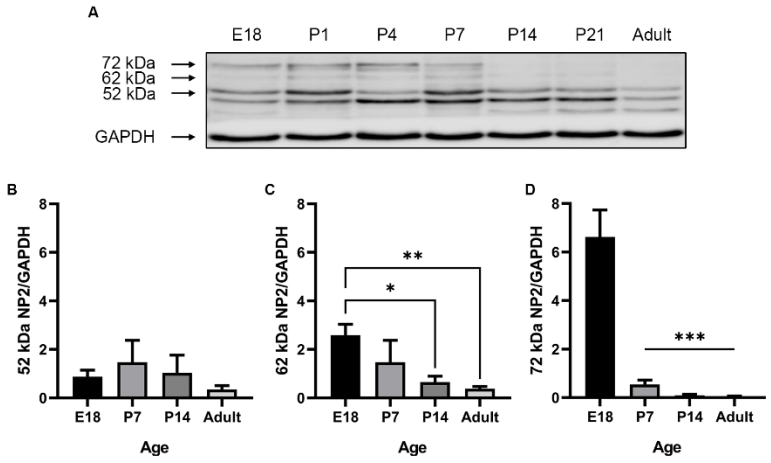

Figure 3-1: Developmental decline in NP2 protein expression in retina.
(A) Representative western blot analyses depicting the protein level of NP2 in E18, P1, P4, P7, P14, P21 and adult mouse retina protein extracts. (B-D) Histogram representing NP2 levels normalized to GAPDH. Bars represent mean ± SEM of 4-8 biological replicates per group. Statistical analyses were carried out by using one-way ANOVA followed by Bonferroni's post hoc test, *$p < 0.05$, **$p < 0.01$, ***$p < 0.001$.

On Western blots, NP2 protein has been found as a single band around ~46-60 kDa depending on the tissue type (Dodds et al., 1997; O'Brien et al., 1999; Reti and Baraban, 2000; Tsui et al., 1996; Xu et al., 2003). For example, in rat brain and spinal neurons, NP2 has been recognized at ~56 kDa and ~58 kDa, respectively (O'Brien et al., 1999). So there seems to be some variability in the migration of NP2 on wester blot assays

depending on tissue type. Close examination of western blot images of cultured hippocampus neurons by Margia *et al.* showed a diffused double band, although the kDa was not specified (Mariga et al., 2015). Furthermore, since the recombinant NP2 appeared as a doublet at ~52 kDa, we believe the ~52 kDa bands we saw are similar to previously reported NP2.

This is the first study, to quantify developmental NP2 protein expression in the retina, where we have identified 3 unique band sets. The identification of the higher bands was unexpected. We do not think these bands reflect multimerization of NP2 since O'Brien *et al.* demonstrated that the NP2 multimeric complex dissociates when incubated with β-mercaptoethanol (O'Brien et al., 1999). Furthermore, NP2 multimers migrate at > 220 kDa (Reti and Baraban, 2000; Xu et al., 2003). To our knowledge, this is the first study to identify and report unique bands at ~62 and 72 kDa. Though studies have examined the developmental changes in NP2 protein expression postnatally, we are the first to look at NP2 protein expression at the embryonic stage. This might explain why these bands have not be previously reported.

Critical analysis of published western blots further supports the notion that tissue difference might explain the multiple bands we saw in our study. Xu *et al.* examined NP2 protein expression in the cerebella, hippocampi, cortices and brainstems (Xu et al., 2003). First, they did not detect NP2 in cerebellum, indicating difference in NP2 expression depending on tissue area. Second, and most interestingly, NP2 appeared as multiple bands (3 bands) in the brainstem while as a single band in the hippocampus and cortex. Unfortunately, the authors did not provide the kDa of these bands nor investigate this

difference. It is important to note that most of the western blot analysis of NP2 developmental expression has been performed using hippocampus tissue (Tsui et al., 1996). Collectively, these lines of evidence indicate that there are 3 NP2 variants in the retina, and that their expression is developmentally regulated.

3.4.2 Decline in N-glycosylated NP2 protein expression with retinal development

We were interested in characterizing the nature of the observed NP2 bands and postulated that the ~62 and ~72 kDa bands could be N-glycosylated forms of NP2. NP2 is known to have three potential N-glycosylation sites based on its primary amino acid sequence (Tsui et al., 1996). Previous work by others has demonstrated that NP2 undergoes post-translational glycosylation events (Tsui et al., 1996; Xu et al., 2003). Protein glycosylation events can be recognized using endoglycosidases (Berry et al., 2013). In previous studies, treatment with endoglycosidase H resulted in a downward shift of NP2 band from ~58 kDa to ~44 kDa due to the removal of N-glycans (Tsui et al., 1996; Xu et al., 2003).

To determine whether the unique bands we observed at ~62 and ~72 kDa were due to N-glycosylation of NP2, E18 mouse retina protein extracts were treated with peptide-*N*-Glycosidase F (PNGase F), a type of glycosidase that can remove N-linked glycans. The change in protein migration after enzymatic deglycosylation, using PNGase F treatment, of E18 retina samples is shown in Figure 3-2A. After treatment with PNGase F, there was a slight downward shift in the ~72 kDa band and a relative decrease in the level of the ~62 kDa band, which we believe is likely an indication of glycan removal. The increase in expression of the ~52 kDa band in the E18 samples following PNGase F treatment,

indicated that ~52 kDa band is likely representative of the deglycosylated NP2 protein. PNGase F treatment of adult retinae samples showed no change in protein migration (*data not shown*). Therefore, we can infer that embryonic and early postnatal retinas highly express glycosylated NP2, while late postnatal and adult retinae express the deglycosylated form of NP2. These results suggest that the expression of the glycosylated form of NP2 is developmentally regulated.

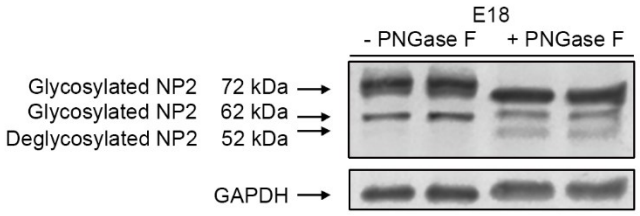

Figure 3-2: Decline in N-glycosylated NP2 protein expression with retinal development. Representative western blot analyses of the expression of N-glycosylated (~72 kDa ~62 kDa) and non-glycosylated (~52 kDa) NP2 in retinal protein extracts from E18 mouse. Samples were treated with peptide N-glycosidase F (PNGase F) or phosphate buffered saline (control) according to manufacturer's protocol prior to SDS-Page separation.

Although, these results are informative in terms of the presence of N-glycan, we do have to point out that treatment with PNGase F did not result in the full removal of neither the ~72 nor ~62 kDa bands. One possibility is that the N-glycan is tightly linked so that we were not able to remove it. It would be worthwhile to repeat these experiments with a different endoglycosidase, such as endoglycosidase H. As discussed, the multiple bands of NP2 are likely to be due in part to differential glycosylation, however there may be other possibilities. Neuronal pentraxin receptor also appears as multiple bands, and it has been hypothesized that in addition to glycosylation events, it could be due to alternative initiation sites (Dodds et al., 1997). This possibility could be extended to NP2. Additional

biochemical experiments are necessary to fully elucidate if the different NP2 variants are due to the use of alternative initiation sites or other post-translational modifications.

Overall, there is less NP2 protein expressed in postnatal and adult retina in general, suggesting a developmentally regulated decline in NP2 expression. The physiological significance of the amount of NP2 in the retina with age is unknown. We hypothesized that the level of NP2 may influence the developmental decline in neurite outgrowth. Embryonic CNS tissues show a greater regenerative ability compared to postnatal and adult CNS neurons (Goldberg et al., 2002a).

3.4.3 NP2 promotes survival and neurite outgrowth of P7 retinal cultures

It has been previously reported that the regeneration ability of P7 RGCs is diminished but not completely lost (Goldberg et al., 2002b). Also, since NP2 levels start to decline at P7 (although not significantly different from E18), we used P7 retinal cultures to determine whether NP2 treatment can promote cell survival and enhance the intrinsic neurite growth ability of RGCs *in vitro*. Given the decrease in NP2 expression with age, we hypothesized that exogenous NP2 would promote cell survival and neurite formation and growth of RGCs. Therefore, retinal cultures were incubated with increasing concentrations of NP2 protein (vehicle control, 0.1, 1 and 10 nM), based on previously published effective doses (Tsui et al., 1996).

Cell survival is an important factor that can influence a cell's ability to regenerate. An unhealthy cell will not be able to regrow its connections as effectively. Therefore, before considering the potential regenerative effects of NP2 on neurite outgrowth, the impact on cell survival must be considered. RNA-binding protein with multiple splicing (RBPMS)

is a reliable, selective somatic marker of RGCs and was used to assess the number of RGC in culture. Our results revealed that NP2 had a beneficial effect on cell survival; 1 nM NP2 treated cells showed significantly more cells surviving compared to vehicle control (Figure 3-3A; $F(3,8) = 4.336$, $p < 0.05$). The other NP2 concentrations showed similar level of survival of RGCs to vehicle control. This indicates that 1 nM NP2 may be an optimal dose to promote the strongest response of RGC survival in P7 RGC cultures.

Next, we evaluated the number of RGC bearing neurites. There was approximately a 100% increase in the number of $RBPMS^+$ RGC bearing $\beta3\text{-Tubulin}^+$ neurites in the 1 nM NP2 treatment group compared to the other treatment groups (Figure 3-3B and D; $F(3,12) = 32.02$, $p < 0.0001$). Increasing the concentration of NP2 beyond 1 nM resulted in a decrease in the number of $RBPMS^+$ RGC bearing neurites to levels comparable to vehicle control. In the vehicle control, 17% of the RGCs had neurites, while treatment with 1 nM NP2 increased the percent of RGCs bearing neurites to 39% ($p < 0.0001$). These results suggest that NP2 is neuroprotective and promotes RGC neurite growth initiation.

Treatment with 1 nM NP2 also significantly increased the length of $\beta3\text{-Tubulin}^+$ neurites compared to the control group. In the vehicle control RGC cultures, the average longest neurite length after three days was 205.10 ± 12.61 μm, whereas 1 nM NP2-treated RGC cultures had an average longest neurite length of up to 272.50 ± 9.35 μm (Figure 3-3C; $F(3,12) = 9.113$, $p < 0.01$). Lower (0.1 nM) and higher (10 nM) concentrations of NP2 were not as effective at inducing neurite growth compared to 1 nM NP2. Representative images for the length of $\beta3\text{-Tubulin}^+$ neurites in the NP2-treated and control retinal

cultures are shown in Figure 3-3E. These results suggest that NP2 is a potent RGC neuritogenic factor.

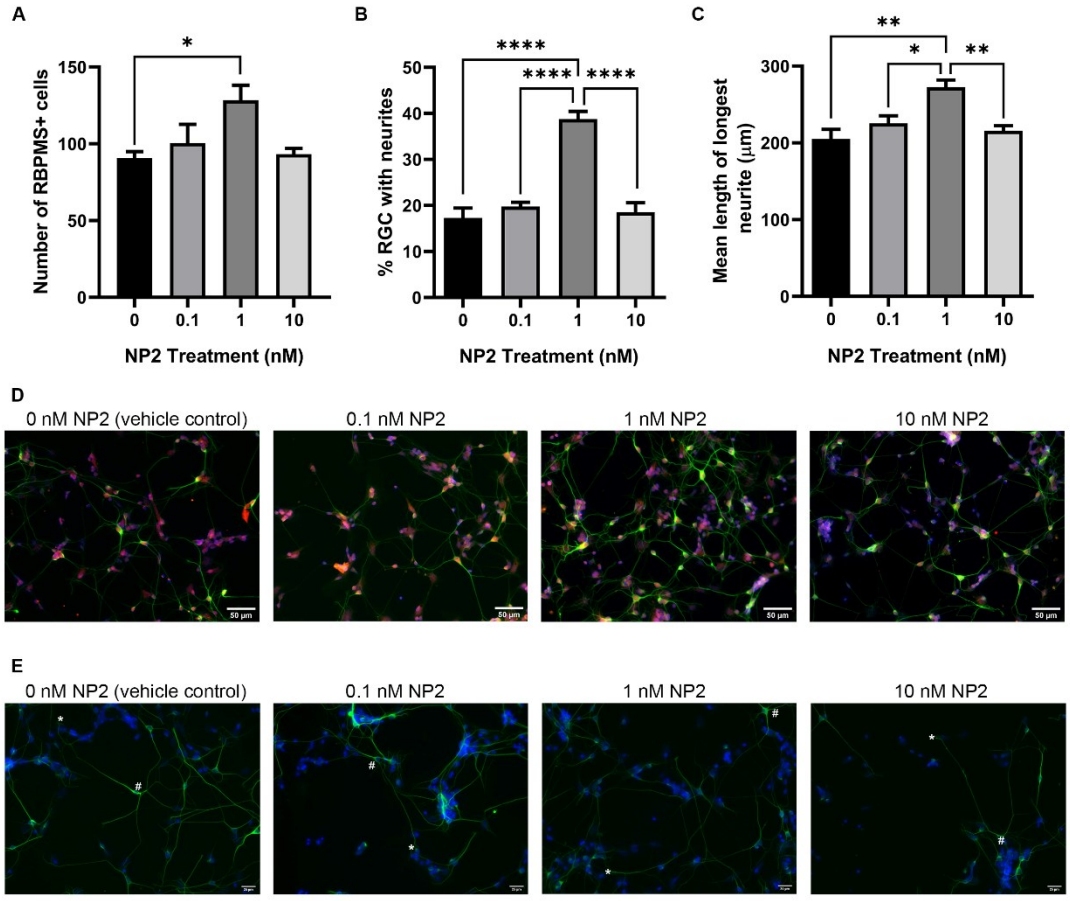

Figure 3-3: NP2 promotes survival and neurite outgrowth in P7 retinal cultures.
(A) Quantification of the number of surviving RBPMS-positive cells following NP2 treatment. (B) Quantification of the percentage of RBPMS$^+$ RGC bearing β3-Tubulin$^+$ neurites following NP2 treatment. (C) Quantification of mean length of longest β3-Tubulin$^+$ neurite following NP2 treatment. Bars represent mean ± SEM of 3-4 biological replicates per group. Statistical analyses were carried out by using one-way ANOVA followed by Bonferroni's post hoc test, *$p < 0.05$, **$p < 0.01$, ****$p < 0.0001$. (D) Representative immunofluorescence images of RBPMS$^+$ RGC (red) with β3-Tubulin$^+$ neurites (green) counterstained with DAPI$^+$ nuclei (blue). Scale bar = 50 μm. (E) Representative immunofluorescence images of NP2-induced neurites. The neurites were visualized by immunodetection of β3-Tubulin (green). Extensive neurite growth was observed in 1 nM NP2-treated RGCs, whereas control-treated RGCs show minimal neurite growth. #, cell somata; *, neurite terminal. Scale bar = 25 μm. RBPMS = RNA-binding protein wth multiple splicing; DAPI = 4′,6-diamidino-2-phenylindole.

3.4.4 NP2 promotes axon growth of P14 retinal cultures

Given that previous research has shown a developmental decline in RGC axon growth ability (Goldberg et al., 2002), we investigated whether NP2 had an impact on older RGCs: P14 and adult developmental stages. Similar to adults, at P14 we had seen low levels of the ~62 and ~72 NP2 bands. Based on the optimal dosage defined in the P7 culture system, we focused on 1 nM NP2, as it was the most effective dose in promoting cell survival and neurite outgrowth *in vitro*. To answer the question of whether the regenerating processes are dendrites or axons, we used Tau-1 antibody, which is a specific axon marker. Due to cell survival issues, we were not able to obtain meaningful data on the impact of NP2 on adult cultures.

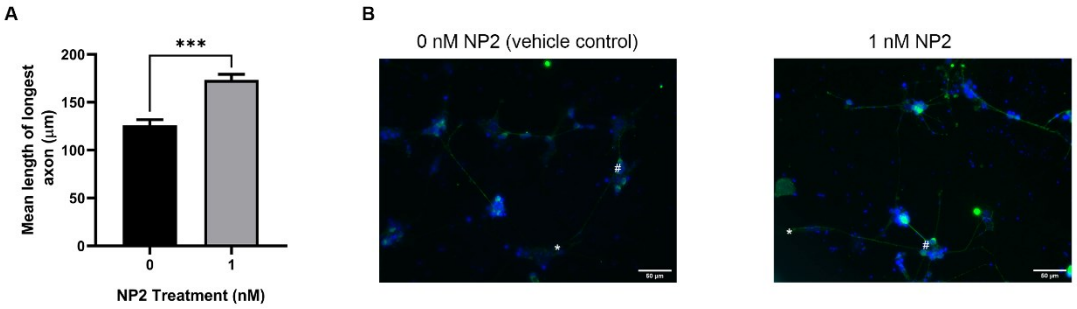

Figure 3-4: NP2 promotes axon growth in P14 retinal cultures.
(A) Quantification of mean length of longest Tau-1+ axon following NP2 treatment. Bars represent mean ± SEM of 5 biological replicates per group. Statistical analyses were carried out by using student's t-test, ***p < 0.001. (B) Representative immunofluorescence images of NP2-induced axons. The axons were visualized by immunodetection of Tau-1 (green) counterstained with DAPI+ nuclei (blue). #, cell somata; *, neurite terminal. Scale bar = 50 µm. DAPI = 4′,6-diamidino-2-phenylindole.

In P14 cultures, treatment with 1 nM NP2 moderately increased the length of Tau-1^{+} axons compared to the control group. In the vehicle control retinal cultures, the average longest axon length after three days was 125.9 µm, whereas 1 nM NP2-treated retinal cultures had an average longest neurite length of up to 173.5 µm (Figure 3-5A; p <

0.001). Representative images for the length of Tau-1^{+} axons in the NP2-treated and control retinal cultures are shown in Figure 3-5B. These results suggest that NP2 treatment promotes axonal outgrowth at a developmental stage at which growth is known to be diminished. This study also demonstrates that NP2 can promote axonal outgrowth and is not limited to dendritic outgrowth only. Previous studies using cortical neurons suggested that NP2 might play a role in promoting neuronal dendritic outgrowth since in culture the neurites labelled positive for MAP2, which is marker for dendrites and not Tau, which is a marker for axons (Tsui et al., 1996). Here it is shown that the P14 neurites label positive for Tau indicating that NP2 can promote axonal outgrowth. While *in vitro* RGC culture system is a powerful model to quickly examine the effects of a therapeutic agent, these results indicate the response of RGCs in isolation from their neighboring cells. Therefore, an *ex vivo* retinal explant system was used to see if these responses could be replicated.

3.4.5 NP2 promote neurite outgrowth of E18 and P7 retinal explants.

Given the increase in neurite growth of P7 and P14 RGCs *in vitro*, we asked if NP2 could also promote neurite growth *ex vivo*. To address this question, we used a previously characterized retinal explant system (Hanea et al., 2016). *Ex vivo* cultures are an ideal model system since they more closely resemble the *in vivo* system compared to *in vitro* cell culture models. We used this method to investigate the effect of NP2 on RGC neurite outgrowth in E18, P7, P14 and adult retinal explants. Due to technical issues, we were not able to obtain meaningful data on the impact of NP2 on P14 and adult retinal tissue. Experimental design and schematic of *ex vivo* retinal explant model is shown in Figure 3-5A and 3B, respectively.

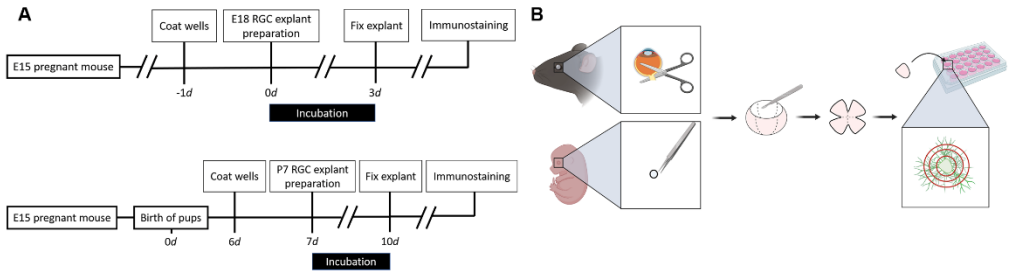

Figure 3-5: NP2 promote neurite outgrowth in E18 and P7 retinal explants.
(A) Experimental design and (B) schematic of ex *vivo* retinal explant model. Retinal explants were prepared from freshly enucleated E18 and P7 mouse eyes. After a 3-day incubation period at 37°C and 5% CO_2, explants were fixed in 4% paraformaldehyde followed by immunostaining.

Based on the optimal dosage defined in the RGC culture system, we focused on 1 nM NP2, as it was the most effective dose in promoting cell survival and neurite outgrowth *in vitro*. Growing neurites were visualized with β3-Tubulin staining, in which neurites appeared emerging from the edge of the retinal explants. Many neurites from NP2-treated E18 explants were able to grow greater than 800 µm from the edge of the explant (Figure 3-7A; $F(11,66) = 9.538$, $p < 0.0001$). We observed baseline growth in the control (vehicle treated) explants from E18 retina and an enhancement in the numbers and length of neurites extending from the explant when it was treated with 1 nM NP2 (Figure 3-6B). Compared to the control, 1 nM NP2 also stimulated neurite outgrowth in explants prepared from P7 mouse retinae. Like E18 explants, many neurites from the P7 explants were able to grow from the edge of the explant when exposed to 1 nM NP2 (Figure 3-7C; $F(11, 88) = 82.34$, $p < 0.0001$). We did not observe growing neurites extending from the edge of the P7 control (vehicle treated) retinal explants (Figures 3-7D). As mentioned above, we attempted P14 and adult explant experiments, however, the explants did not adhere consistently to the substate to allow effective analysis of the growth, therefore, we were not able to evaluate these samples.

Overall, we noticed that E18 RGC extended neurites further than P7 RGCs, however P7 RGCs extended more neurites than E18 RGCs. The difference in neurite length between the two age groups is expected since it has been established that there is an intrinsic decline in axon regenerative ability with age (Goldberg et al., 2002). A similar trend in terms of difference in age was also seen in our *in vitro* RGC cultures, where P7 RGCs exhibited greater neurite outgrowth in comparison to P14 RGCs. This indicates that although NP2 can enhance neurite outgrowth in both population of cells, it does so to different extent.

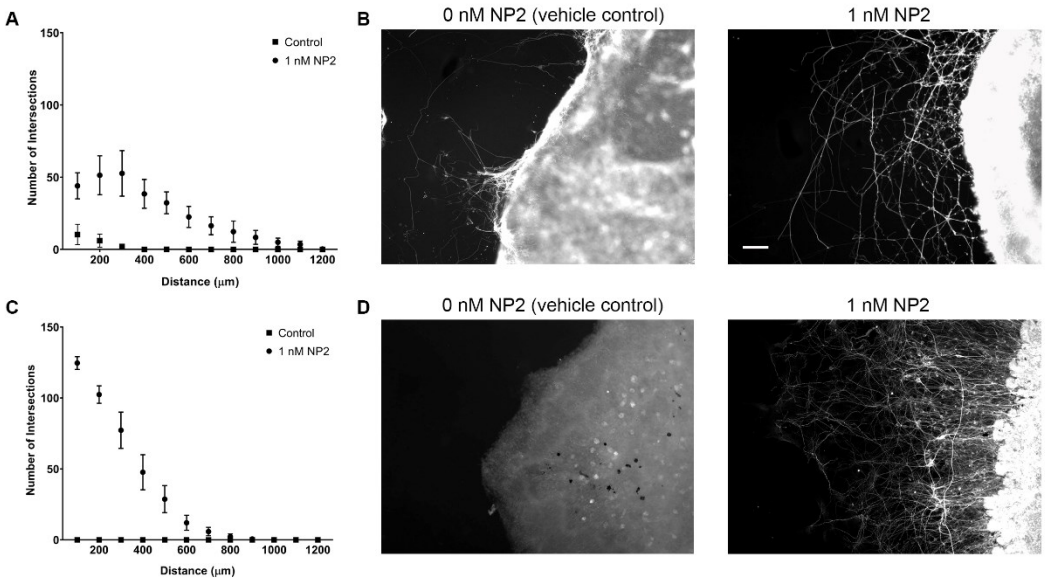

Figure 3-6: NP2 promote neurite outgrowth in E18 and P7 retinal explants.
(A) Quantification of the number of neurite intersections against the distance from the explant body of E18 retinal explants. (B) Representative immunofluorescence images of β3-Tubulin^{+} neurite emerging from vehicle control and 1 nM NP2 treated E18 retinal explants. (C) Quantification of the number of neurite intersections against the distance from the explant body of P7 retinal explants. (D) Representative immunofluorescence images of β3-Tubulin^{+} neurite emerging from vehicle control and 1 nM NP2 treated P7 retinal explants. Points represent mean ± SEM of 4-5 biological replicates per group. Scale bar = 100 μm.

The present study clearly shows that NP2 is sufficient to promote neurite outgrowth in E18, P7 and P14 RGCs. The exact mechanism of NP2-induced neurite outgrowth is not known. It has been reported that neurite outgrowth can be promoted by increasing neural

activity of RGCs by electrical stimulation both *in vitro* and in mouse retinal explant models (Goldberg et al., 2002a; Lee and Chiao, 2016). Based on this concept, it was found that when RGC neural activity was modulated using blue light stimulation for 1 hour, there was enhanced neurite outgrowth of postnatal explants after five days *in vitro* via facilitation by gap junctions that spread neural activity across the whole retina (Lin and Chiao, 2019). Although, the extent of neurite outgrowth (~200 μm) was not as robust as what we saw in our studies. NP2 mRNA expression is rapidly induced in neurons by electrical stimulation (Tsui et al., 1996). It is possible that NP2-induced neurite growth works through similar mechanism as electrical stimulation. It is postulated that active neurons would survive and extend neurites or axons better than less active neurons.

It has been demonstrated that increased neural activity is able to promote RGC axon growth via the recruitment of neurotrophic signalling (Corredor and Goldberg, 2009). NP2 can be transcriptionally upregulated through the BDNF-TrkB signaling mechanisms (Mariga et al., 2015). In another study, electrical stimulation at high frequency was found to increase neural activity and subsequently increase the rapid release of BDNF in the dorsal root ganglia (Lever et al., 2001). It is possible that NP2 is promoting neurite outgrowth in a similar mechanism involving BDNF. As such, one of the limitations of this study is that the molecular mechanisms of NP2-mediated RGC survival and neurite outgrowth was not examined and warrants further investigation. Future studies could explore this avenue of research.

3.5 Conclusion

In the present study, we found that there was a decline in NP2 protein expression in mouse retinal tissue with increase in age. Further assessment revealed that the decline in expression was specific to the glycosylated form of NP2. We have shown that NP2 is neuroprotective and enhanced the number of RGCs with neurites. Furthermore, we have shown that NP2 treatment promotes neurite and axon growth in both embryonic and postnatal retinal tissue above and beyond the normal intrinsic growth ability. NP2 is a potential axon-inducing factor that could be used to promote regeneration of CNS neurons. Future research will evaluate the potential physiological impact of NP2 administration, using a well-established optic nerve crush injury model.

3.6 Supplemental Figure

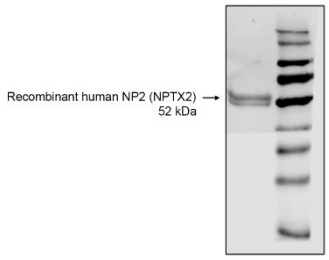

S 3-1: Western blot of recombinant human neuronal pentraxin 2 protein.
Under reducing conditions, the recombinant human neuronal pentraxin 2 protein (NPTX2; R&D Systems) appeared as a doublet at ~52 kDa.

Chapter 4: **Neuronal Pentraxin 2 promotes cell survival following optic nerve crush**

4.1 Abstract

Axons in the adult mammalian CNS fail to spontaneously regenerate after injury. The molecular complexities surrounding axon regeneration in the adult CNS can be attributed to both the inhibitory extracellular environment and the intrinsic characteristics of adult neurons that are not inherently permissive to regeneration by default. Neuronal pentraxin 2 (NP2) has been shown to promote survival and neurite outgrowth of embryonic and postnatal retinal ganglion cells (RGCs) *in vitro*. We therefore investigated whether NP2 can promote regeneration and/or survival of adult RGCs *in vivo*. We used the well-defined optic nerve crush (ONC) injury model, and intravitreal injections were used to deliver NP2 or saline to the RGC within the retina. The structural and functional response of the RGCs and optic nerve were examined. Our findings demonstrated that NP2 promotes RGC survival following ONC injury up to at least 4-weeks post crush. However, NP2 was not sufficient to promote axon regeneration when measured at four weeks post-injury. Furthermore, NP2 did not promote functional recovery. This study highlights the importance of monitoring visual function when investigating potential regeneration-inducing factors since structural outcomes may not directly correlate with functional outcome.

Keywords: retinal ganglion cell; NP2; neuronal survival; optic nerve crush; electroretinography; visual evoked potentials

4.2 Introduction

The lack of spontaneous regeneration in the adult central nervous system (CNS) in a major hurdle that limits recovery post CNS injury. This inability to regenerate has been postulated to be the result of both the inhibitory extrinsic environment of the CNS and diminished intrinsic growth ability of mature CNS neurons (Crair and Mason, 2016). Previous work has reported limited axon regeneration when extrinsic inhibitory molecules present within the CNS microenvironment were repressed (Dergham et al., 2002; Kim et al., 2003; Lee et al., 2010; Zheng et al., 2003). There has been vast interest in characterizing and stimulating the intrinsic growth ability of mature CNS neurons post-injury (Cai et al., 2001; Kaplan et al., 2015; Park et al., 2008; Smith et al., 2009). Much effort has been deployed to discover possible therapeutic interventions, however, the efficacy of these mechanisms in promoting functional recovery remains controversial.

The retinal ganglion cells (RGC) are the only neuronal type to relay visual information from the retina to the brain through the optic nerve. The mouse optic nerve crush (ONC) injury lesions RGC axons and leads to optic nerve degeneration and subsequent RGC loss. Due to its reproducibility, this model has been widely used to investigate mechanisms underlying neuroprotection, axonal injury-induced RGC death and axon regeneration (Park et al., 2008; Smith et al., 2009; Surguchov et al., 2018). This model has been vital towards the advancement of understanding the molecular mechanisms underlying CNS repair. Many factors have been shown to promote RGC survival and/or long-distance structural regeneration post ONC (Cai et al., 2001; Kaplan et al., 2015; Park et al., 2008; Smith et al., 2009). However, the functional aspect of RGC survival and long-distance regeneration has been rarely explored. Monitoring RGC and optic nerve

function via electroretinography (ERG) and visual evoked potentials (VEPs) is an important aspect of this study. ERG and VEPs are a useful tool to assess retinal function noninvasively (Porciatti, 2015; Ridder and Nusinowitz, 2006). An ERG records response of retinal cells to visual stimuli. Similarly, VEPs are the measure of electrical signals generated by the visual cortex in response to visual stimulation.

There are currently no effective treatments for cell loss and promotion of axon regeneration following CNS injury, therefore novel therapeutics to prevent RGC death or promote axonal regeneration are a priority. Neuronal pentraxin 2 (NP2) is a secreted polypeptide and is part of the highly conserved multifunctional pentraxin family (Tsui et al., 1996). Previous work suggests that NP2 has the potential to promote dendritic outgrowth in embryonic cortical explants (Tsui et al., 1996). We have shown that NP2 enhances neurite growth in both embryonic and postnatal retinal tissue *in vitro* and *ex vivo*. This led us to ask whether NP2 would promote functional axon regeneration *in vivo* under physiological conditions. It is important to fill this void in knowledge in order to better understand the potential role of NP2 in promoting functional neural repair.

The aim of this study was two-fold. First, using an established *in vivo* ONC model, we evaluated the impact of NP2 administration on RGC survival and axon regeneration. Second, we evaluated the impact of NP2 administration on RGC and optic nerve function post-ONC using electrophysiological measurements of visual-induced activity in the retina and brain by ERG and VEP analysis, respectively. Our results demonstrate that exogenous administration of NP2 promotes RGC survival but does not improve functional recovery.

4.3 Methods

4.3.1 Animals

All experiments were conducted according to the guidelines of the Canadian Council on Animal Care (CCAC) and approved by the Carleton University Animal Care Committee. All experiments except for the functional analysis experiments were performed on C57BL/6N wild-type male mice purchased from Charles River Laboratories (Montreal, Quebec, Canada). Functional Analysis experiments were additionally approved by the University of Ottawa Animal Care and Veterinary Service and were performed on C57BL/6J wild-type male mice purchased from Jackson Laboratories (Bar Harbor, Maine). All animals were housed with consistent 12-hour light-dark cycle, with access to food and water *ad libitum*.

4.3.2 Optic nerve crush surgery and intravitreal injection

All animals were randomly assigned to experimental groups. Adult mice were anaesthetized with isoflurane (inhaled; 1-5%) and given 4 mg/kg slow-release Meloxicam analgesic, according to the guidelines of the Canadian Council on Animal Care (CCAC).

The ONC surgeries were performed as previously described with minor modifications (Park et al., 2008; Smith et al., 2009). Briefly, the optic nerve was exposed by making a small incision in the left eye in the superior posterior area of the conjunctiva and crushed at a point ~1 mm behind the optic disc for 10 seconds with jeweler's forceps (Dumont #5; Fine Science Tools). Care was taken to not damage the nearby retinal blood vessels or blood supply that could potentially cause retinal ischemia. For animals receiving intravitreal injections, immediately following the ONC, a Hamilton syringe was used to

withdraw 1 µl of the vitreous humor, followed immediately by the injection of 1 µl of either the vehicle control (saline) or 1 nM recombinant human Neuronal Pentraxin 2 Protein (NPTX2; R&D Systems) into the vitreous chamber. The injection needle was angled to avoid hitting the lens. A total of 5 treatment groups were used: ONC group (ONC only), ONC+saline group (saline injection immediately following ONC; vehicle control group), ONC+NP2 group (1 nM NP2 injection immediately following ONC), saline group (saline injection only) and NP2 group (1 nM NP2 injection only).

The optic nerves were anterogradely labelled with cholera toxin β subunit (CTB) by injecting 1 µl of a 1 mg/mL CTB solution into the vitreous chamber of the left eye. CTB injections were performed 3-4 days prior to tissue collection. Animals were sacrificed by CO_2 asphyxiation. Eye and optic nerve tissues were harvested for both histological and Western blot analyses.

4.3.3 Anesthesia for electrophysiology

Animals were anesthetized with a Ketamine-medetomidine cocktail (50-75 mg/kg and 0.5-1.0 mg/kg IP, respectively) and given subcutaneous saline for hydration. Following electroretinography, the anesthetic was reversed using antipamezole (0.1-1.0 mg/kg), 1 hour post induction of anesthesia. The animals were left to recover on heating pads before returning them to the animal facility.

4.3.4 Visual electrophysiology

Mouse functional testing was performed by Dr. Pamela Lagali (Tsilfidis Lab) via electroretinography and visual evoked potential recordings (Espion, Diagnosys). Briefly,

mice (5-8/ experimental group) were dark adapted overnight and tested the following morning under dim red light. The pupils were dilated with 1% tropicamide (Mydriacyl, Alcon) and 2.5% phenylephrine hydrochloride (Mydfrin, Alcon), and a topical corneal anesthetic, 0.5% proparacaine HCL (Alcain, Alcon), was applied prior to testing. Throughout testing, the animals were kept on a heated surface to maintain body temperature. Ag/AgCl contact lens type electrodes were placed on corneas simultaneously, with a drop of lubricating eye gel (Systane, Alcon) to maintain corneal hydration and contact. A reference electrode was placed in the mouth and a needle ground was placed subcutaneously into the tail. A second needle electrode was inserted subcutaneously beneath the scalp near the visual cortex as the active VEP electrode.

A flash stimulus was presented to the eyes at a frequency of 1 Hz and an intensity of 0.05 $cd.s/m^2$ to elicit a-waves, b-waves, and VEPs. For the flash stimulus, 100 traces were averaged to achieve one readout per eye. A pattern stimulus consisting of alternating horizontal black and white bars presented at a frequency of 0.155 cycles/degree with 2.1 reversals/second and at 100% contrast was used to generate pattern ERGs. For pattern stimulus, 300 traces were averaged to achieve one readout per eye.

The electrophysiology tests were performed two days prior to ONC surgery (baseline values) and then again four days before sacrifice (post-crush values). Post-crush values were normalized to baseline values to account for intra-animal differences. Fundus imaging (Micron III, Phoenix Technology Group) was performed to visually inspect the eyes of each animal both pre- and post-surgery to detect surgical damage as well as to follow morphological changes to the retina during experiments.

4.3.5 Visual electrophysiology analysis

For full-field scotopic flash ERG, the first negative trough in the waveform was designated as the a-wave and the third positive peak as the b-wave. The a-wave amplitudes were measured from the baseline to the negative a-wave trough while the b-wave amplitudes were measured from the a-wave trough to the positive peak of the b-wave. For PERG, the small negative trough was designated as N1, the maximum positive peak as P1, and the broad negative trough as N2. P1 was typically around 100 milliseconds. P1 was measured from N1 trough to the positive peak of P1. N2 was measured from the positive peak of P1 to the negative trough of N2. For the single stimulus VEP, the peak before the dip was designated as P1, the lowest negative trough as N1 and the peak before leveling off as P2. N1 was measured from the positive peak of P1 to the negative trough of N1. P2 was measured from the negative trough of N1 to the positive peak of P2. For all recordings, we normalized the post-intervention values to their respective baseline values to minimize the variation inherent in electrophysiological recordings in live animals.

4.3.6 Western blot for quantifying NP2 expression post ONC

ONC was performed, as described above, without intravitreal injections of saline or NP2. Eyes from mice were enucleated 1-, 3-, 7- and 14-days post crush (3-4 mice/timepoint) and used to extract protein in RIPA buffer containing phosphatase and proteinase inhibitors (Cell Signalling). Proteins were separated by SDS-PAGE and transferred to PVDF membranes. Primary antibodies for NPTX2 (1:250; ThermoFisher Scientific) and glyceraldehyde 3-phosphate dehydrogenase (GAPDH; 1:10 000; Cell Signalling) were used overnight. Primary antibodies were visualized with infrared dye 680/800 CW goat

anti-rabbit IgG (1:10 000, LiCor Biosciences). Membrane was imaged with the Odyssey Imaging System (LI-COR; 680/800 channel). Bands were quantified by densitometry using Image Studio Lite (LI-COR) and normalized to glyceraldehyde 3-phosphate dehydrogenase (GAPDH) signal.

4.3.7 *In Vivo* retinal ganglion cell survival analysis, using retinal wholemounts

The eyes were enucleated and fixed in 4% paraformaldehyde (PFA) and stored in a series of sucrose solutions with ascending concentration (10% and 20%) at 4°C. The eyes were submerged in 1X PBS and dissected using micro-scissors and micro-forceps under a dissection microscope. The dissected retinae were cut into a four-leaf clover shape and washed with 1% Triton X-100 solution three times, every 15 minutes, to remove any remaining vitreous matter and to permeabilize tissues. The retinas were stained with guinea pig anti-RNA-binding protein with multiple splicing (RBPMS) antibody (1:250, Phosphosolutions), diluted in a 1% Triton X-100 solution in 24-well plates (Sarstedt) at 4°C for 3 days. The samples were then washed with 1X PBS three times for 15 minutes, and then incubated with anti-guinea pig IgG conjugated to AlexaFluor 488 (1:200, Invitrogen), diluted in 1% Triton X-100 solution, for 2 hours at 4°C. This was followed by three washes with 1X PBS for 15 minutes and staining with 4′,6-diamidino-2-phenylindole (DAPI; 1:10 000; Thermo Scientific) overnight to label cell nuclei.

To quantify RGC survival for each retina (3-4 mice/experimental group), three random square (400 × 400 μm^2 per microscope field) areas of each quadrant (superior, inferior,

temporal and nasal) were imaged by using a confocal microscope (LSM 800, Zeiss) at 20X magnification. The number of RGCs per field was manually counted.

4.3.8 Axonal cryosection

The optic nerves were extracted and fixed in 4% PFA for 48 hours. They were then placed into 10% sucrose for 24 hours and then transferred to 20% sucrose and stored at 4°C until cryosection preparation. After embedding in Optimal Cutting Temperature compound, the samples were frozen on dry ice and cryosectioned. The sections were collected on glass slides (14 μm for longitudinal axonal sections).

Slides containing optic nerve sections were washed three times with 1X PBS before applying DAPI (1:10 000, Thermo Scientific) to label cell nuclei. Images of the sample areas around the ONC sites were captured by Zeiss Axio Imager Upright Microscope (Zeiss) at 20X magnification.

4.3.9 Statistical analysis

Statistical analysis was performed using GraphPad Prism (version 6.0). One-way analysis of variance (ANOVA) was used to compare the differences between the experimental groups. Significant findings were followed up using Bonferroni's posthoc test. In all analyses, a p-value of ≤ 0.05 was considered significant. All data are presented as mean ± standard error of the mean (SEM).

4.4 Results/Discussion

4.4.1 NP2 expression is altered following optic nerve crush

We had previously found that NP2 protein expression is developmentally regulated in the mouse retina. We had identified three different variants of this protein in the retina corresponding to a double band around ~52 kDa, a single band at ~62 kDa and another single band at ~72 kDa. The predicted molecular weight of monomeric NP2 is 46.2 kDa (Tsui et al., 1996), but there is ample evidence supporting post-translational modification of the protein (Tsui et al., 1996; Xu et al., 2003). As such we found that ~62 kDa and ~72 kDa bands may represent glycosylated versions of NP2. Both the ~62 kDa and 72 kDa bands were selectively expressed in E18 and early postnatal samples (up to P7), while their expression was diminished in late postnatal and adult samples. These findings lead us to ask whether NP2 protein expression would differ following ONC. To investigate the endogenous expression of NP2 in response to ONC, NP2 protein expression levels were measured 1, 3 7 and 14-days after ONC using western blot assays (Figure 4-1A). The western blot analyses revealed that NP2 is expressed in the retina post ONC and that the time course of its expression changes following ONC. Post ONC, a double band at ~52 kDa and a faint single band at ~72 kDa were visible (Figure 4-1B).

The expression of the ~52 kDa double band varied across the time points (Figure 4-1C; $F(4,13) = 8.6670$, $p < 0.01$). Overall, at 1-, 7- and 14-days post crush, the expression of the ~52 kDa variant relative to GAPDH was decreased compared to the non-injured animals. The decrease was statistically significant at both 7- and 14-days post crush ($p < 0.05$). At 3-days post crush the expression of the ~52 kDa variant was comparable to the non-injured animals. The expression of the protein at 3-days post crush was also statistically

significantly higher than at the other post-crush time points.

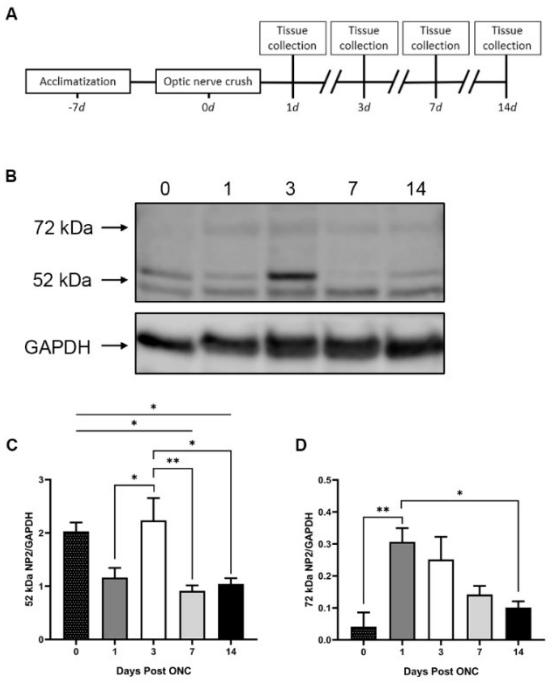

Figure 4-1: NP2 expression is altered following optic nerve crush.
(A) Timeline of tissue collection post optic nerve crush. Experimental animals were euthanized 1-, 3-, 7- and 14-days post crush. Day 0 represents animals that were not subjected to optic nerve crush. (B) Representative western blot image depicting the protein level of NP2 following no crush and 1-, 3-, 7- and 14-days post crush in adult mouse retinal protein extracts. GAPDH was used as the loading control. (C-D) Histogram representing NP2 levels normalized to GAPDH. Bars represent mean ± SEM of 3-4 biological replicates per group. Statistical analyses were carried out by using one-way ANOVA followed by Bonferroni's post hoc test, *$p < 0.05$, **$p < 0.01$. GAPDH: glyceraldehyde-3-phosphate dehydrogenase.

Even though the ~72 kDa band was barely detectable in non-crushed adult samples, the ~72 kDa NP2 isoform was significantly upregulated on day 1 after ONC (Figure 4-1D; $F(4, 3) = 7.073$; $p < 0.01$). Then, there was a gradual decrease in the ~72 kDa NP2 isoform expression over time. By 14-days post ONC there was a decrease in its expression by two-thirds compared to 1-day post crush ($p < 0.05$). It is important to note that the ~72 kDa isoform was expressed at much lower levels than the ~52 kDa isoforms. Considering our evidence that the ~72 kDa variant/isoform was only expressed in E18

and early postnatal samples, the upregulation of this variant of NP2 in response to ONC was quite interesting.

In a study by Fischer and colleagues, NP2 mRNA was shown to decline following axotomy alone but increase above baseline after axotomy combined with lens injury (Fischer, 2004). Although mature RGCs normally fail to regenerate axons through the injury site, they show regenerative potential following combined axotomy and lens injury (Fischer, 2004). Furthermore, using immunocytochemistry, it was found that NP2 protein expression was undetectable 4 days after axotomy but was strongly enhanced in RGCs after axotomy plus lens injury (Fischer, 2004). The possible role of elevated NP2 protein expression in the context of increased regenerative potential following combined axotomy and lens injury was not explored. We are the first to document the time course change of NP2 protein expression in the retina following ONC. Since the expression of the ~52 kDa variant decreased over time post ONC, we hypothesized that increasing NP2 expression through exogenous administration may aid in RGC survival or regeneration post ONC.

4.4.2 NP2 promotes RGC survival *in vivo* after optic nerve crush

Survival of RGCs after ONC is vital for any attempt to promote regeneration and eventually retore visual function. We had previously found that 1 nM NP2 can promote cell survival *in vitro*. We were interested in determining whether NP2 can promote RGC survival post insult *in vivo* under physiological conditions. To answer this question, we determined RGC survival after ONC and intravitreal administration of either 1 nM NP2 or saline by retinal whole-mount immunohistochemistry using RNA-binding protein with

multiple splicing (RBPMS) which is a reliable and selective somatic marker of RGCs. Two weeks after ONC, there was a significant decrease in the number of RGCs in all experimental groups (Figure 4-2A and C; $F(3, 12) = 142.3$; $p < 0.0001$). As expected, ONC injury led to a substantial reduction in the number of RBPMS-positive RGCs. The number of RGCs declined significantly by approximately 75% in the ONC and ONC+saline retinas compared to the intact uninjured retinas ($p < 0.0001$). This coincides with other published studies which indicate that there is a marked progressive loss of RGCs following ONC (Agudo et al., 2008; Li et al., 2020; Liu et al., 2014; Villegas-Pérez et al., 1993). There was no significant difference in RGC survival between ONC and ONC+saline mice, indicating that the intravitreal injection procedure does not further affect RGC survival.

Delivery of NP2 to the retina at the time of ONC significantly increased the number of RBPMS-positive RGCs, compared to injured eyes injected with or without saline ($p < 0.0001$). The magnitude of the percent difference in cell survival between the ONC and ONC+NP2 groups was nearly 300%. In comparison to the uninjured group, 70% of the RGCs in the ONC+NP2 survived. These results suggest that 1 nM NP2 treatment may be neuroprotective post ONC.

The progressive decrease in the number of RGCs was still evident 4-weeks after ONC (Figure 4-2B and D; $F(2,7) = 2015$, $p < 0.0001$). By 4-weeks, there was a dramatic decrease in the number of RGCs in the ONC and ONC+saline groups. This indicates that with time there was further decline in RGC survival. These findings are in agreement with other published studies which indicate that at 4 weeks post ONC, only 8-9% RGCs

remain (Li et al., 2020; Liu et al., 2014). NP2 injection post ONC was still neuroprotective at the four-week timepoint. There was a statistically significant increase in the number of surviving RGCs with NP2 treatment compared to ONC or ONC+saline treatment ($p < 0.0001$). These results further illustrate that 1 nM NP2 treatment may be neuroprotective post ONC.

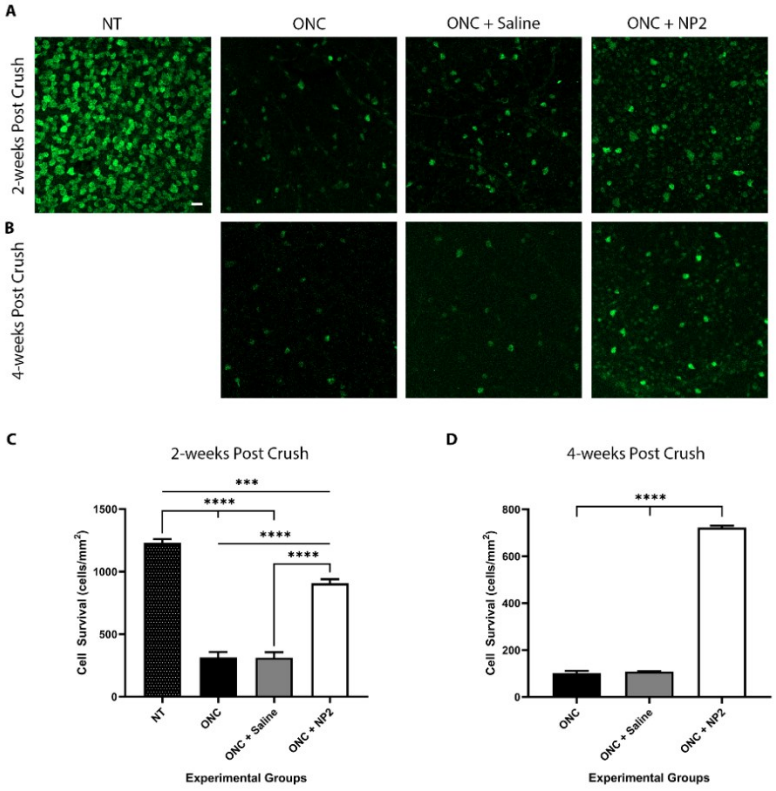

Figure 4-2: NP2 administration promotes adult RGC survival post ONC injury.
(A, B) Retinal wholemounts were double labeled with DAPI and anti-RBPMS antibody, 2- and 4-weeks post crush. The ganglion cell layer is shown in the confocal images. (C, D) Density of RBPMS-positive cells (cells per mm^2) 2- and 4-weeks post crush. Bars represent mean ± SEM from 3-4 animals per experimental group. Statistical analyses were carried out by using one-way ANOVA followed by Bonferroni's post hoc test, *** $p < 0.001$, **** $p \leq 0.0001$. Scale bar = 20 µm. NT = no treatment (uninjured group).

Taken together, these results suggests that the 1 nM NP2 treatment was able to promote RGC survival following ONC injury up to at least 4-weeks post crush. Our findings are further supported by an *in vitro* study, in which NP2 had neuroprotective function against *in vitro* ischemia oxygen-glucose deprivation (OGD) induced cytotoxicity (Cai et al.,

2019). The overexpression of NP2 mRNA in primary neuronal cultures showed approximately 50% protection against OGD-induced cell death (Cai et al., 2019). Although preservation of the ganglion cell bodies is an important aspect of protection, it is also necessary to test whether the neurons were merely saved from cell death or if they are functional as well.

4.4.3 NP2 does not enhance functional recovery after optic nerve crush

Several neuroprotective agents have been identified as possible candidates for therapeutic intervention following ONC based on histological findings (Legacy et al., 2013; Smith et al., 2009). Less is known about protection of RGC function. Surviving RGCs may not be functional. Given that 1 nM NP2 was protective of the number of RGC that survived both *in vitro* and *in vivo* post ONC, this led us to ask whether these cells were functional. Therefore, we used electroretinography to measure retinal function before and following ONC and intravitreal administration of either 1 nM NP2 or saline (Figure 4-3).

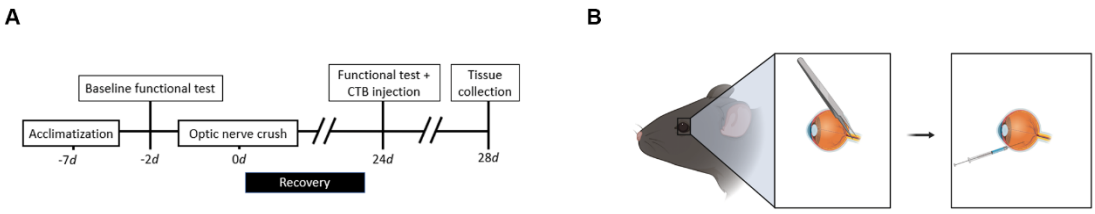

Figure 4-3: *In vivo* functional analysis experimental design.
(A) Timeline for in vivo functional analysis experiment. Functional analysis was performed before and after optic nerve crush injury. (B) Schematic of the optic nerve crush procedure.

A total of 5 treatment groups were used: ONC group (ONC only), ONC+saline group (saline injection immediately following ONC; vehicle control group), ONC+NP2 group (1 nM NP2 injection immediately following ONC), saline group (saline injection only)

and NP2 group (1 nM NP2 injection only). The right eye of the saline injection group served as the no treatment group.

A series of *in vivo* visual function tests were used to assess retinal and optic nerve function. The scotopic full-field flash ERG amplitudes and latencies were measured to assess outer retinal function. This test generates a waveform with two components: a negative a-wave and a positive b-wave, which correspond to photoreceptor and inner retina (mainly bipolar cell) function, respectively (Heckenlively et al., 2006). This test is critical to determine whether the ONC surgery or the intravitreal injection procedures affect cells other than the RGCs. Since RGCs are downstream of multiple cell types, the proper function of the upstream retinal cells is key to delineating the effects of ONC surgery and/or intravitreal injection procedure on RGC specifically.

To establish a baseline, scotopic full-field flash ERG was recorded before any intervention. Figure 4-4A shows the ERG waveforms for each experimental group before (baseline) and 4-weeks following intervention. The red lines show the bassline records acquired before ONC and/or intravitreal injection, and the black and grey lines show responses 4-weeks after the surgical intervention. Analysis of the waveforms indicated that the outer retina function was not affected by the surgical procedure nor the treatment interventions. Neither the a-wave (Figure 4-4B; $F(5,37) = 2.201$, $p > 0.05$) nor b-wave (Figure 4-4D; $F(5,37) = 1.291$, $p > 0.05$) peak amplitudes were statistically different between the experimental groups 4-weeks post ONC. Similarly, there were no statistical differences between the experimental groups in terms of the a-wave (Figure 4-4C; $F(5,37) = 0.0828$; $p > 0.05$) and b-wave (Figure 4-4E; $F(5,37) = 0.1282$; $p > 0.05$)

latencies. This suggests that the function of the photoreceptor and bipolar cells are maintained under these experimental manipulations. This also means that any changes observed in RGC function and optic nerve function is not due to impairment of upstream neuronal signaling through the retina (Liu et al., 2014).

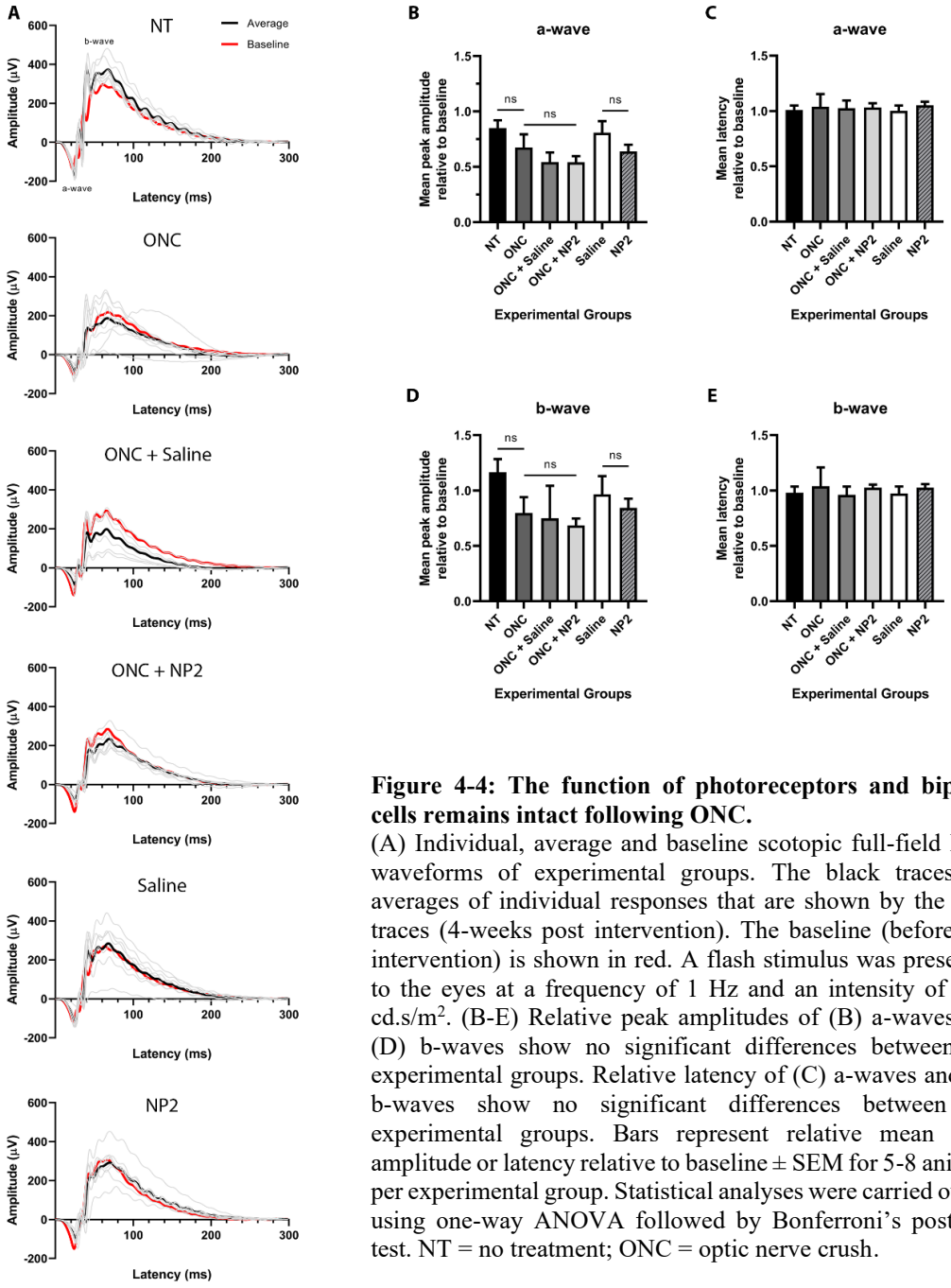

Figure 4-4: The function of photoreceptors and bipolar cells remains intact following ONC.
(A) Individual, average and baseline scotopic full-field ERG waveforms of experimental groups. The black traces are averages of individual responses that are shown by the gray traces (4-weeks post intervention). The baseline (before any intervention) is shown in red. A flash stimulus was presented to the eyes at a frequency of 1 Hz and an intensity of 0.05 cd.s/m^2. (B-E) Relative peak amplitudes of (B) a-waves and (D) b-waves show no significant differences between the experimental groups. Relative latency of (C) a-waves and (E) b-waves show no significant differences between the experimental groups. Bars represent relative mean peak amplitude or latency relative to baseline ± SEM for 5-8 animals per experimental group. Statistical analyses were carried out by using one-way ANOVA followed by Bonferroni's post hoc test. NT = no treatment; ONC = optic nerve crush.

The pattern ERG (PERG) test was used to assess the functionality of RGCs. In this test, an alternating horizontal black and white striped pattern is presented as the visual stimulus, which results in a waveform with three components: a negative trough (termed N1), followed by a positive peak (termed P1) and a broad second negative trough (termed N2). To establish a baseline, PERG was recorded before any intervention. Figure 4-5A shows the PERG traces for each experimental group before (baseline) and 4-weeks following intervention. Analysis of the waveforms indicated that RGC function was impaired in the experimental animals that received ONC and animals that received NP2 injection alone.

A one-way ANOVA revealed that the difference in PERG P1 amplitude (Figure 4-5B; $F(5,36) = 6.191$; $p < 0.001$) and latency (Figure 4-5C; $F(5,34) = 2.827$; $p < 0.05$) post intervention was significant. Post hoc comparisons using Bonferroni indicated that the P1 amplitude (Figure 4-5B, $p < 0.05$) and latency (Figure 4-5C, $p < 0.01$) were statistically significantly lower in the ONC experimental group compared to the no treatment group. The P1 amplitude and latency of animals that received 1 nM NP2 post ONC were not statistically different from ONC-only or ONC+saline animals. Although not statistically significant, the P1 amplitude of animals that received NP2 intravitreal injection-only was lower in comparison to the intravitreal saline injection-only experimental animals. There was no statistical difference between saline and NP2-injection only experimental groups in terms of P1 latency.

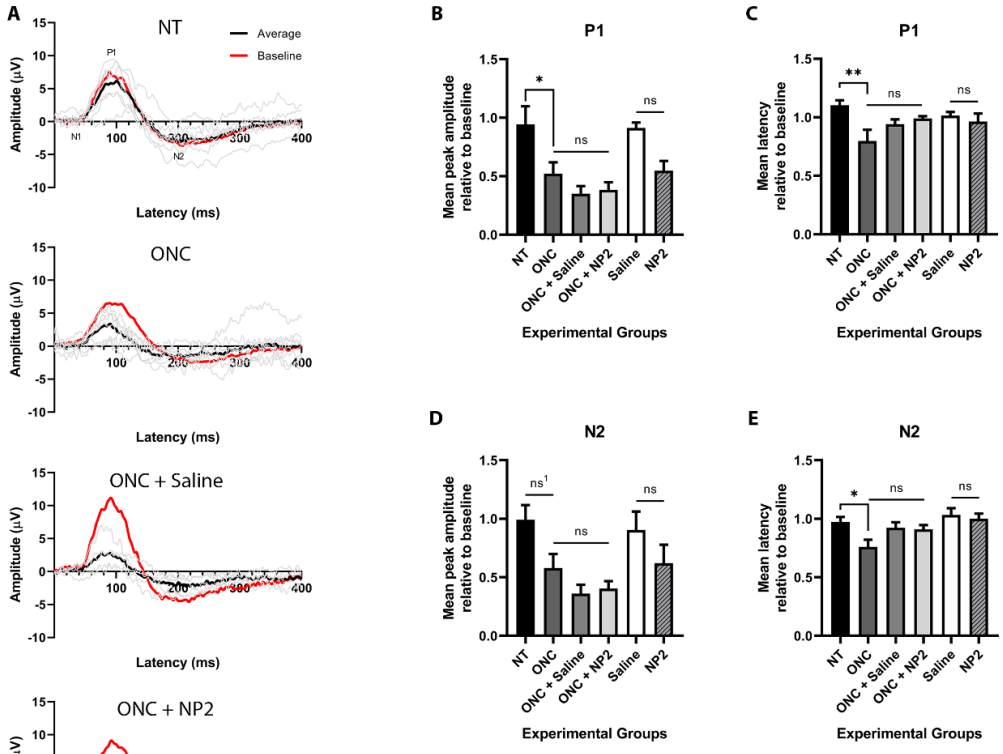

Figure 4-5: NP2 does not protect against RGC dysfunction following ONC.
(A) Individual, average and baseline PERG waveforms of experimental groups. The black traces are averages of individual responses that are shown by the gray traces (4-weeks post intervention). The baseline (before any intervention) is shown in red. A pattern stimulus consisting of alternating horizontal black and white bars was presented to the eyes at a frequency of 0.155 cycles/degree with 2.1 reversals/second and at 100% contrast. Quantification of (B) amplitude of P1 (C) latency of P1 (D) amplitude of N2 and (E) latency of N2 of PERG recordings at 4 weeks post-crush. Bars represent mean peak amplitude or latency relative to baseline ± SEM for 5-8 animals per experimental group. Statistical analyses were carried out by using one-way ANOVA followed by Bonferroni's post hoc test, ns = not significant, *$p < 0.05$, ***$p < 0.001$. NT = no treatment; ONC = optic nerve crush. [1] Statistical significance was seen in 7/8 animals in the ONC group compared to NT.

There was a trend for lower N2 amplitude in experimental animals that received ONC or NP2 intravitreal injection-only, however these differences did not reach statistical

significance (Figure 4-5D). This may be due to the increased variability between animals in the same experimental group. Although there was no statistical difference in N2 amplitude between the no treatment and ONC experimental animals' cohort-wise, statistically lower N2 amplitude was seen in 7 of the 8 animals that received ONC. The N2 amplitudes of animals that received 1 nM NP2 post ONC was not statistically different from ONC-only or ONC+saline animals. The N2 amplitude of animals that received 1 nM NP2 injection was not statistically different from saline injection animals.

A one-way ANOVA revealed a significant effect of surgical intervention for N2 latency (Figure 4-5E; $F(5,35) = 4.169$; $p < 0.01$). Post hoc comparisons using Bonferroni indicated that the N2 latency were statistically significantly lower in the ONC experimental group compared to the no treatment group ($p < 0.05$). The N2 latency of animals that received 1 nM NP2 post ONC was not statistically different from ONC-only or ONC+saline animals. The N2 latency of animals that received 1 nM NP2 injection was not statistically different from saline injection animals.

The interpretation of changes in RGC function is based on alterations in both amplitude and latency of the PERG components. The decrease in P1 and N2 amplitudes and changes in latencies were considered reflective of RGC dysfunction. As expected, our results indicate that ONC injury results in decreased RGC function. The PERG response has been reported to decrease or diminish following direct and indirect RGC injury (Chou et al., 2013; Liu et al., 2014; Saszik et al., 2002; Takeda et al., 2000; Villegas-Pérez et al., 1993). Our results regarding the decrease in PERG amplitudes and latency in the ONC group are in agreement with these published findings.

Unexpectedly, our results revealed that 1nM NP2 does not protect against RGC functional loss triggered by ONC. Based on the number of RGC surviving with NP2 treatment following ONC, we had hypothesized that the function of RGCs would remain intact following ONC. However, this was not the case. One way to interpret our histological and functional findings is that some RGCs that are viable are not functional. The mechanisms responsible for rendering an RGC dysfunctional, yet viable are poorly understood (Mead and Tomarev, 2016). Different ocular injury models have shown that RGC dysfunction precedes loss of RGC density, more specifically PERG can be altered before histological loss of RGCs (Liu et al., 2014; Porciatti, 2015). Structural studies using glaucoma models, showed axonal and dendritic dysfunction preceding the loss of RGC somas (Buckingham et al., 2008; Williams et al., 2013). A study examining the longitudinal morphological and functional changes of RGC after ONC in mouse found that the PERG demonstrated an early RGC functional deficit in response to ONC, before significant RGC death was evident (Li et al., 2020). In this study they found that the correlation between P1 amplitude and RGC survival was very poor (Li et al., 2020). In terms of our findings, this could explain why we saw structural RGC survival with NP2 administration but there was a lack of RGC function. This also means that the PERG can detect RGC pathologies prior to cell death when the RGCs may be still curable. Therefore, the time lag between RGC dysfunction and RGC death could be another window of opportunity for therapeutic intervention. If RGC dysfunction precedes death, then potential function-restoring agents could be administered during this time.

Despite the sensitivity of PERG to detect RGC dysfunction, whether it reliably displays the function of all RGC subtype is unclear. PERG quantifies population responses. The

PERG waveform has be found to be completely absent following ONC even though certain RGC subtypes demonstrate impressive resistance to ONC (Liu et al., 2014). Certain RGC subtypes such as melanopsin RGCs have been reported to be more resistant to death than other subtypes following optic nerve trauma (Sánchez-Migallón et al., 2018). It has been found that just like how different RGC subtypes are more susceptible to death, RGC dysfunction is also subtype dependent (Chen et al., 2015; Puyang et al., 2017). For example, following ONC model there was a more significant decline in function in the OFF-RGC subtype compared to ON-RGC subtype (Puyang et al., 2017). The P1 and N2 components of the mouse PERG are believed to originate in part from the ON- and OFF-centre ganglion cells, respectively (Miura et al., 2009). However, there are over 30-types of RGCs and large portion of them are still less defined (Puyang et al., 2017). How the other different RGC subtypes contribute to the PERG waveforms has not been fully elucidated, neither has addressing how this may impact the disparity between RGC survival and RGC function. Therefore, it is possible that NP2 is neuroprotective towards a certain subpopulation of RGC subtypes, whose function is not being captured by the PERG since the PERG measures the whole retinal response.

A study by Xia and colleagues (2014), found that a single-injection of ciliary neurotrophic factor (CNTF), a widely known neuroprotective agent, protected against RGC functional loss at eight days after ONC (Xia et al., 2014). However, the same CNTF-treated animals displayed lower PERG amplitudes 15-days after ONC and flat PERG amplitudes 22 days after ONC (Xia et al., 2014). This indicates that with time the neuroprotective effect in terms of function may ware off. The study authors did not quantify the number of surviving RGCs at the 22-day timepoint. We only assessed PERG

responses 4-weeks post treatment. It is possible that if we had assessed PERG responses 7- or 14-days post treatment, we may have seen similar responses to that seen with CNTF. A longitudinal study on the impact of NP2 administration has not been conducted. One limitation of the NP2 treatment in terms of function could be related to the half-life of the protein. Following maximal electroconvulsive seizures (MECS), NP2 mRNA levels in the hippocampus and cortex have been shown to stay elevated for at least 8 hours (Tsui et al., 1996). The half-life of NP2 has been reported to be 30 hours (Sowmya, 2019). However, the half-life of intravitreally injected NP2 has not been elucidate. Furthermore, we did not investigate the intravitreal half-life of injected NP2 in our experiment. We reason that it is possible that the impact of NP2 may ware off with time. Therefore, it is possible that sustained delivery of NP2 may be needed for functional recovery.

We found that NP2 injection itself might impair RGC function when injected into a non-damaged eye. It is likely that overexpression of NP2 in healthy eyes may be detrimental. Intraocular injection of CNTF, a neuroprotective agent for retinal degeneration, reduced ERG amplitude when injected into healthy eyes (McGill et al., 2007). The decrease in RGC function in NP2-only injection group cannot be linked to the intravitreal injection procedure since the animals that received saline injection-only had comparable PERG responses before and after intravitreal injection. This suggest that the intravitreal injection procedure did not cause the RGC dysfunction.

Overall, the PERG results demonstrate that, although RGCs were protected after treatment with NP2, their function was still impaired. This finding highlights the

importance of electrophysiological assessment of RGC function as a necessary outcome measure in ONC models. While the number of surviving RGCs have been quantified to report neuroprotective effects of potential therapeutic agents, the functionality of these surviving RGCs is rarely examined. Therefore, the function of surviving RGCs is also a necessary parameter that should be examined to determine treatment efficacy.

Given that 1 nM NP2 enhanced neurite outgrowth in both embryonic and postnatal retinal tissue *in vitro* and *ex vivo*, this led us to ask whether NP2 would promote axon regeneration *in vivo* under physiological conditions following ONC. The animals in this study were injected with CTB anterograde tracer to label regenerating axons. Since we were injuring the optic nerve, functional tests were also performed to evaluate optic nerve function. VEP is used to assess the functional integrity of the visual pathway, from the retina via the optic nerve to the visual cortex. Any abnormality that affects the visual pathways or visual cortex in the brain can affect the VEP. VEP can indicate abnormalities in the visual pathway induced by ONC (Mead and Tomarev, 2016). Therefore, we performed flash VEP tests before and following ONC and intravitreal administration of either 1 nM NP2 or saline. The flash VEP elicits a reproducible waveform with three components: a small positive peak (termed P1), followed by a negative trough (termed N1) and a second positive peak (termed P2) (You et al., 2011). The amplitudes of N1 and P2 components correlate with axonal loss (You et al., 2011).

Similar to the other two functional tests, to establish a baseline, VEPs were recorded before any intervention. Figure 4-6A shows the flash VEP traces for each experimental group before (baseline) and 4-weeks following surgical intervention. Analysis of the

waveforms indicated that the optic nerve function was significantly impaired in the experimental animals that received ONC. The VEP traces were mostly flat in the animals that received ONC, ONC+saline and ONC+NP2, which indicates severe damage to the optic neve. Analysis of the N1 peak amplitudes showed that there were statistically significant differences between the no treatment and ONC animals (Figure 4-6B; $F(5,32) = 14.98$; $p < 0.0001$). The N1 amplitude of animals that received 1 nM NP2 post ONC were not statistically different from ONC-only or ONC+saline animals. There was no statistical difference between saline and NP2-injection only experimental groups in terms of N1 amplitude. Findings for P2 amplitudes were similar to N1 amplitudes for all the experimental groups. Notably, P2 amplitudes were statistically significantly lower in animals that received ONC compared to the no treatment group (Figure 5C; $F(5,34) = 11.07$; $p <0.0001$). Since the optic nerve is composed of the RGC axons, these findings correlate with our PERG findings, which indicated RGC dysfunction.

In the animals that received the ONC, since the optic nerve is severely damaged, there is no signal transmission from the retina to the brain, which is why the VEPs were essentially flat. The latencies of the N1 and P2 components are believed to be an accurate measurement of the level of optic nerve myelination (Marenna et al., 2019). Due to the change in the VEP waveform of the ONC, ONC+saline and ONC+NP2 experimental groups an accurate analysis of the component's latency could not be made. We expected to see reductions in VEP signaling in the ONC animals because we were directly crushing the optic nerve. Altogether, our findings show that ONC resulted in the disruption of signal from the retina to the visual cortex. This finding coincides with the very few studies that had addressed optic nerve functional loss following ONC injury (Li

et al., 2018; Passaglia et al., 2018; Shao et al., 2016). The analysis of the VEP traces suggest that 1nM NP2 does not aid in restoring the disruption of signal from the retina to the visual cortex triggered by ONC.

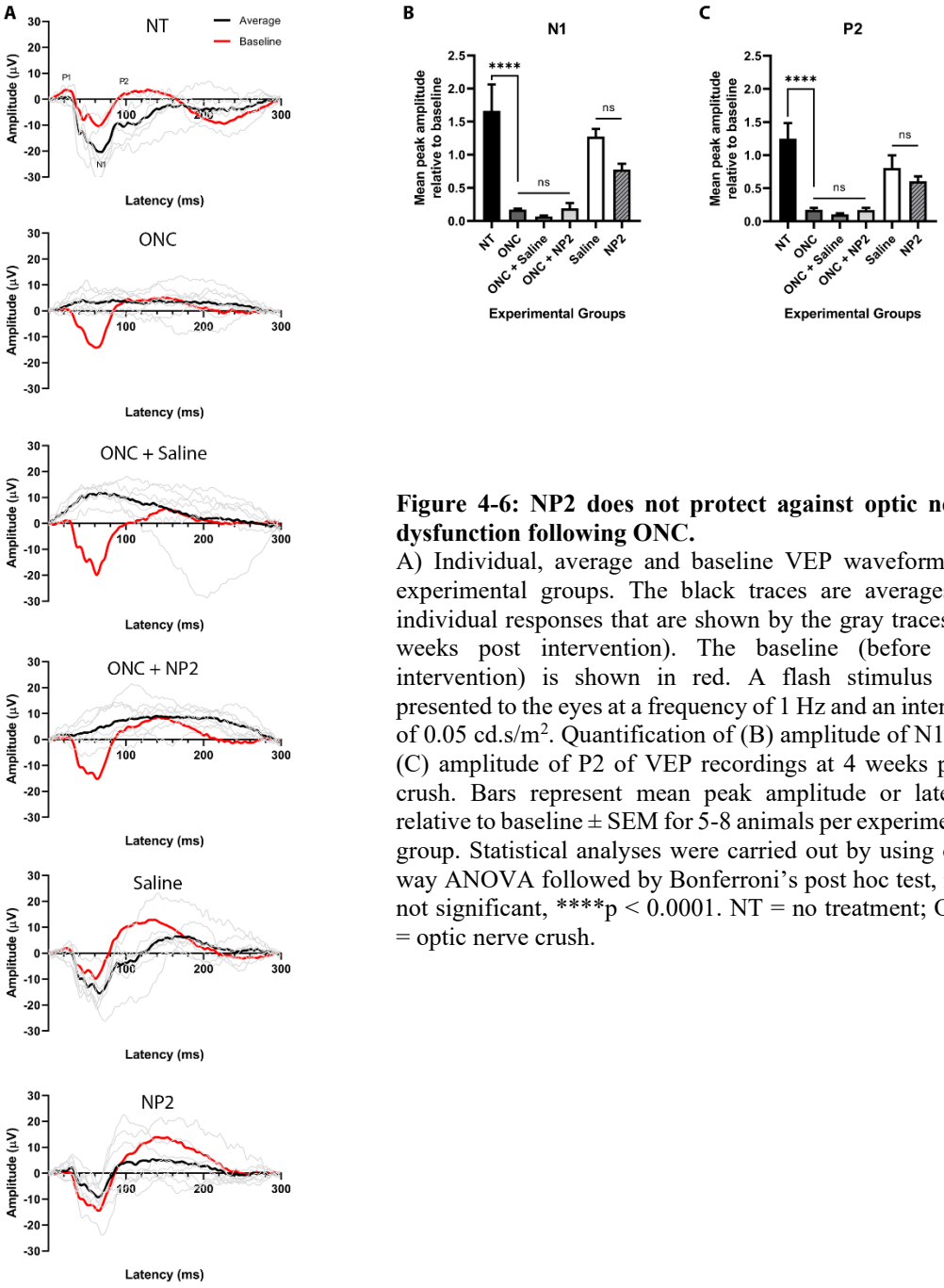

Figure 4-6: NP2 does not protect against optic nerve dysfunction following ONC.
A) Individual, average and baseline VEP waveforms of experimental groups. The black traces are averages of individual responses that are shown by the gray traces (4-weeks post intervention). The baseline (before any intervention) is shown in red. A flash stimulus was presented to the eyes at a frequency of 1 Hz and an intensity of 0.05 cd.s/m^2. Quantification of (B) amplitude of N1 and (C) amplitude of P2 of VEP recordings at 4 weeks post-crush. Bars represent mean peak amplitude or latency relative to baseline ± SEM for 5-8 animals per experimental group. Statistical analyses were carried out by using one-way ANOVA followed by Bonferroni's post hoc test, ns = not significant, ****$p < 0.0001$. NT = no treatment; ONC = optic nerve crush.

A limitation of this study is that we were unable to properly visualize the CTB anterograde tracer in the samples. It appears NP2 was not sufficient to promote robust axon regeneration following ONC (*data not shown*). Based on our *in vitro* and *ex vivo* results, we had hypothesized that there would be some degree of axon regeneration. However, this was not the case. As noted in an opinion piece by Pernet and Schwab (2014), functional recovery of vision would imply that damaged axons regenerate at least until the lateral geniculate nucleus and the superior colliculus – a distance of more than 8 mm from the site of injury in mice (Pernet and Schwab, 2014). Both *in vitro* and *ex vivo*, we had only observed 250 µm and 500 µm of neurite outgrowth. Taken together, our data suggest that 1 nM NP2 was not adequate to reach therapeutical action to facilitate sufficient structural nor functional axon regeneration of the injured optic neve.

Based on the evidence that NP2 expression is significantly lower in adult RGCs compared to embryonic RGCs and that its expression changes post ONC, we hypothesized that increasing NP2 expression would promote adult RGC survival and enhance regeneration after ONC. Since 1 nM NP2 promoted neurite outgrowth *in vitro* and *ex vivo*, we decided to inject the same concentration of NP2 into the eye immediately after ONC. Two and four-weeks after ONC, the 1 nM NP2 promoted survival of adult RGCs. However, the same concentration of NP2 was not sufficient to induce axon regeneration after ONC. Our results highlight the importance of functional testing when investigating future therapeutic agents. While factors may promote axonal regrowth *in vitro* and *ex vivo*, it is important to follow-up these studies *in vivo*, especially with functional testing.

4.5 Conclusion

This study highlights the importance of monitoring visual function when investigating potential regeneration-inducing factors. Even though 1 nM NP2 enhanced neurite outgrowth *in vitro* and *ex vivo*, it did not demonstrate the same potential *in vivo*. Furthermore, although NP2 promoted RGC survival *in vivo* post ONC, it appears as though these RGC's activity is significantly impaired. Although preservation of RGC is an important aspect of neuroprotection, it important to consider whether these surviving cells are responsive to stimuli and/or elicit a response, which this study tested. When using the ONC injury model to address axon regeneration, electrophysiological assessment appears to be a sensitive and necessary outcome measure for determining the full therapeutic potential of factors. Therefore, the development of potential therapies requires accurate and reliable assessment of RGC numbers along with appropriate testing of RGC function.

Chapter 5: **General Discussion**

This thesis examined the possibility that NP2 is neuroprotective toward RGCs and promotes axon regeneration following visual system injury. The developmental expression pattern of NP2 was characterized to determine whether there was a relationship between developmental changes in NP2 expression and the established decline in axon regeneration ability of RGCs (Goldberg et al., 2002a). Additionally, the impact of NP2 treatment on RGC survival, using an *in vitro* RGC culture model, was evaluated. Furthermore, the ability of NP2 to enhance RGC neurite outgrowth, using both *in vitro* and *ex vivo* model systems, was examined. To assess the *in vivo* impact of exogenous NP2 administration on RGC survival and axon regeneration, a well established ONC model was utilized. The effect of NP2 administration on functional recovery following ONC was also evaluated, using ERG and VEPs.

The developmental expression of NP2 in the brain has not been well defined. Furthermore, detailed expression profile of NP2 protein in the retina has also not been thoroughly studied. The present study is thus the first report delineating this relationship. The results showed a decline in NP2 protein expression with an increase in age. It was found that NP2 migrates as 3 unique set of bands in western blot analyses: ~52 (double band), ~62 and ~72 kDa. Western blot analyses identified two band at ~72 kDa and ~62 kDa in embryonic and early postnatal samples, while late postnatal and adult samples do not largely express these bands. Following treatment with PNGase F, there was a slight downward shift in the ~72 kDa band and a relative decrease in the level of the ~62 kDa

band, which is likely an indication of glycan removal. Based on these results, it was hypothesized that the ~72 kDa and ~62 kDa bands represent the glycosylated versions of NP2. Under reducing conditions, NP2 protein migrated as a single band in western blots from ~46-60 kDa in brain tissues (Dodds et al., 1997; O'Brien et al., 1999; Reti and Baraban, 2000; Tsui et al., 1996; Xu et al., 2003). NP2 expression has been extensively studied in certain brain region but not in the retina. It is possible that the NP2 variants that were observed in the retina are expressed at varying levels in other tissues/brain regions or not expressed at all. Further research is needed to fully elucidate the developmental expression pattern of the different variants of NP2 in the CNS.

Based on the presented data it can not be ascertained that the developmental changes in NP2 protein expression is specific to a certain population of cells in the retina. Since the overall NP2 expression in the retina was analyzed, it remains to be answered whether there are changes in the pattern of NP2 protein expression in RGCs, with development. Immunohistochemistry was used to localize NP2 in the retina, however, the NP2 signal could not be clearly differentiated using the available experimental resources. Similar difficulties with commercially available NP2 antibodies have been reported (Van't Spijker et al., 2019). Bjartmar and colleagues (2006) used their own lab-generated NP2 antibodies and localized NP2 protein expression in postnatal mice to the GCL, inner nuclear and inner plexiform layers (Bjartmar et al., 2006). Future studies could examine potential methods to localize NP2 to specific cells in the retina and examine whether the expression changes developmentally. Previous studies have reported that NP2 is enriched in the somatodendritic areas of neurons while others have found that NP2 is expressed in the axon and axon terminals (Mariga et al., 2015; O'Brien et al., 1999; Reti et al., 2002b;

Xu et al., 2003). Future studies could clarify whether NP2 is constantly expressed in the optic nerve or whether it is induced by neural activity in the RGC soma and then rapidly transported to axon terminals as seen in other neuronal cell populations (Xu et al., 2003).

Under naïve conditions, the expression of the ~72 kDa NP2 variant in the adult retina is maintained at very low levels. In the present study, it was demonstrated that the ~72 kDa NP2 variant was rapidly upregulated 1-day after ONC before declining. The ~62 kDa NP2 variant was not detected post injury. Whereas the ~52 kDa variant's expression declined to almost 50% of the non-injured samples. Based on these results, it was concluded that treatment with exogenous NP2 (~52 kDa variant) may be beneficial post injury.

Cell survival is a very important factor that contributes to the ability of axons to regenerate. Therefore, when considering the regenerative effects of NP2 on axon growth, the impact on cell survival must also be considered. $RBPMS^+$ RGC count was used as an indicator of morphologic damage to correlate with RGC functional loss. The presented results indicate that NP2 has a beneficial effect on survival of RGCs both *in vitro* and *in vivo*. It was found that ONC induced significant neuronal loss, while 1 nM NP2 treatment promoted cell survival. The number and the function of surviving RGCs are necessary parameters to determine treatment efficacy. To verify whether the surviving RGC's were functional PERG analysis was used. PERG findings did not correlate with retinal morphologic changes. Based on the number of $RBPMS^+$ RGCs remaining post NP2 exposure, it was hypothesized that there would be intact or slightly lower RGC function in NP2 treated ONC animals compared to the ONC-only or ONC+saline groups.

However, there was no significant difference in terms of RGC function between these experimental groups. The PERG requires uninterrupted retrograde optic nerve signaling (Li et al., 2020). It is possible that while NP2 was necessary to promote RGC survival it could not sufficiently promote the function of the RGCs. The highlight of the *in vivo* experiment is the long-lasting survival effect of a single treatment with NP2 (at least 4 weeks). At present, it remains to be elucidated how a single administration of NP2 engages an RGC survival program.

The presented data revealed that treatment with NP2 promotes neurite outgrowth of both embryonic and postnatal RGCs. Although the efficacy of neurite outgrowth differed depending on the age of the RGCs. It is well established that the loss of intrinsic regenerative ability is highly correlated with development of CNS neurons (Goldberg et al., 2002b). Post ONC, exogenous administration of NP2 is necessary but is not sufficient to promote axon regeneration. Thus, lack of sufficient axon regeneration *in vivo* seems to be somewhat misaligned with the *in vitro* and *ex vivo* observations, where neurite outgrowth was significantly enhanced by exogenous NP2 treatment. There remain some challenges in interpreting outcomes of the *in vivo* study. A few possibilities are reflected below regarding reasons that the *in vivo* data did not confirm the findings from *in vitro* and *ex vivo* experiments.

It is important to consider the differences between the *in vitro, ex vivo* and *in vivo* models. Dissociated *in vitro* RGC cultures allow for the determination of RGC's intrinsic response to a factor by isolating the RGC from their normal environment (Romano and Hicks, 2007). This means the enhancement of neurite outgrowth observed *in vitro*

highlights the ability of NP2 to modulate RGC's intrinsic regeneration mechanism positively. However, since the RGCs are dissociated during the isolation procedure, it does not take into consideration the interaction of other retinal cells. Organotypic retinal explant cultures are multicellular *ex vivo* models, in which RGCs remain embedded in contact with accompanying cells. When the retina is removed from the eyeball during dissection, even though the cellular composition is intact, the RGC axons are damaged creating an injury model in a dish. Since robust neurite outgrowth was seen *ex vivo*, this indicates that in the presence of other retinal cells NP2 is still able to enhance RGC's intrinsic regeneration mechanism positively. In this model, the response of the retinal cells are being studied in isolation from the rest of the eye (Schaeffer et al., 2020). While the retinal explant isolation procedure severs the RGC axons, thereby somewhat mimicking an optic nerve injury model, it does not take into consideration the cascade of cellular responses that are turned on *in vivo* post injury. Inflammatory cells and myelin-associated factors that play an important role during Wallerian degeneration *in vivo* are absent *ex vivo*. Another important consideration is the role of extracellular matrix (ECM) components. In the *in vitro* and *ex vivo* experiments, the ECM was made of exogenous factors, laminin and PDL, whereas *in vivo* the extracellular matrix is intricately comprised and likely disrupted due to the injury.

Apart from the differences in the extrinsic factors between these models, the intrinsic factors also need to be addressed. Embryonic and postnatal *in vitro* and *ex vivo* cultures were used to address NP2's regulation of neurite outgrowth. While embryonic cultures have been commonly used to address similar questions, the intrinsic ability of young neurons to regrow their axon induces a bias regarding the molecular and cellular

mechanisms of axon growth in mature neurons (Goldberg et al., 2002b). Therefore, this approach presents a major caveat. Indeed, unlike mature neurons, embryonic neurons or young neurons (until P5-P6 in mice) have a high regrowth potential (Goldberg et al., 2002b). This could explain partially why neurite growth was seen *in vitro* and *ex vivo* but not *in vivo*. However, it should be noted that NP2 was able to promote neurite growth of P7 and P14 RGCs; age points which consistently show weakened regrowth ability. There were marked differences in the number and length of neurite outgrowth of NP2 treated P7 and P14 RGCs in comparison to respective controls.

Another difference between the models used in this study is the delivery method. Both *in vitro* and *ex vivo*, the cell or tissue were fully immersed in NP2 solution. This means that the ganglion cell body and the damaged axonal ends are in direct contact with NP2 in solution. Whereas *in vivo*, injection of NP2 into the vitreous body means that the NP2 is accessible to only the cell bodies and not the leading edge of the damaged axons. In the *in vivo* setting, the RGCs are being manipulated while the optic nerve at the injury is no being directly treated. The most important of these questions, is whether levels of NP2 sufficient to elicit growth was achieved using the intravitreal injection method. The amount of NP2 used *in vitro* and *ex vivo* cultures was sufficient to achieve survival and neurite growth of RGCs. Furthermore, the level of administered NP2 protein *in vivo* was sufficient to enhance RGC survival up to at least 4-weeks post ONC. Thus, while it cannot be concluded with certainty that higher levels of NP2 would not support optic nerve regeneration, it can be concluded that exogenous NP2 at levels sufficient to support growth of RGC axons *in vitro* and *ex vivo* and that enhance RGC survival *in vivo* are not equally capable of supporting optic nerve regeneration *in vivo*. The possibility that the

exogenous NP2 *in vivo* could be much more readily degraded should also be taken into consideration. As another avenue of research, modulation of NP2 protein levels by using another *in vivo* delivery technique may be helpful to examine.

The presented study has not directly tested whether NP2 injected into the eye is taken up by RGCs. There is the possibility that NP2 might be acting on other cells present in the eye when administered *in vivo*. Based on the *in vitro* RGC culture model, NP2 does seem to act directly on RGCs to induce neurite outgrowth. It can be speculated that this may also be the case *in vivo* because of the anatomy of the eye is such that RGCs are the first cells encountered by NP2 following its injection into the vitreous body. However, there is the possibility that the compound may diffuse into the other layers of the retina. Similarly, the question remains whether if NP2 after being up taken is being transported to the injury site. Under naïve conditions, NP2 is rapidly upregulated in the soma following neural activity and then trafficked down axons to terminal (Reti et al., 2002b, 2008; Xu et al., 2003). Whether this same mode of transport occurs post injury remains to addressed. This could partially explain the disparity we saw between our *in vitro* and *in vivo* results in terms of regeneration ability of NP2. Therefore, future studies could explore whether treatment of NP2 at the injury site would sufficiently enhance functionally relevant axon regeneration.

Since the inhibitory CNS environment has also been shown to play a major role in the lack of regeneration that is seen following ONC injury, combinatorial therapies that both increase intrinsic regenerative capability of axons and decrease extrinsic inhibitory factors within the CNS environment, will likely be most effective when treating CNS

injuries. Since NP2 has a demonstrated role in prolonging RGC survival, potential function-restoring agents and robust axon regeneration-inducing agents could be co-administered. In an *in vivo* study, it was found that the enhancement of neural activity in combination with the activation of mTOR, was able to promote long-distance and target-specific regeneration of adult retinal axons (Lim et al., 2016). NP2 could promote survival of the RGCs long enough to allow regeneration by other more effective regeneration stimulating factors *in vivo*. One advantage of NP2 as a possible therapeutic agent is the fact that it is already present in the retina and injecting it into the eye is simply adding more to what is already present. This obviates the need of administering compounds that are not endogenous to the human body.

RGC loss leading to visual impairment occurs in diabetic retinopathy, optic neuropathies, and glaucoma (Almasieh et al., 2012). Given NP2's ability to promote robust RGC survival, it is possible that NP2 might be useful in the context of these diseases. Therefore, future studies could examine the therapeutic potential of NP2 in other disease models where RGC survival is vital.

There are limitations in this study. First, the possible neurotoxic nature of NP2 was not examined. Though the studies show that NP2 is neuroprotective, whether NP2 could cause cell death was not fully characterized. This could be examined using markers for cell death. Another limitation in this study is that the molecular mechanisms of NP2-mediated RGC survival was not possible to examine in the available timeframe. Future studies could explore these avenues of research. To explore the mechanism underlying the NP2-mediated cell survival, the expression of neuronal pentraxin receptor (NPR), the

known receptor for NP2, could be examined. NPR has been shown to expressed in the GCL in postnatal animals (Bjartmar et al., 2006). Whether it is expressed in adults and how its expression changes post injury is not known. If NPR is present, it is possible that NP2 is exerting its effects via the NPR. Expression of NPR mRNA post ONC has been shown using RNA sequencing (unpublished findings), whether this translates to protein expression could be explored.

Another possible mechanism of action could be via a BDNF-dependent pathway. NP2 has been shown to be a direct transcriptional target of BDNF (Mariga et al., 2015). The results of our study correspond with previously published results regarding the effects of BDNF administration in the CNS (Giehl and Tetzlaff, 1996; Lu et al., 2001). BDNF promoted survival of corticospinal motor neurons after subcortical axotomy (Giehl and Tetzlaff, 1996; Lu et al., 2001) but did not promote corticospinal axonal regeneration (Hiebert et al., 2002).

NP2 was originally isolated as an IEG induced by seizures in the rat hippocampus (Tsui et al., 1996). Later NP2 was shown to form clusters with NP1 and bind to NPR. NP1 and NP2 clusters play a key role in inducing synaptic clustering of AMPA receptors in both primary neurons and HEK-293 cells (O'Brien et al., 1999; Xu et al., 2003). It has been proposed that when NPR transmembrane domain is cleaved, there is internalization of the neuronal pentraxin complex (NP1-NP2-NPR) and the associated AMPA receptors via endocytosis (Cho et al., 2008). Following ONC, there is a release of excess glutamate that leads to excitotoxicity. It is possible that NP2-NP1-NPR induced internalization of AMPA receptors may reduce the cell's response to glutamate. Therefore the upregulation

of NP2 may protect neurons from glutamate excitotoxicity through internalization of AMPA receptors (Schwarz et al., 2002). Future studies could investigate these possible avenues of research.

Chapter 6: **Conclusion**

This study presents data that supports the possible therapeutic potential of NP2 in targeting repair following CNS injury. Like other CNS repair inducing factors, NP2 protein expression is developmentally regulated. Furthermore, NP2 yields neuroprotection *in vitro* and *in vivo,* following ONC injury. However, single injection of NP2 failed to provide functional recovery following optic nerve injury. Further studies are required to assess the full extent of NP2's neuroprotective abilities (multiple injection or combinatory approach) before it can be ruled out as an effective therapy. The results of this thesis are an important step forward in understanding the role of NP2 in the damaged CNS and provides clues to potential therapeutic strategies that could be employed to promote CNS repair.

References

Agrawal, A., Singh, P.P., Bottazzi, B., Garlanda, C., and Mantovani, A. (2009). Pattern Recognition by Pentraxins. Advances in Experimental Medicine and Biology *653*, 98–116.

Agudo, M., Pérez-Marín, M.C., Lönngren, U., Sobrado, P., Conesa, A., Cánovas, I., Salinas-Navarro, M., Miralles-Imperial, J., Hallböök, F., and Vidal-Sanz, M. (2008). Time course profiling of the retinal transcriptome after optic nerve transection and optic nerve crush. Molecular Vision *14*, 1050–1063.

Almasieh, M., Wilson, A.M., Morquette, B., Cueva Vargas, J.L., and Di Polo, A. (2012). The molecular basis of retinal ganglion cell death in glaucoma. Progress in Retinal and Eye Research *31*, 152–181.

Anderson, M.A., Burda, J.E., Ren, Y., Ao, Y., O'Shea, T.M., Kawaguchi, R., Coppola, G., Khakh, B.S., Deming, T.J., and Sofroniew, M. V (2016). Astrocyte scar formation aids central nervous system axon regeneration. Nature *532*, 195–200.

Baker, N.E., Li, K., Quiquand, M., Ruggiero, R., and Wang, L.H. (2014). Eye development. Methods *68*, 252–259.

Balhara, J., Koussih, L., Zhang, J., and Gounni, A.S. (2013). Pentraxin 3: An immuno-regulator in the lungs. Frontiers in Immunology *4*, 1–10.

Belin, S., Nawabi, H., Wang, C., Tang, S., Latremoliere, A., Warren, P., Schorle, H., Uncu, C., Woolf, C.J., He, Z., et al. (2015). Injury-Induced Decline of Intrinsic Regenerative Ability Revealed by Quantitative Proteomics. Neuron *86*, 1000–1014.

Benowitz, L.I. (2010). Optic Nerve Regeneration. Archives of Ophthalmology *128*, 1059.

Benowitz, L., and Yin, Y. (2008). Rewiring the injured CNS: Lessons from the optic nerve. Experimental Neurology *209*, 389–398.

Benowitz, L.I., He, Z., and Goldberg, J.L. (2017). Reaching the brain: Advances in optic nerve regeneration. Experimental Neurology *287*, 365–373.

Berardi, N., Domenici, L., Gravina, A., and Maffei, L. (1990). Pattern ERG in rats following section of the optic nerve. Experimental Brain Research *79*, 539–546.

Berry, L.R., Van Walderveen, M.C., Atkinson, H.M., and Chan, A.K.C. (2013). Comparison of N-linked glycosylation of protein C in newborns and adults. Carbohydrate

Research *365*, 32–37.

Bjartmar, L., Huberman, A.D.D., Ullian, E.M.M., Rentería, R.C.C., Liu, X., Xu, W., Prezioso, J., Susman, M.W.W., Stellwagen, D., Stokes, C.C.C., et al. (2006). Neuronal Pentraxins Mediate Synaptic Refinement in the Developing Visual System. Journal of Neuroscience *26*, 6269–6281.

Bosse, F., Hasenpusch-Theil, K., Küry, P., and Müller, H.W. (2006). Gene expression profiling reveals that peripheral nerve regeneration is a consequence of both novel injury-dependent and reactivated developmental processes. Journal of Neurochemistry *96*, 1441–1457.

Breviarios, F., Aniellos, E.M., Golay, J., Bottazzis, B., Bairochll, A., Sacconell, S., Marzellass, R., Predazziss, V., Rocchi, M., Vallell, G. Della, et al. (1992). Interleukin-1-inducible Genes in Endothelial Cells. Journal of Biological Chemistry *267*, 22190–22197.

Bringmann, A., Pannicke, T., Grosche, J., Francke, M., Wiedemann, P., Skatchkov, S.N., Osborne, N.N., and Reichenbach, A. (2006). Müller cells in the healthy and diseased retina. Progress in Retinal and Eye Research *25*, 397–424.

BrosiusLutz, A., and Barres, B.A. (2014). Contrasting the Glial Response to Axon Injury in the Central and Peripheral Nervous Systems. Developmental Cell *28*, 7–17.

Buckingham, B.P., Inman, D.M., Lambert, W., Oglesby, E., Calkins, D.J., Steele, M.R., Vetter, M.L., Marsh-Armstrong, N., and Horner, P.J. (2008). Progressive ganglion cell degeneration precedes neuronal loss in a mouse model of glaucoma. Journal of Neuroscience *28*, 2735–2744.

Bull, N.D., Johnson, T. V., Welsapar, G., DeKorver, N.W., Tomarev, S.I., and Martin, K.R. (2011). Use of an adult rat retinal explant model for screening of potential retinal ganglion cell neuroprotective therapies. Investigative Ophthalmology and Visual Science *52*, 3309–3320.

Cai, D., Qiu, J., Cao, Z., McAtee, M., Bregman, B.S., and Filbin, M.T. (2001). Neuronal cyclic AMP controls the developmental loss in ability of axons to regenerate. Journal of Neuroscience *21*, 4731–4739.

Cai, M., Zhu, Y., Li, Z., Josephs-Spaulding, J., Zhou, Y., Hu, Y., Chen, H., Liu, Y., He, W., and Zhang, J. (2019). Profiling the Gene Expression and DNA Methylation in the Mouse Brain after Ischemic Preconditioning. Neuroscience *406*, 249–261.

Chang, S., Bok, P., Tsai, C.Y., Sun, C.P., Liu, H., Deussing, J.M., and Huang, G.J. (2018). NPTX2 is a key component in the regulation of anxiety. Neuropsychopharmacology *43*, 1943–1953.

Chapman, G., Shanmugalingam, U., and Smith, P.D. (2020). The Role of Neuronal Pentraxin 2 (NP2) in Regulating Glutamatergic Signaling and Neuropathology. *13*, 1–6.

Chen, D.F., Jhaveri, S., and Schneider, G.E. (1995). Intrinsic changes in developing retinal neurons result in regenerative failure of their axons. Proceedings of the National Academy of Sciences of the United States of America *92*, 7287–7291.

Chen, H., Zhao, Y., Liu, M., Feng, L., Puyang, Z., Yi, J., Liang, P., Zhang, H.F., Cang, J., Troy, J.B., et al. (2015). Progressive degeneration of retinal and superior collicular functions in mice with sustained ocular hypertension. Investigative Ophthalmology & Visual Science *56*, 1971–1984.

Cho, R.W., Park, J.M., Wolff, S.B.E.E., Xu, D., Hopf, C., Kim, J., Reddy, R.C., Petralia, R.S., Perin, M.S., Linden, D.J., et al. (2008). mGluR1/5-Dependent Long-Term Depression Requires the Regulated Ectodomain Cleavage of Neuronal Pentraxin NPR by TACE. Neuron *57*, 858–871.

Chou, T.-H., Park, K.K., Luo, X., and Porciatti, V. (2013). Retrograde Signaling in the Optic Nerve Is Necessary for Electrical Responsiveness of Retinal Ganglion Cells. Investigative Ophthalmology & Visual Science *54*, 1236–1243.

Cooper, M.L., Collyer, J.W., and Calkins, D.J. (2018). Astrocyte remodeling without gliosis precedes optic nerve axonopathy. Acta Neuropathologica Communications *6*, 38.

Corredor, R.G., and Goldberg, J.L. (2009). Electrical activity enhances neuronal survival and regeneration. Journal of Neural Engineering *6*, 55001.

Crair, M.C., and Mason, C.A. (2016). Reconnecting Eye to Brain. The Journal of Neuroscience *36*, 10707–10722.

David, S., and Aguayo, A.J. (1981). Axonal Elongation into Peripheral Nervous System `` Bridges ' ' after Central Nervous System Injury in Adult Rats Author (s): Samuel David and Albert J . Aguayo Published by : American Association for the Advancement of Science Stable URL : http://www.js. *214*, 931–933.

Dergham, P., Ellezam, B., Essagian, C., Avedissian, H., Lubell, W.D., and McKerracher, L. (2002). Rho signaling pathway targeted to promote spinal cord repair. Journal of Neuroscience *22*, 6570–6577.

Dodds, D., Omeis, I., Cushman, S., Hekms, J., and Perin, M. (1997). Neuronal pentraxin receptor, a noval putative integral membrane pentraxin that interacts with neuronal pentraxin 1 and 2 and taipoxin-associated calcium-binding protein. Journal of Biological Chemistry *272*, 21488–21494.

Dowton, S.B., and McGrew, S.D. (1990). Rat serum amyloid P component. Biochem. J. *270*, 571–585.

Dräger, U.C. (1974). Autoradiography of tritiated proline and fucose transported transneuronally from the eye to the visual cortex in pigmented and albino mice. Brain Research *82*, 284–292.

Ertürk, A., Hellal, F., Enes, J., and Bradke, F. (2007). Disorganized microtubules underlie the formation of retraction bulbs and the failure of axonal regeneration. The Journal of Neuroscience : The Official Journal of the Society for Neuroscience *27*, 9169–9180.

Faulkner, J.R., Herrmann, J.E., Woo, M.J., Tansey, K.E., Doan, N.B., and Sofroniew, M. V (2004). Reactive astrocytes protect tissue and preserve function after spinal cord injury. The Journal of Neuroscience : The Official Journal of the Society for Neuroscience *24*, 2143–2155.

Fawcett, J.W. (2015). Chapter 10 - The extracellular matrix in plasticity and regeneration after CNS injury and neurodegenerative disease. In Sensorimotor Rehabilitation, N. Dancause, S. Nadeau, and S.B.T.-P. in B.R. Rossignol, eds. (Elsevier), pp. 213–226.

Fawcett, J.W. (2018). The Paper that Restarted Modern Central Nervous System Axon Regeneration Research. Trends in Neurosciences *41*, 239–242.

Fawcett, J.W., and Verhaagen, J. (2018). Intrinsic Determinants of Axon Regeneration. Developmental Neurobiology 890–897.

Fawcett, J.W., Housden, E., Smith-Thomas, L., and Meyer, R.L. (1989). The growth of axons in three-dimensional astrocyte cultures. Developmental Biology *135*, 449–458.

Fischer, D. (2004). Switching Mature Retinal Ganglion Cells to a Robust Growth State In Vivo: Gene Expression and Synergy with RhoA Inactivation. Journal of Neuroscience *24*, 8726–8740.

Fischer, D., and Leibinger, M. (2012). Promoting optic nerve regeneration. Progress in Retinal and Eye Research *31*, 688–701.

George, R., and Griffin, J.W. (1994). The proximo-distal spread of axonal degeneration in the dorsal columns of the rat. Journal of Neurocytology *23*, 657–667.

Giehl, K.M., and Tetzlaff, W. (1996). BDNF and NT-3, but not NGF, prevent axotomy-induced death of rat corticospinal neurons in vivo. European Journal of Neuroscience *8*, 1167–1175.

Gobrecht, P., Andreadaki, A., Diekmann, H., Heskamp, A., Leibinger, M., and Fischer, D. (2016). Promotion of Functional Nerve Regeneration by Inhibition of Microtubule Detyrosination. Journal of Neuroscience *36*, 3890–3902.

Goldberg, J.L., Espinosa, J.S., Xu, Y., Davidson, N., Kovacs, G.T.A., and Barres, B.A. (2002a). Retinal ganglion cells do not extend axons by default: promotion by

neurotrophic signaling and electrical activity. Neuron *33*, 689–702.

Goldberg, J.L., Klassen, M.P., Hua, Y., and Barres, B.A. (2002b). Amacrine-signaled loss of intrinsic axon growth ability by retinal ganglion cells. Science *296*, 1860–1864.

Goodman, A.R., Cardozo, T., Abagyan, R., Altmeyer, A., Wisniewski, H.-G., and Vilcekt, J. (1996). Long Pentraxins: an Emerging Group of Proteins with Diverse Functions. Cytokine & Growth Factor *7*, 191–202.

Hanea, S.T., Shanmugalingam, U., Fournier, A.E., and Smith, P.D. (2016). Preparation of embryonic retinal explants to study CNS neurite growth. Experimental Eye Research *146*, 304–312.

Hanson, J.E. (2017). Identifying faulty brain circuits. ELife *6*, e26942.

Harrison, J.M., O'Connor, P.S., Young, R.S., Kincaid, M., and Bentley, R. (1987). The pattern ERG in man following surgical resection of the optic nerve. Investigative Ophthalmology & Visual Science *28*, 492–499.

He, Z., and Jin, Y. (2016). Intrinsic Control of Axon Regeneration. Neuron *90*, 437–451.

Heckenlively, J.R., Arden, G.B., and Bach, M. (2006). Principles and practice of clinical electrophysiology of vision (MIT press).

Hiebert, G.W., Khodarahmi, K., McGraw, J., Steeves, J.D., and Tetzlaff, W. (2002). Brain-derived neurotrophic factor applied to the motor cortex promotes sprouting of corticospinal fibers but not regeneration into a peripheral nerve transplant. Journal of Neuroscience Research *69*, 160–168.

Hsu, Y.-C., and Perin, M.S. (1995). Human neuronal pentraxin II (NPTX2): Conservation, genomic structure, and chromosomal localization. Genomics *28*, 220–227.

Huebner, E. a, and Strittmatter, S.M. (2009). Axon Regeneration in the Peripheral and Central Nervous Systems. Results and Problems in Cell Differentiation *48*, 339–351.

James, S.L., Bannick, M.S., Montjoy-Venning, W.C., Lucchesi, L.R., Dandona, L., Dandona, R., Hawley, C., Hay, S.I., Jakovljevic, M., Khalil, I., et al. (2019). Global, regional, and national burden of traumatic brain injury and spinal cord injury, 1990-2016: A systematic analysis for the Global Burden of Disease Study 2016. The Lancet Neurology *18*, 56–87.

Kaplan, A., Ong Tone, S., and Fournier, A.E. (2015). Extrinsic and intrinsic regulation of axon regeneration at a crossroads. Frontiers in Molecular Neuroscience *8*, 27.

Kim, J.E., Li, S., Grand Pré, T., Qiu, D., and Strittmatter, S.M. (2003). Axon regeneration in young adult mice lacking Nogo-A/B. Neuron *38*, 187–199.

Kirkpatrick, L.L., Matzuk, M.M., Dodds, D.C., and Perin, M.S. (2000). Biochemical interactions of the neuronal pentraxins. Neuronal pentraxin (NP) receptor binds to taipoxin and taipoxin-associated calcium-binding protein 49 via NP1 and NP2. Journal of Biological Chemistry *275*, 17786–17792.

Kozaczek, M., Bottje, W., Greene, E., Lassiter, K., Kong, B., Dridi, S., Korourian, S., and Hakkak, R. (2019). Comparison of liver gene expression by RNAseq and PCR analysis after 8 weeks of feeding soy protein isolate- or casein-based diets in an obese liver steatosis rat model. Food & Function *10*, 8218–8229.

Kretz, A., Marticke, J.K., Happold, C.J., Schmeer, C., and Isenmann, S. (2007). A primary culture technique of adult retina for regeneration studies on adult CNS neurons. Nature Protocols *2*, 131–140.

Laha, B., Stafford, B.K., and Huberman, A.D. (2017). Regenerating optic pathways from the eye to the brain. Science *356*, 1031–1034.

Lee, M.-J., and Chiao, C.-C. (2016). Short-term Alteration of Developmental Neural Activity Enhances Neurite Outgrowth of Retinal Explants. Investigative Ophthalmology & Visual Science *57*, 6496–6506.

Lee, D.H., Luo, X., Yungher, B.J., Bray, E., Lee, J.K., and Park, K.K. (2014). Mammalian target of rapamycin's distinct roles and effectiveness in promoting compensatory axonal sprouting in the injured CNS. J Neurosci *34*, 15347–15355.

Lee, G.W., Lee, T.H., and Vilcek, J. (1993). TSG-14, a tumor necrosis factor- and IL-1-inducible protein, is a novel member of the pentaxin family of acute phase proteins. Journal of Immunology (Baltimore, Md. : 1950) *150*, 1804–1812.

Lee, J.K., Geoffroy, C.G., Chan, A.F., Tolentino, K.E., Crawford, M.J., Leal, M.A., Kang, B., and Zheng, B. (2010). Assessing Spinal Axon Regeneration and Sprouting in Nogo-, MAG-, and OMgp-Deficient Mice. Neuron *66*, 663–670.

Lee, S.-J.J., Wei, M., Zhang, C., Maxeiner, S., Pak, C.H., Calado Botelho, S., Trotter, J., Sterky, F.H., Südhof, T.C., Botelho, S.C., et al. (2017). Presynaptic neuronal pentraxin receptor organizes excitatory and inhibitory synapses. Journal of Neuroscience *37*, 1062–1080.

Legacy, J., Hanea, S., Theoret, J., and Smith, P.D. (2013). Granulocyte macrophage colony-stimulating factor promotes regeneration of retinal ganglion cells in vitro through a mammalian target of rapamycin-dependent mechanism. Journal of Neuroscience Research *91*, 771–779.

Leinonen, H., and Tanila, H. (2018). Vision in laboratory rodents—Tools to measure it and implications for behavioral research. Behavioural Brain Research *352*, 172–182.

Lever, I.J., Bradbury, E.J., Cunningham, J.R., Adelson, D.W., Jones, M.G., McMahon, S.B., Marvizón, J.C., and Malcangio, M. (2001). Brain-derived neurotrophic factor is released in the dorsal horn by distinctive patterns of afferent fiber stimulation. The Journal of Neuroscience : The Official Journal of the Society for Neuroscience *21*, 4469–4477.

Li, H.-J., Sun, Z.-L., Yang, X.-T., Zhu, L., and Feng, D.-F. (2017). Exploring Optic Nerve Axon Regeneration. Current Neuropharmacology *15*, 861–873.

Li, H.J., Pan, Y.B., Sun, Z.L., Sun, Y.Y., Yang, X.T., and Feng, D.F. (2018). Inhibition of miR-21 ameliorates excessive astrocyte activation and promotes axon regeneration following optic nerve crush. Neuropharmacology *137*, 33–49.

Li, L., Huang, H., Fang, F., Liu, L., Sun, Y., and Hu, Y. (2020). Longitudinal Morphological and Functional Assessment of RGC Neurodegeneration After Optic Nerve Crush in Mouse. Frontiers in Cellular Neuroscience *14*, 1–9.

Lim, J.H.A., Stafford, B.K., Nguyen, P.L., Lien, B. V., Wang, C., Zukor, K., He, Z., and Huberman, A.D. (2016). Neural activity promotes long-distance, target-specific regeneration of adult retinal axons. Nature Neuroscience *19*, 1073–1084.

Lima, S. De, Koriyama, Y., Kurimoto, T., Oliveira, T., Yin, Y., Li, Y., Gilbert, H.H.-Y., Maria, A., Martinez, B., Benowitz, L., et al. (2012). Correction for de Lima et al., Full-length axon regeneration in the adult mouse optic nerve and partial recovery of simple visual behaviors. Proceedings of the National Academy of Sciences *109*, 13465–13465.

Lin, C.I., and Chiao, C.C. (2019). Blue light promotes neurite outgrowth of retinal explants in postnatal ChR2 mice. ENeuro *6*, 1–17.

Liu, Y., McDowell, C.M., Zhang, Z., Tebow, H.E., Wordinger, R.J., and Clark, A.F. (2014). Monitoring Retinal Morphologic and Functional Changes in Mice Following Optic Nerve Crush. Investigative Ophthalmology & Visual Science *55*, 3766–3774.

London, A., Benhar, I., and Schwartz, M. (2013). The retina as a window to the brain - From eye research to CNS disorders. Nature Reviews Neurology *9*, 44–53.

Lu, P., Blesch, A., and Tuszynski, M.H. (2001). Neurotrophism without neurotropism: BDNF promotes survival but not growth of lesioned corticospinal neurons. Journal of Comparative Neurology *436*, 456–470.

Ludwin, S.K. (1990). Oligodendrocyte survival in Wallerian degeneration. Acta Neuropathologica *80*, 184–191.

Lye-Barthel, M., Sun, D., and Jakobs, T.C. (2013). Morphology of Astrocytes in a Glaucomatous Optic Nerve. Investigative Ophthalmology & Visual Science *54*, 909–917.

Maekawa, Y., Onishi, A., Matsushita, K., Koide, N., Mandai, M., Suzuma, K., Kitaoka, T., Kuwahara, A., Ozone, C., Nakano, T., et al. (2016). Optimized Culture System to Induce Neurite Outgrowth From Retinal Ganglion Cells in Three-Dimensional Retinal Aggregates Differentiated From Mouse and Human Embryonic Stem Cells. Current Eye Research *41*, 558–568.

Marenna, S., Castoldi, V., d'Isa, R., Marco, C., Comi, G., and Leocani, L. (2019). Semi-invasive and non-invasive recording of visual evoked potentials in mice. Documenta Ophthalmologica *138*, 169–179.

Mariga, A., Glaser, J., Mathias, L., Xu, D., Xiao, M., Worley, P., Ninan, I., and Chao, M. V. (2015). Definition of a Bidirectional Activity-Dependent Pathway Involving BDNF and Narp. Cell Reports *13*, 1747–1756.

Martinez de la Torre, Y., Fabbri, M., Jaillon, S., Bastone, A., Nebuloni, M., Vecchi, A., Mantovani, A., and Garlanda, C. (2010). Evolution of the Pentraxin Family: The New Entry PTX4. The Journal of Immunology *184*, 5055–5064.

McGill, T.J., Prusky, G.T., Douglas, R.M., Yasumura, D., Matthes, M.T., Nune, G., Donohue-Rolfe, K., Yang, H., Niculescu, D., Hauswirth, W.W., et al. (2007). Intraocular CNTF Reduces Vision in Normal Rats in a Dose-Dependent Manner. Investigative Ophthalmology & Visual Science *48*, 5756–5766.

McKinley, W.O., Jackson, A.B., Cardenas, D.D., and De Vivo, M.J. (1999). Long-term medical complications after traumatic spinal cord injury: A regional model systems analysis. Archives of Physical Medicine and Rehabilitation *80*, 1402–1410.

Mead, B., and Tomarev, S. (2016). Evaluating retinal ganglion cell loss and dysfunction. Experimental Eye Research *151*, 96–106.

Miura, G., Wang, M.H., Ivers, K.M., and Frishman, L.J. (2009). Retinal pathway origins of the pattern ERG of the mouse. Experimental Eye Research *89*, 49–62.

Miyake, K., Yoshida, M., Inoue, Y., and Hata, Y. (2007). Neuroprotective Effect of Transcorneal Electrical Stimulation on the Acute Phase of Optic Nerve Injury. Investigative Ophthalmology & Visual Science *48*, 2356–2361.

Morimoto, T., Miyoshi, T., Matsuda, S., Tano, Y., Fujikado, T., and Fukuda, Y. (2005). Transcorneal electrical stimulation rescues axotomized retinal ganglion cells by activating endogenous retinal IGF-1 system. Investigative Ophthalmology & Visual Science *46*, 2147–2155.

Müller, A., Hauk, T.G., Leibinger, M., Marienfeld, R., and Fischer, D. (2009). Exogenous CNTF stimulates axon regeneration of retinal ganglion cells partially via endogenous CNTF. Molecular and Cellular Neuroscience *41*, 233–246.

Murali, A., Ramlogan-Steel, C.A., Andrzejewski, S., Steel, J.C., and Layton, C.J. (2019). Retinal explant culture: A platform to investigate human neuro-retina. Clinical and Experimental Ophthalmology *47*, 274–285.

Nathan, F.M., Ohtake, Y., Wang, S., Jiang, X., Sami, A., Guo, H., Zhou, F.-Q., and Li, S. (2020). Upregulating Lin28a Promotes Axon Regeneration in Adult Mice with Optic Nerve and Spinal Cord Injury. Molecular Therapy *28*, 1902–1917.

Noonan, V.K., Fingas, M., Farry, A., Baxter, D., Singh, A., Fehlings, M.G., and Dvorak, M.F. (2012). Incidence and Prevalence of Spinal Cord Injury in Canada: A National Perspective. Neuroepidemiology *38*, 219–226.

O'Brien, R., Xu, D., Mi, R., Tang, X., Hopf, C., and Worley, P. (2002). Synaptically Targeted Narp Plays an Essential Role in the Aggregation of AMPA Receptors at Excitatory Synapses in Cultured Spinal Neurons. Journal of Neuroscience *22*, 4487–4498.

O'Brien, R.J., Desheng, X., Petralia, R.S., Steward, O., Huganir, R.L., and Worley, P. (1999). Synaptic clustering of AMPA receptors by the extracellular immediate- early gene product Narp. Neuron *23*, 309–323.

Omeis, I.A., Hsu, Y.-C., and Perin, M.S. (1996). Mouse and Human Neuronal Pentraxin 1 (NPTX1): Conservation , Genomic Structure, and Chromosomal Localization. Genomics *36*, 543–545.

Park, K.K., Liu, K., Hu, Y., Smith, P.D., Wang, C., Cai, B., Xu, B., Connolly, L., Kramvis, I., Sahin, M., et al. (2008). Promoting axon regeneration in the adult CNS by modulation of the PTEN/mTOR pathway. Science (New York, N.Y.) *322*, 963–966.

Passaglia, C.L., Siddiq, M.M., Zorina, Y., Davis, S., Kaplan, E., Blitzer, R., and Iyengar, R. (2018). A four-drug combination promotes functional axonal regeneration in the rat optic nerve crush model. Investigative Ophthalmology & Visual Science *59*, 2510.

Pernet, V., and Schwab, M.E. (2014). Lost in the jungle: New hurdles for optic nerve axon regeneration. Trends in Neurosciences *37*, 381–387.

Porciatti, V. (2015). Electrophysiological assessment of retinal ganglion cell function. Experimental Eye Research *141*, 164–170.

Porciatti, V., Pizzorusso, T., Cenni, M.C., and Maffei, L. (1996). The visual response of retinal ganglion cells is not altered by optic nerve transection in transgenic mice overexpressing Bcl-2. Proceedings of the National Academy of Sciences *93*, 14955–14959.

Puyang, Z., Gong, H.-Q., He, S.-G., Troy, J.B., Liu, X., and Liang, P.-J. (2017). Different functional susceptibilities of mouse retinal ganglion cell subtypes to optic nerve crush

injury. Experimental Eye Research *162*, 97–103.

Ramon y Cajal, S., and May, R.M. (1928). Degeneration & regeneration of the nervous system, (London: Oxford University Press, Humphrey Milford).

Reid, M.S., and Blobel, C.P. (1994). Apexin, an acrosomal pentaxin. Journal of Biological Chemistry *269*, 32615–32620.

Reti, I.M., and Baraban, J.M. (2000). Sustained increase in Narp protein expression following repeated electroconvulsive seizure. Neuropsychopharmacology *23*, 439–443.

Reti, I.M., Reddy, R., Worley, P.F., and Baraban, J.M. (2002a). Selective expression of Narp, a secreted neuronal pentraxin, in orexin neurons. Journal of Neurochemistry *82*, 1561–1565.

Reti, I.M., Reddy, R., Worley, P.F., and Baraban, J.M. (2002b). Prominent Narp expression in projection pathways and terminal fields. Journal of Neurochemistry *82*, 935–944.

Reti, I.M., Miskimon, M., Dickson, M., Petralia, R.S., Takamiya, K., Bland, R., Saini, J., During, M.J., Huganir, R.L., and Baraban, J.M. (2008). Activity-dependent secretion of neuronal activity regulated pentraxin from vasopressin neurons into the systemic circulation. Neuroscience *151*, 352–360.

Ridder, W.H., and Nusinowitz, S. (2006). The visual evoked potential in the mouse - Origins and response characteristics. Vision Research *46*, 902–913.

Romano, C., and Hicks, D. (2007). Adult retinal neuronal cell culture. Progress in Retinal and Eye Research *26*, 379–397.

Sánchez-Migallón, M.C., Valiente-Soriano, F.J., Nadal-Nicolás, F.M., Di Pierdomenico, J., Vidal-Sanz, M., and Agudo-Barriuso, M. (2018). Survival of melanopsin expressing retinal ganglion cells long term after optic nerve trauma in mice. Experimental Eye Research *174*, 93–97.

Saszik, S.M., Robson, J.G., and Frishman, L.J. (2002). The scotopic threshold response of the dark-adapted electroretinogram of the mouse. The Journal of Physiology *543*, 899–916.

Schaeffer, J., Delpech, C., Albert, F., Belin, S., and Nawabi, H. (2020). Adult Mouse Retina Explants: From ex vivo to in vivo Model of Central Nervous System Injuries. Frontiers in Molecular Neuroscience *13*, 1–19.

Schlimgen, A.K., Helms, J.A., Vogel, H., and Perin, M.S. (1995). Neuronal pentraxin, a secreted protein with homology to acute phase proteins of the immune system. Neuron *14*, 519–526.

Schwalbe, R.A., Dahlback, B., Coe, J.E., and Nelsestuen, G.L. (1992). Pentraxin family of proteins interact specifically with phosphorylcholine and/or phosphorylethanolamine. Biochemistry *31*, 4907–4915.

Schwarz, D.A., Barry, G., Mackay, K.B., Manu, F., Naeve, G.S., Vana, A.M., Verge, G., Conlon, P.J., Foster, A.C., and Maki, R.A. (2002). Identification of differentially expressed genes induced by transient ischemic stroke. Molecular Brain Research *101*, 12–22.

Shao, W.-Y., Liu, X., Gu, X.-L., Ying, X., Wu, N., Xu, H.-W., and Wang, Y. (2016). Promotion of axon regeneration and inhibition of astrocyte activation by alpha A-crystallin on crushed optic nerve. International Journal of Ophthalmology *9*, 955–966.

Shoichet, M.S., Tate, C.C., Baumann, M.D., and LaPlaca, M.C. (2008). Strategies for Regeneration and Repair in the Injured Central Nervous System. W.M. Reichert, ed. (Boca Raton (FL)), p.

Sia, G.M., Béïque, J.C., Rumbaugh, G., Cho, R., Worley, P.F., and Huganir, R.L. (2007). Interaction of the N-Terminal Domain of the AMPA Receptor GluR4 Subunit with the Neuronal Pentraxin NP1 Mediates GluR4 Synaptic Recruitment. Neuron *55*, 87–102.

Smith, P.D., Sun, F., Park, K.K., Cai, B., Wang, C., Kuwako, K., Martinez-Carrasco, I., Connolly, L., and He, Z. (2009). SOCS3 Deletion Promotes Optic Nerve Regeneration In Vivo. Neuron *64*, 617–623.

Sowmya, H. (2019). A Comparative Study of Homology Modeling Algorithms for NPTX2 Structure Prediction. Research J. Pharm. and Tech. *12*, 1895–1900.

Strauss, O. (2005). The retinal pigment epithelium in visual function. Physiological Reviews *85*, 845–881.

Surguchov, A., Soto, I., Shindler, K., Crish, S.D., Pietrucha-Dutczak, M., Amadio, M., Smedowski, A., Govoni, S., and Lewin-Kowalik, J. (2018). The Role of Endogenous Neuroprotective Mechanisms in the Prevention of Retinal Ganglion Cells Degeneration. *12*.

Takeda, M., Kato, H., Takamiya, A., Yoshida, A., and Kiyama, H. (2000). Injury-specific expression of activating transcription factor-3 in retinal ganglion cells and its colocalized expression with phosphorylated c-Jun. Investigative Ophthalmology & Visual Science *41*, 2412–2421.

Templeton, J.P., and Geisert, E.E. (2012). A practical approach to optic nerve crush in the mouse. Molecular Vision *18*, 2147–2152.

Torres-Espín, a, Santos, D., González-Pérez, F., Del Valle, J., and Navarro, X. (2014). Neurite-J: an Image-J Plug-in for Axonal Growth Analisys in Organotypic Cultures.

Journal of Neuroscience Methods *236*, 1–14.

Tsui, C.C., Copeland, N.G., Gilbert, D.J., Jenkins, N. a, Barnes, C., and Worley, P.F. (1996). Narp, a novel member of the pentraxin family, promotes neurite outgrowth and is dynamically regulated by neuronal activity. The Journal of Neuroscience : The Official Journal of the Society for Neuroscience *16*, 2463–2478.

Van't Spijker, H.M., Rowlands, D., Rossier, J., Haenzi, B., Fawcett, J.W., and Kwok, J.C.F. (2019). Neuronal Pentraxin 2 Binds PNNs and Enhances PNN Formation. Neural Plasticity *2019*.

Varadarajan, S.G., and Huberman, A.D. (2018). Assembly and repair of eye-to-brain connections. Current Opinion in Neurobiology *53*, 198–209.

Vargas, M.E., and Barres, B.A. (2007). Why is Wallerian degeneration in the CNS so slow? Annual Review of Neuroscience *30*, 153–179.

Vecino, E., Rodriguez, F.D.D., Ruzafa, N., Pereiro, X., and Sharma, S.C. (2016). Glia–neuron interactions in the mammalian retina. Progress in Retinal and Eye Research *51*, 1–40.

Viczian, A.S., and Zuber, M.E. (2014). Retinal Development. Principles of Developmental Genetics: Second Edition 297–313.

Villegas-Pérez, M.P., Vidal-Sanz, M., Rasminsky, M., Bray, G.M., and Aguayo, A.J. (1993). Rapid and protracted phases of retinal ganglion cell loss follow axotomy in the optic nerve of adult rats. Journal of Neurobiology *24*, 23–36.

Whitehead, A.S., Zahedi, K., Rits, M., Mortensen, R.F., and Lelias, J.M. (1990). Mouse C-reactive protein. Generation of cDNA clones, structural analysis, and induction of mRNA during inflammation. The Biochemical Journal *266*, 283–290.

Williams, P.A., Howell, G.R., Barbay, J.M., Braine, C.E., Sousa, G.L., John, S.W.M., and Morgan, J.E. (2013). Retinal ganglion cell dendritic atrophy in DBA/2J glaucoma. PloS One *8*, e72282.

Wong, K., Babetto, E., and Beirowski, B. (2017). Axon degeneration: make the Schwann cell great again. Neural Regeneration Research *12*, 518.

van Wyk, M., Wässle, H., and Taylor, W.R. (2009). Receptive field properties of ON- and OFF-ganglion cells in the mouse retina. Visual Neuroscience *26*, 297–308.

Wyndaele, M., and Wyndaele, J.-J. (2006). Incidence, prevalence and epidemiology of spinal cord injury: what learns a worldwide literature survey? Spinal Cord *44*, 523–529.

Xia, X., Wen, R., Chou, T.-H., Li, Y., Wang, Z., and Porciatti, V. (2014). Protection of

Pattern Electroretinogram and Retinal Ganglion Cells by Oncostatin M after Optic Nerve Injury. PLOS ONE *9*, e108524.

Xiao, M.-F., Xu, D., Craig, M.T., Pelkey, K.A., Chien, C.-C., Shi, Y., Zhang, J., Resnick, S., Pletnikova, O., Salmon, D., et al. (2017). NPTX2 and cognitive dysfunction in Alzheimer's Disease. ELife *6*, 3–5.

Xu, D., Hopf, C., Reddy, R., Cho, R.W., Guo, L., Lanahan, A., Petralia, R.S., Wenthold, R.J., O'Brien, R.J., and Worley, P. (2003). Narp and NP1 form heterocomplexes that function in developmental and activity-dependent synaptic plasticity. Neuron *39*, 513–528.

Yiu, G., and He, Z. (2006). Glial Inhibition of CNS axon regeneration. Nature Review Neuroscience *7*, 617–627.

You, Y., Klistorner, A., Thie, J., and Graham, S.L. (2011). Improving reproducibility of VEP recording in rats: electrodes, stimulus source and peak analysis. Documenta Ophthalmologica. Advances in Ophthalmology *123*, 109–119.

Zheng, B., Ho, C., Li, S., Keirstead, H., Steward, O., and Tessier-Lavigne, M. (2003). Lack of enhanced spinal regeneration in Nogo-deficient mice. Neuron *38*, 213–224.